

2019

Effect of FDM process parameters on the mechanical properties of CFR-PEEK

Rama Srikar Mutyala
Iowa State University

Follow this and additional works at: <https://lib.dr.iastate.edu/etd>



Part of the [Industrial Engineering Commons](#)

Recommended Citation

Mutyala, Rama Srikar, "Effect of FDM process parameters on the mechanical properties of CFR-PEEK" (2019). *Graduate Theses and Dissertations*. 17753.
<https://lib.dr.iastate.edu/etd/17753>

This Thesis is brought to you for free and open access by the Iowa State University Capstones, Theses and Dissertations at Iowa State University Digital Repository. It has been accepted for inclusion in Graduate Theses and Dissertations by an authorized administrator of Iowa State University Digital Repository. For more information, please contact digirep@iastate.edu.

Effect of FDM process parameters on the mechanical properties of CFR-PEEK

by

Rama Srikar Mutyala

A thesis submitted to the graduate faculty

in partial fulfillment of the requirements for the degree of

MASTER OF SCIENCE

Major: Industrial Engineering

Program of Study Committee:

Gül E. Okudan Kremer, Major Professor

John Jackman

Michael Helwig

Mark Mba-Wright

The student author, whose presentation of the scholarship herein was approved by the program of study committee, is solely responsible for the content of this thesis. The Graduate College will ensure this thesis is globally accessible and will not permit alterations after a degree is conferred.

Iowa State University

Ames, Iowa

2019

Copyright © Rama Srikar Mutyala, 2019. All rights reserved.

DEDICATION

I would like to dedicate my work to my beloved parents Mr. Srinivas Rao, Mrs. Mutyala Sailaja and sister, Sravani Mutyala for supporting me throughout my efforts and for their unconditional love and support. I am very thankful to you for believing in me and letting me pursue my dreams. I am very blessed to have them in my life.

TABLE OF CONTENTS

	Page
LIST OF FIGURES	v
LIST OF TABLES	viii
NOMENCLATURE	ix
ACKNOWLEDGMENTS	xii
ABSTRACT	xiii
CHAPTER 1	
INTRODUCTION	
1.1 Motivation	1
1.2 Overview of Proposed Framework	3
1.3 Thesis Road Map	4
CHAPTER 2	
LITERATURE REVIEW	
2.1 Rapid Prototyping Overview	6
2.1.1 Computer Aided Design Rapid Prototyping Interface	11
2.1.1.1 Computer Aided Design Software	11
2.1.1.2 Rapid Prototyping Machine Software	14
2.2. Fused Deposition Modelling	17
2.3 FDM Part Quality	20
2.4 Studies Done So Far	23
2.5 Research Gap, Challenges and Problems	33
2.6 Review	36
CHAPTER 3	
MATERIALS AND METHODS	
3.1 Introduction	39
3.1.1 Disadvantages of Materials Being Used as Implants	41
3.2 Potentiality of CFR-PEEK as an Implant	43
3.3 Methodology	47
3.3.1 Specimen Fabrication	47
3.3.2 Test Requirements and Measurements	51

3.3.2.1 Tensile test	51
3.3.2.2 Compressive test	52
3.3.2.3 Number of specimens	53
3.3.2.4 Speed of testing	54
3.3.2.5 Test requirements	54
3.4 Selection of Process Parameters	56
3.4.1 Layer Thickness	56
3.4.2 Orientation	58
3.4.3 Printing Speed	60
CHAPTER 4 RESULTS AND DISCUSSION	
4.1 Tensile specimen	66
4.1.1 ANOVA Analysis	68
4.1.2 Contour Plots for Tensile Strength	76
4.1.3 Surface Plots	78
4.1.4 Optimal factor for Tensile Strength	80
4.2 Compression specimen	82
4.2.1 ANOVA Analysis	83
4.2.2 Contour Plots for Compression Strength	90
4.2.3 Surface Plots	94
4.2.4 Optimal factor for Compression Strength	96
4.3 Comparison with other studies	97
CHAPTER 5 CONCLUSION	98
5.1 Uniqueness of this study	101
5.2 Scope of future work	102
CHAPTER 6 REFERENCES	103
APPENDIX SELECTIVE LASER SINTERING	117
APPENDIX 3D PRINTING	119
APPENDIX LAMINATED OBJECT MANUFACTURING	120
APPENDIX MULTIJET MODELLING	122

LIST OF FIGURES

		Page
Figure 1.1	Illustration of proposed framework	4
Figure 2.1	Position of layered manufacturing in comparison to other manufacturing techniques in terms of complexity and quantity	8
Figure 2.2	The main stages involved in Rapid Prototyping processes	10
Figure 2.3	Tessellation of 3D model and the effect of increased tessellation	12
Figure 2.4	Stages involved in the slicing process	15
Figure 2.5	Detailed diagram of slicing, polygons created and order of their presentation	16
Figure 2.6	Schematic diagram of Fused Deposition Modelling (FDM) method	18
Figure 2.7	Stair case effect observed in inclined surfaces	21
Figure 3.1	Comparison of stiffness of different materials	43
Figure 3.2	APIUM P220 Series FDM printer	47
Figure 3.3a	SolidWorks model of the specimen	48
Figure 3.3b	STL files of the SolidWorks model	48
Figure 3.4	Schematic diagram showing the Fused Deposition Modelling printer working	49
Figure 3.5	Tensile test specimen and dimensions	50
Figure 3.6 a	Compressive test specimen and dimensions	51
Figure 3.6 b	Compression test fixture	52
Figure 3.7	800 Series UTM fatigue test machine	54
Figure 3.8	Layer thickness	55
Figure 3.9	Part orientation of the dog bone structure in X, Y and Z direction	58

Figure 4.1	Stress-strain graphs obtained for various combinations of tensile strength	68
Figure 4.1.2	Main effects plot	70
Figure 4.1.3	Interaction Plot	71
Figure 4.1.4	Interaction plot figure created to understand the interactions	72
Figure 4.1.5	Effect of tension load (tensile strength) on the layers of the part stacked	73
Figure 4.1.6	Full interaction plot for tensile strength	74
Figure 4.1.7	Variations in tensile strengths of parts printed with various combinations of process parameters	76
Figure 4.1.8	Contour Plots: Tensile strength vs Orientation, Layer thickness	77
Figure 4.1.9	Contour Plots: Tensile strength vs Layer thickness, Printing speed	77
Figure 4.1.10	Contour Plots: Tensile strength vs Orientation, Printing speed	78
Figure 4.1.11	Surface Plots: Tensile strength vs Orientation, Printing speed	79
Figure 4.1.12	Surface Plots: Tensile strength vs Orientation, Layer thickness	79
Figure 4.1.13	Surface Plots: Tensile strength vs Layer thickness, Printing speed	80
Figure 4.1.14	Tensile: Optimal factors obtained using MINITAB software	81
Figure 4.2.3	Compression: Main effects plot	85
Figure 4.2.4	Interactions plot for compression strength	86
Figure 4.2.5	Effect of compression load (compressive strength) on the layers of the part stacked	88
Figure 4.2.6	Full interaction plot for compression strength	89
Figure 4.2.7	Variations in compression strengths of parts printed with various combinations of process parameters	90
Figure 4.2.8	Contour Plots: Compression strength with respect to Layer Thickness and Orientation	91
Figure 4.2.9	Contour Plots: Compression strength with respect to Layer thickness and Printing speed	92

Figure 4.2.10	Contour Plots: Compression strength with respect to Printing speed and Orientation	93
Figure 4.2.11	Surface Plots: Compression strength with respect to Orientation and printing speed	94
Figure 4.2.12	Surface plots: Compression strength with respect to Layer Thickness and Orientation	95
Figure 4.2.13	Surface plots: Compression strength with respect to Layer Thickness and Printing speed	95
Figure 4.2.14	Compressive: Optimal factors obtained using MINITAB software	96
Figure 7.1	Categorization of rapid prototyping processes based on the initial material form	117
Figure 7.2	Schematic diagram of selective laser sintering	119
Figure 7.3	Schematic diagram of 3D printing	121
Figure 7.4	Laminated object manufacturing	122
Figure 7.5	Multi jet modelling	123

LIST OF TABLES

	Page	
Table 2.1	Available standard interfaces	11
Table 2.2	Comparison between various Rapid Prototyping methods	20
Table 2.3	Summary of the literature review done so far on the effect of process parameters on strength of Fused Deposition Modelling parts	29
Table 3.1	Specification of the Fused Deposition Modelling printer	47
Table 3.2	Values of varying process parameters	61
Table 3.3	Possible combinations of all three parameters	62
Table 3.4 a	Randomization of tensile tests	63
Table 3.5 b	Randomization of compressive tests	64
Table 4.1	Combinations and the obtained tensile strengths in Mpa	67
Table 4.2	Combinations and their compression values obtained.	83
Table 4.1.1	Analysis of variance table for tensile test results	69
Table 4.2.2	Analysis of variance table for compression test results	84

NOMENCLATURE

2D	Two dimensional
3D	Three dimensional
3DW	Three-Dimensional Welding
ABS	Acrylonitrile Butadiene Styrene
AM	Additive Manufacturing
ASCII	American Standard Code for Information Interchange
BIS	Beam Interference Solidification
BPM	Ballistic Particle Manufacture
CAD	Computer Aided Design
CAM	Computer Aided Manufacturing
CNC	Computer Numerical Control
CT	Computer Topography
DMD	Direct Metal Deposition
DFM	Design for Manufacture
DMLS	Direct Metal Laser Sintering
DOE	Design of Experiment
DSPC	Direct Shell Production Casting
DXF	Drawing Exchange Format
ECF	Enterocutaneous Fistula
EDM	Electrical Discharge Machining
ES	Electro Setting
FDM	Fused Deposition Modelling

FEA	Finite Element Analysis
FPM	Freeform Powder Molding
GPD	Gas Phase Deposition
FFF	Freeform Fabrication
HIS	Holographic Interface Solidification
IGES	Initial Graphics Exchange Specification
LEAF	Layer Exchange ASCII format
LENS	Laser Engineered Net Shaping
LM	Layered Manufacturing
LOM	Laminated Object Manufacturing
LTP	Liquid Thermal Polymerization
MJM	Multi Jet Modelling
MJS	Multi-phase Jet Solidification
OQP	Object Quadra Process
PA-12	Polyamide 12
PC	Polycarbonate
PLS	Paper Lamination System
PLT	Paper Lamination Technology
PPSU	Poly-phenyl-sulphone
PS	Polystyrene
RFP	Rapid Freezing Prototyping
RM	Rapid Manufacturing
RP	Rapid Prototyping
RPS	Rapid Prototyping System
RT	Rapid Tooling

SAHP	Selective Adhesive and Hot Press
SCS	Solid Creation System
SDM	Shape Deposition Manufacturing
SF	Spatial Forming
SFP	Solid Foil Polymerization
SGC	Solid Ground Curing
SL	Stereo lithography
SLM	Selective Laser Melting
SLS	Selective Laser Sintering
SOUP	Solid Object Ultraviolet-laser Plotting
STEP	Shape Transfer Exchange Protocol
STL	Stereo-lithography File
TSF	Topographic Shell Fabrication
UV	Ultra violet

ACKNOWLEDGMENTS

First of all, I would like to thank the almighty for providing me with such an opportunity and platform to excel and showcase my skills.

I would like to express my sincere gratitude to my advisor Prof. Gül Kremer for her continuous support throughout my research work. I am very grateful for her invaluable guidance, untiring encouragement, and immense motivation. I am also indebted to Prof. Kijung Park for his stimulating suggestions and indispensable support throughout my research work.

I am fortunate and ever obligated to have both of them for adding great dimensions to my research and making it unique.

I owe my wholehearted thanks to my father for his ever-supporting words of wisdom that has always been my driving and motivating force. I also owe sincere thanks to my mother for her unconditional love and blessing which is beyond any limits and my sister for always being by my side.

I would also like to thank Gayeon Kim for her support in my research work, which she has extended to me as a colleague.

ABSTRACT

Carbon reinforced Poly-ether-ether-ketone (CFR-PEEK) is a poly-aromatic semi-crystalline thermoplastic that is widely used in the biomedical field because of its in vivo bio-compatibility and human bone-like elastic modulus. It is being used in different surgical fields such as orthopedic, facial and spinal surgeries, and is considered as an ideal material for articulating implants. Additive manufacturing is an ideal fit to create the medical implants because of its ability to print customized patient-specific products in comparatively less time and cost.

One such additive manufacturing technique known as Fused Deposition Modelling has been proven to be the best alternative for fabricating CFR-PEEK samples. However, the product quality of parts manufactured by FDM technique mainly depends on the process parameters and the wide range of parameters makes it a complex process. Additionally, the FDM parameter effects vary widely for different materials. Therefore, there is a need to understand the effect of these parameters on the new and potential materials like CFR-PEEK.

This study investigates the effects three crucial FDM parameters (layer thickness, orientation and printing speed) on the mechanical properties of CFR-PEEK material. Layer thickness and Orientation play an important role in tensile and compressive strength of the CFR-PEEK parts. Printing speed too has an effect

on the tensile strength but has minimal to no effect on the compressive strength of CFR-PEEK. Understanding the relationship between the process parameters and part quality would help medical industry in fabricating customized or patient specific implants.

CHAPTER 1

INTRODUCTION

1.1 Motivation

In today's competitive world, industries are looking forward to cost savings, improved product life, higher quality and reliability of products. The growing demand of customized products in different fields such as aviation, automobile with complicated geometry and nuance features has led to a rise in the usage of Rapid Prototyping (RP) technology. This technology has proved to be an efficient alternative for the industries to produce complex parts with less manual effort at a faster pace while completely removing the need of tooling and Design for Manufacturing (DfM) related constraints to a large extent. Among several RP technologies available in the current scenario, Fused Deposition Modelling (FDM) has been chosen as the area of focus because of its special characteristics such as the ability to build complex structures in a layer-by-layer method starting from a Computer Aided Design (CAD) file and capability to use different kinds of materials in the fabrication. Affordability and feasibility to control the process remotely to produce customized consumer goods made this innovative technology as a favorable means of fabrication across various industries (Palermo, 2013).

Despite the wide range of benefits offered by FDM, a large number of barriers exist related to this process. FDM technology needs to be improved in terms of

geometrical stability, part quality and product performance. A proper understanding of the processes and their traits is crucial to overcome these limitations (Sood, 2011).

A significant amount of importance is given to the mechanical strength of RP fabricated parts as the mechanical properties are considered to be the most important indices for evaluating the fabrication quality of the process (Deng et al., 2018). Though FDM has been evolving from prototyping to manufacturing parts for their direct usage in application, parts fabricated by FDM have poor mechanical properties (Rajpurohit et al., 2018). The product quality and material properties of the FDM part depends a lot on the process parameters such as orientation, infill density, feed rate, raster angle, and layer thickness among others (Masood et al., 2010; Smith et al., 2013; Bagsik et al., 2010). These wide range of parameters available in the FDM technology makes it a complex process (Casavola et al., 2016). Therefore, the need to understand the effect of process parameters on the mechanical properties of the parts is highly crucial (Vaezi et al., 2011). This study would help in understanding the relationship between the process parameters and the part quality. Understanding this relationship will aid in identifying the optimal (among the ones used for this study) process parameter combination required to obtain parts with a desired strength.

Moreover, the effects of the FDM parameters differ from material to material, which means that the optimal combination of parameters obtained for one material may not be the same for a different material (Gebisa et al., 2018). Research in this direction until now is focused more on typical materials such as ABS (Ismail et al., 2014), PLA (Chacón et al., 2017), ULTEM 9085 (Schöppner et al., 2011). This calls for the need to

investigate the effect of parameters on newly emerging materials such as CFR-PEEK (Carbon-Reinforced Polyether ether ketone). CFR-PEEK, a relatively new material, is a composite of PEEK (Polyether ether ketone). Unlike PEEK, this material can be made anisotropic by altering the carbon fibers to meet the demand of specific products especially in medical applications (Green et al., 2007). Among other available polymers today, CFR-PEEK has advantages of improved stiffness and wear resistance, high toughness and load carrying capacity (Green et al., 2001; Li et al., 2015). However, not much attention has been given to the possibility of fabricating CFR-PEEK samples with low cost 3D/FDM printers. This study will examine the effects of FDM process parameters on the mechanical properties of CFR-PEEK test coupons.

Overall, there is a lot of opportunity in the field of additive manufacturing especially in Fused Deposition Modelling (FDM) technology. With the emergence of new materials, the need to use them for fabricating products with minimum cost is highly increasing. FDM, among the other additive manufacturing methods, provides a relatively inexpensive way of fabricating parts and hence is the most popular and fast-growing three-dimensional printing method.

1.2 Overview of Proposed Framework

The goal of this study is to investigate the effect of process parameters such as layer thickness, orientation and printing speed on the part quality (CFR-PEEK material) using an FDM printer. Part quality is measured in terms of the mechanical strength of parts. This study aims at explaining the effect of each parameter on the mechanical

properties including tensile and compressive strength of the parts. The overall objectives of this study are as follows:

- Investigating the effect of FDM process parameters on the quality of CFR-PEEK parts.
- Analysis of experimental-based results using statistical methods. Investigating and determining the relationship between the FDM process parameters and the mechanical properties.
- Finding the optimum combination of process parameters to obtain products with improved part quality.

Figure 1.1 shows the summary of the proposed framework.

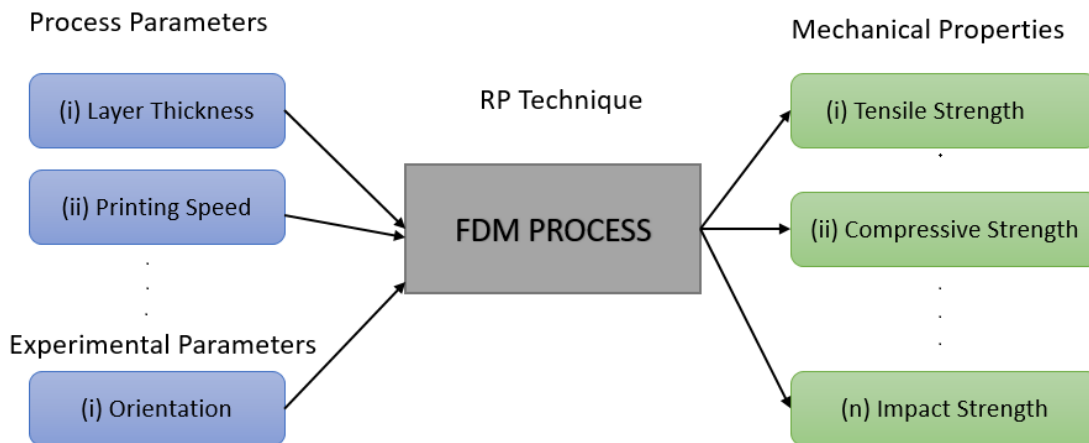


Figure 1.1. Illustration of proposed framework

1.3 Thesis Road Map

In the literature, materials such as Acrylonitrile Butadiene Styrene (ABS) and Polylactic Acid (PLA) have been extensively used to study the effect of process parameters

on the mechanical strength of the parts. As the effects of these parameters mainly depend on the material being used, the experimental results obtained in the studies were found to be inconsistent (Khan et al., 2005). This study focuses on the parameters having the maximum effect on the mechanical properties of the build parts. Chapter 2 consists of a detailed literature review on the Rapid Prototyping (RP) technologies available and few of the challenges being faced. Exploring the literature review also reveals that limited study has been done on few RP technologies. Chapter 2 also discusses the research done thus far using various materials to find out the effect of process parameters on the strength of the parts.

Chapter 3 contains a systematic description of the proposed framework along with figures and tables, which would enable the reader to get a better understanding of the experiments conducted as part of this research. This chapter gives details of the material being used and the design of the sample that is being fabricated using Fused Deposition Modelling method. It also includes the list of experiments being performed and additional details regarding them.

Chapter 4 includes the analysis of the experiments and studies the effect of process parameters on part quality. Part quality will be measured in terms of tensile and compressive strength of the samples being fabricated using Fused Deposition Modelling technique. It includes a comprehensive investigation on the individual effect of the parameters on part quality. Finally, from the analysis, the optimal process parameter combination for the maximum strength will be determined.

Chapter 5 includes conclusions and statement related to scope for future work.

CHAPTER 2

LITERATURE REVIEW

2.1 Rapid Prototyping Overview

With the fast-growing technology and competition, industries are focusing more on faster and easier ways of manufacturing techniques. However, the challenges faced with manufacturing of complex structures made researchers to focus more on the way parts are being fabricated which led to the emergence of a new technology, Rapid Prototyping. The 'rapid' in RP refers to the quick fabrication of models in comparison to traditional subtractive methods of manufacturing processes such as drilling, milling, machining, turning, etc. This technology is capable of fabricating structures with complicated geometry by receiving a CAD (Computer Aided Design) model with minimal or no human effort and tooling which would be impossible with conventional manufacturing machines such as CNCs. Eventually, these advantages paved the path for additive manufacturing into diverse fields such as aerospace, automobile, medical, etc. For example, through RP technology in the medical field, the possibility of fabricating customized and precise geometries has enabled orthopedic surgeons to duplicate lost human organs and prepare medical implants (Li et al., 2015). The inherent property of porosity in RP technologies has been of further advantage in the fabrication of medical scaffolds and implants (Inzana et al., 2014). In yet another study (Wiedemann et al., 1999) related to automobile field, it was found that when compared to traditional manufacturing processes, RP techniques are capable of printing a whole engine mock-up within one-fifth of the total cost. Using

RP techniques to fabricate end-use products is termed as Rapid Manufacturing (Hon, 2007).

Rapid Manufacturing is executed by either adding the material or by removing the material to get the desired shape. This study focuses more on the 'material addition' method of RP also named as Layered Manufacturing. The underlying fundamental of this kind of manufacturing is to break down the structure into building blocks of layers. In other words, any three-dimensional complex structure could be converted into a bunch of simple two-dimensional layers. This technology has facilitated designers the means to overcome the constraints involved in Design for Manufacturing (DfM) principles and has provided them additional time which can be utilized in iterating the designs and optimizing them (Bernard et al., 2002).

Layered Manufacturing, when compared to other manufacturing processes has been able to overcome the geometrical limitations and quantity restrictions and has proved its capability to manufacture complicated geometries (Levy, 2003). Figure 2-1 from Levy's study shows the comparison between different manufacturing processes such as cutting, die casting, milling with that of LM in terms of producing structure complexity and quantity. However, in practical terms, the new emerging and better performing LM technologies will push the borders around the LM technique (as shown in Figure 2-1) towards the higher quantity.

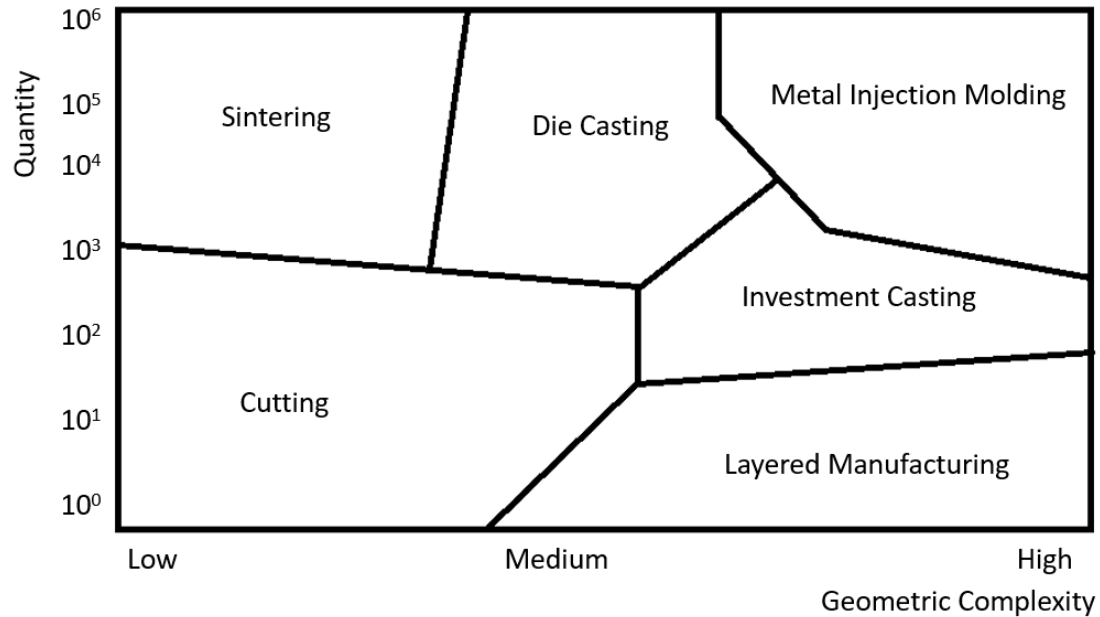


Figure 2.1. Position of LM in comparison to other manufacturing techniques in terms of complexity and quantity. (adapted from Levy, 2003)

Generally, Layered Manufacturing is used for fabricating prototypes, which are extensively used in many fields at the design stage for a given product. Depending upon the complexity and size of the structure being built, LM could take anywhere from one to twenty-four hours to build a part. But when compared with the time required for building a part using other traditional methods, the time taken for LM is much less (Bak, 2003). For example, a traditional method like casting requires a lot of time for designing and building the molds and patterns for a particular product. Additionally, excess time would be required for machining and removing the excess parts. Whereas in the case of LM, there is no need for tooling, and it does not involve much of human skill and effort. Yet another traditional technique, injection molding used for mass manufacturing, requires expensive molds and the success of part quality depends on the skill of the person making the molds of parts.

In most of the LM methods, parts are fabricated by depositing materials layer by layer in a two-dimensional x-y plane, and the third dimension (z) is a result of the layers stacked up along the height of the object. Most of the LM processes are similar to each other as they form objects in a layer-by-layer fashion and then bond them in z-direction (Gebhardt, 2003).

The main stages involved in any RP process are shown in Figure 2-2 (Sood, 2011). The steps involved in an RP process are as following:

- The creation of the Computer-Aided Design (CAD model of the desired object using available software such as SolidWorks, Creo etc.).
- The CAD model is then converted to a standard RP format (STL etc.).
- The model is then sliced using the slicing software such as Stratasys into two-dimensional layers.
- The sliced model is then sent to the printer, which then prints the part layer by layer.
- Post-processing and finishing of the printed part.

The first step depends on the designer and is independent of the RP processes. The next two steps, which are converting to a standard RP format and slicing, are very crucial. These steps are further discussed in the later part of the literature section. The remaining steps depend on the RP processes, which are discussed in section 2.2.

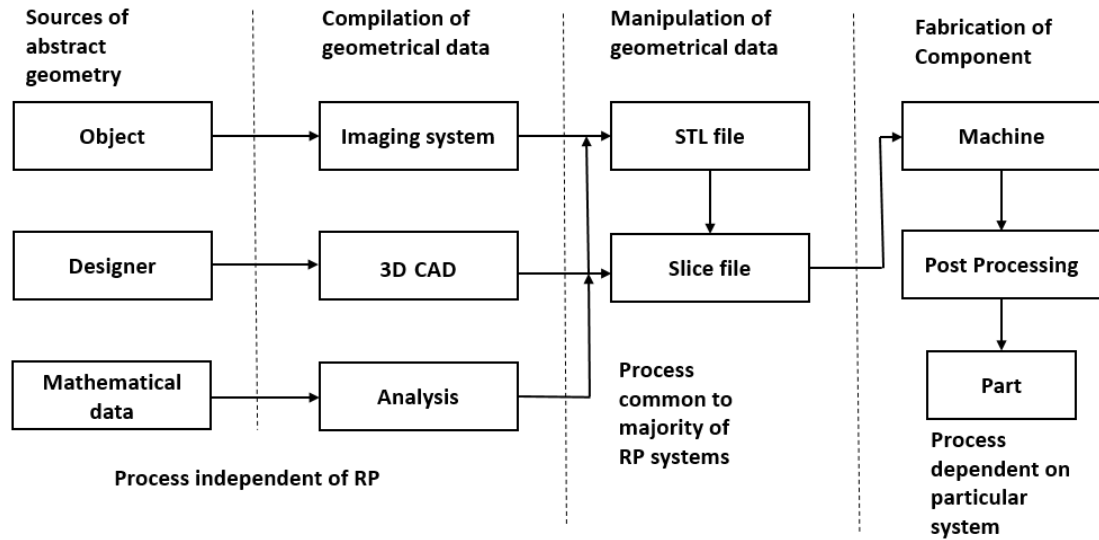


Figure 2.2. The main stages involved in the RP processes. (adapted from Sood, 2011)

All the aforementioned steps can be segregated into two categories:

1. Development of mathematical information or data, which is completely based on the CAD model.
2. The development of the physical model from the CAD model.

The following sections will describe these in detail.

2.1.1 CAD-RP Interface

2.1.1.1 CAD Software

One stage, which is most common and crucial in any RP process, is the conversion of the CAD model to a suitable RP format. Some of the available CAD modeling software are SOLIDWORKS, Pro-E, CATIA, and AUTOCAD among others, which store the designed solid models in the form of mathematical data and then transmit this data using standardized interfaces (standard formats). Some of the standard interfaces in use are as follows (Gebhardt, 2003):

Table 2.1. Available standard interfaces (Gebhardt, 2003)

Interfaces available today	Full form
IGES	Initial Graphic Exchange Specification
STEP	Standard for Exchange of Product data
DXF	Drawing Exchange format
STL	Standard Tessellation Language

Even though a plethora of interfaces are available, the industry standard for any RP file is the STL which stands for Stereolithography (Jamshidi et al., 2005). The algorithms and mathematical data in the CAD model can be transferred using the STL format. The STL format is triangular facets representation of the desired model, which acts as an input to slicing software that slices the model into layers for build process (Muthu et al., 2016). STL files are usually in the ASCII (American Standard Code for Information Interchange) or

in the binary format. The Binary format is usually preferred in 3D printing but if the RP user has to manually inspect the entire STL file for any defects then ASCII is preferred.

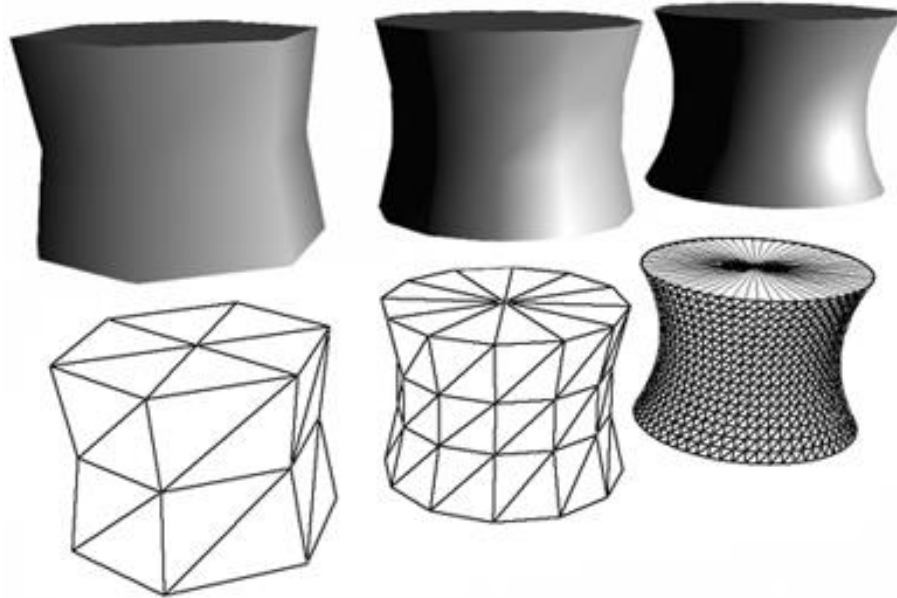


Figure 2.3. As the tessellation increases the accuracy of printed physical model gets close to the CAD model (Blockland forum, Aug 2016)

Before slicing, the CAD model is tessellated, i.e. converted into a mesh of triangles to form the outer shell of the object (as shown in the Figure 2-3) and is stored in the STL format, which is supported by the RP machines. The process of converting the CAD into a mesh of triangles to form the outer surface of the object is called tessellation (Deger et al., 2012). This is an important step as the parameters such as build time, part quality and surface roughness depend on the extent to which the model has been tessellated. The more tessellated a model is, the more is the building time, and more is the dimensional accuracy of the physical model in comparison to the CAD model (Deger et al., 2012). Figure 2-3 (Blockland forum, 2016) shows the effect of tessellation on the part quality. After this stage, the tessellated model is then sliced using a slicing software such as

Stratasys. But before being sliced, the slicing software allows the user to make a choice of the orientation and slice thickness (layer thickness) which greatly impact product building time, material to be used and associated cost, surface quality and the number of additional structures known as support structures.

There are few requirements that the triangles in an STL file must satisfy such as:

1. Each triangle facet must share one and only one edge with the adjacent triangle (Wohlers, 1992).

2. The vertex of any one triangle cannot lie on the edge of any other triangle (Wohlers, 1992). Also, the vertices of the triangle facets should be listed in counter-clockwise direction when the part is looked from outside. The normal vector of each triangle must be pointing outside (Wohlers, 1992). Most of the CAD systems fail to satisfy these requirements and result in defects such as overlapping facets, missing facets, cracks, holes and inaccurate normal (Kai et al., 1997). These mistakes in STL files are the product of the improper part surface orientation. Only a few of these defects such as normal cracks, overlapping facets and inaccurate normal can be corrected automatically by the current day STL file repairing programs. For example, complicated cracks or curves which contain a large number of edges (located in different planes) are difficult for programs to correct. One other disadvantage comes with the file size. As discussed above in reference to Figure 2-3, as the number of triangles increases, the approximation accuracy increases along with the file size. So, one needs to make a compromise between the approximation accuracy needed and the file size. Higher file size also leads to higher

build times. Other disadvantages include lack of topological information and identification of colors used (Barequet et al., 1998).

To overcome these disadvantages, two approaches were developed, of which one is to use other formats such as STEP (Shape Transfer Exchange Protocol), and IGES (Initial Graphics Exchange Specification) (Ma et al., 2001).

2.1.1.2 RP Machine Software

The second stage involved in the CAD-RP interface is the processing of the STL file from the 3D CAD model by the RP machine. RP software packages are used to orient, repair, color, and print the 3D model of the part. Some of the available RP software packages today are CATALYST, ZPRINT, QUICKSLICE etc. These perform the main function of slicing the 3D CAD model of the part into thin slices. The information of these slices is then fed to the printing machine.

The other most important aspect of the RP machine software is to determine the process parameters such as orientation layer thickness, raster fill, density etc. with which the part needs to be built. This aspect is crucial for any RP user as the parameters such as build time, cost and material depend on this selection. The complexity of the RP software varies with the RP process that is being used. Regardless of the RP processes, the basic function of any RP software is to create 2D cross sections by slicing the 3D model with parallel lines creating the contour of each layer (Rodrigo et al., 2017). Slicing can be done with a specific layer thickness or based on adaptive slicing.

The slicing process itself can be divided into four stages as shown in Figure 2-4 (Rodrigo et al., 2017) which can take most of the process planning time. These 2D slices when stacked up together will create the complete part. As the number of 2D slices increases, the build time along with the approximation accuracy increases. This will be further described in detail in section 2.1.2.

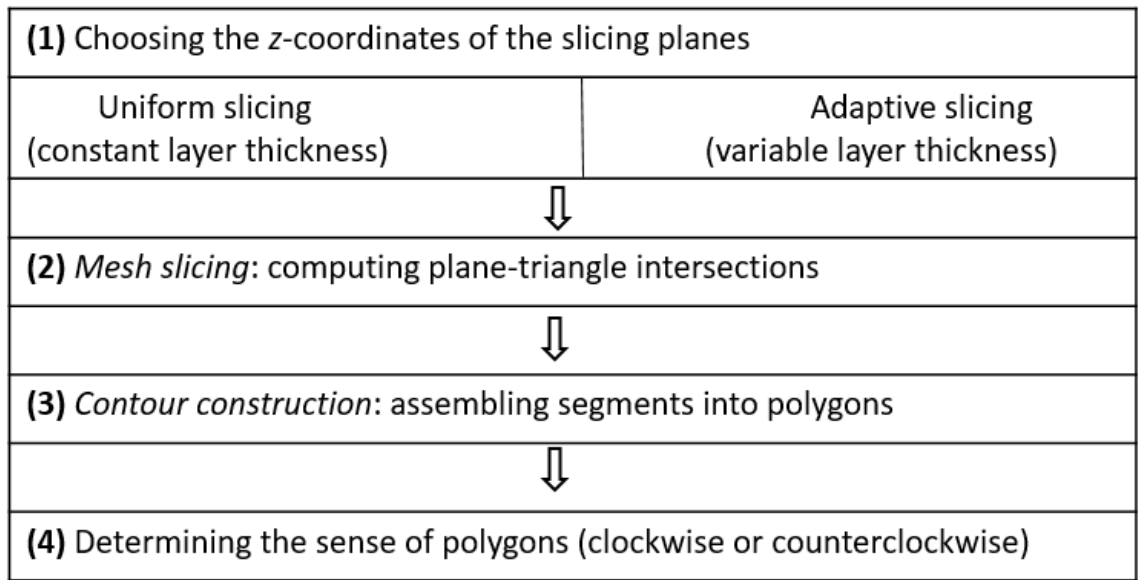


Figure 2.4. Stages involved in Slicing process (adapted from Rodrigo et al., 2017)

The result of the slicing step is the formation of dots or unorganized and unstructured set of line segments in each slice that represent the contour of the part surface. Figure 2-5 shows a detailed diagram of steps in slicing (Rodrigo et al., 2017).

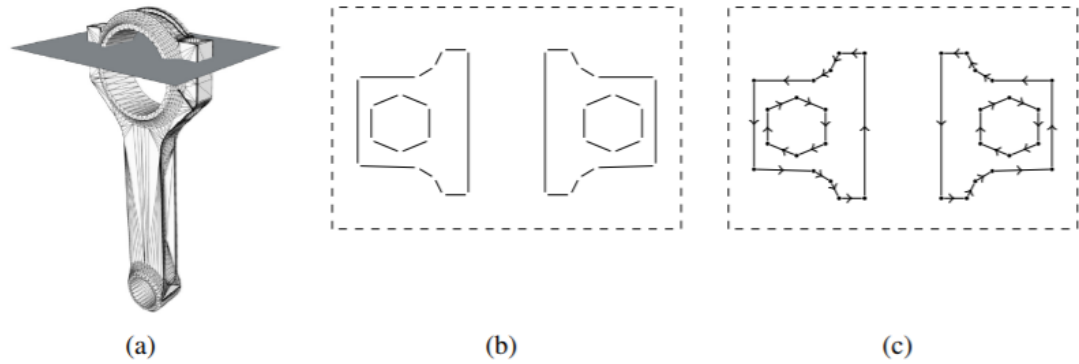


Figure 2.5. a) Slicing of the tessellated model. b) Polygons created in each slice by joining the points created by slicing in step (a). c) Clockwise and counter-clockwise representation of polygons (adopted from Rodrigo et al., 2017)

The unordered line segments form together a set of polygons on each slice which limits the interior region of the part on the particular layer as shown in Figure 2-5 b. Therefore, these segments must be organized into a set of closed polygons. The contour construction step then creates a polygon description of the cross-section. This polygon description process in the contour construction step aids the RP machine in understanding the information of the part's perimeter (to build the part's surface) and the enclosed region in each layer (Rodrigo et al., 2017).

The RP machine then reads the information in the polygons based on whether the polygon is clockwise or counterclockwise. Based on the order of the polygon (clockwise or counter-clockwise) the direction of the normal is decided. The direction of the normal vector decides whether the material should be inside or outside the polygon. This procedure is continued for each slice until the structure or part is built. The software also calculates and generates information regarding the support structures and similar things with the help of algorithms in RP software (Gebhardt, 2013) during the construction of

the part. The generation of supports is not a common step in all RP processes since few of the RP processes such as LOM, SLS, SL do not need support structures, unlike the FDM process. A file with the information regarding the support structure, polygon orders, normal directions etc. is generated and translated into RP machine's processable language. Accordingly, the material is extruded and eventually the part is built.

2.2. Fused Deposition Modelling (FDM)

In this study FDM process has been used but a review of all other additive manufacturing processes has been provided in the Appendix. Developed by Scott Crump in 1988, Fused Deposition Modelling (FDM) is a rapid prototyping technique that is based on surface chemistry, thermal energy and layer manufacturing technology (Christiyan et al., 2016). In FDM, the desired part is initially modeled in CAD and is converted into an STL file (Stereolithography file format), which is checked for defects like, missing facets, dangling edges (Tak et al., 2015). During the build process, filaments of thermoplastic, heated to its melting temperature are extruded layer by layer from a nozzle tip in an extrusion head which moves along the X-Y direction.

The extrusion head consists of two extrusion nozzles of which one is used for extruding build material and the other is used for extruding support material (Pham, 2012). The head, controlled by a motor, lays thin beads of material onto the surface of the platform to form the first layer which solidifies quickly due to the low temperature of the platform (Shofner et al., 2003). The base plate is maintained at a lower temperature to aid the cooling of the material when laid on it.

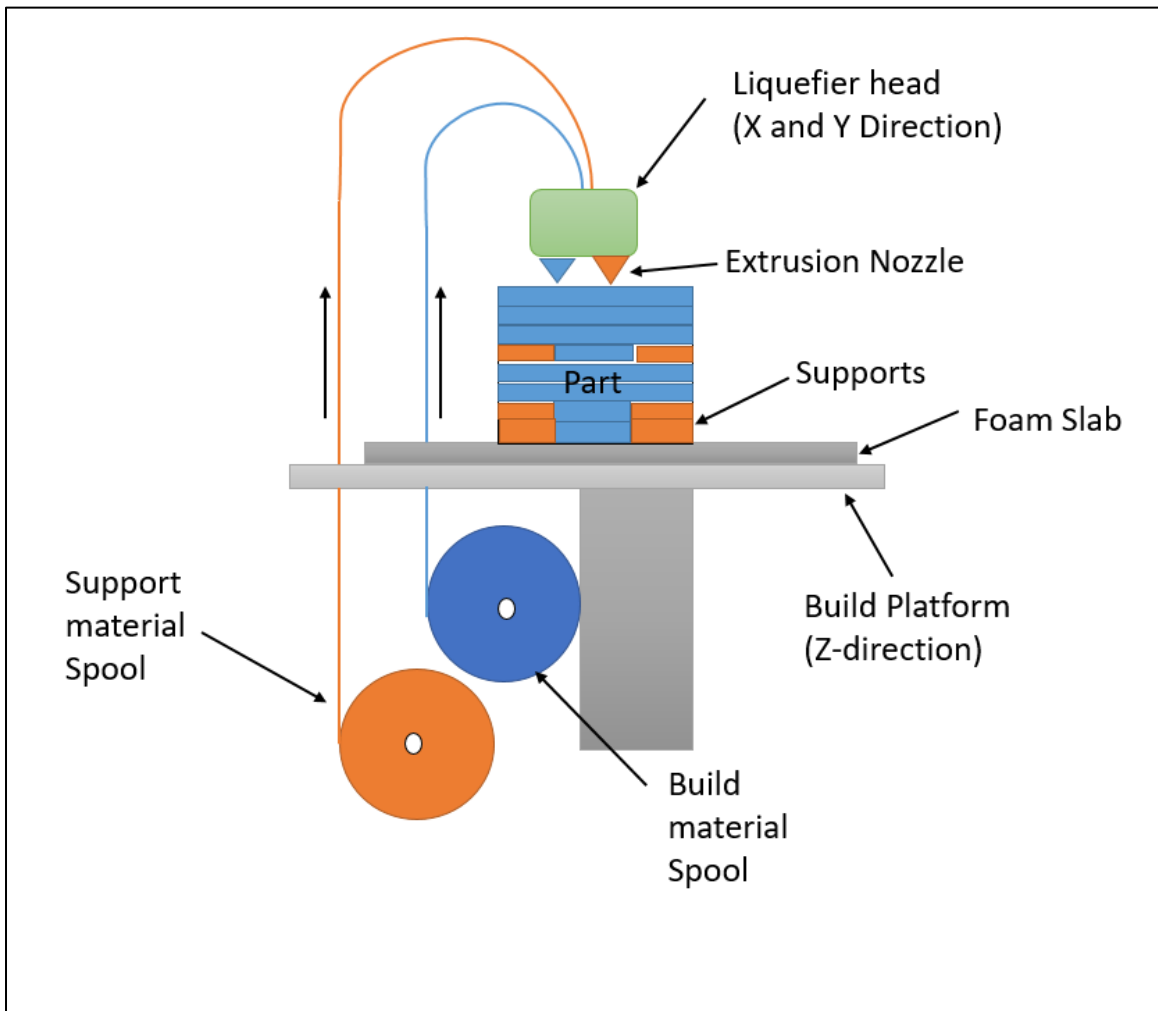


Figure 2.6. Schematic diagram of Fused Deposition Modelling (FDM) method (adapted from Khan Adil, 2016)

The platform then lowers by a specified distance, i.e. for the nozzle to lay the second layer onto it. The extruded material is maintained at 0.5 degrees Celsius above melting temperature so that it gets solidified in about 0.1s and gets cold welded to the adjacent previous layers (Pham et al., 2012). This process continues until the part is built as per the dimensions given in the design input (Russell et al., 1997). Along with the part, build supports are built to support the weaker sections and hanging structures of the part.

A schematic diagram of the FDM process is provided in Figure 2.6 (Khan Adil, 2016).

There are several advantages of FDM process when compared to most other additive manufacturing processes such as lower initial machine purchase costs, ease of use, and reduced risk of material contamination and safety of users (Rahman et al., 2015). These advantages make it a user-friendly method. Other advantages include ease in change the materials, minimal wastage of build material and easy removal of support material (Chua et al., 2010). This study focuses on the use of FDM method to fabricate the parts.

Some of the disadvantages include poor dimensional accuracy, low strength of the parts and higher build time. The build time and cost of an FDM part are influenced by the process parameters used to build the parts. Hence, it is very crucial to make the correct choice of parameters as the part quality including strength, accuracy and surface roughness mainly depend on the process parameters (Sood et al., 2012).

Every RP process has its own advantages and disadvantages, some of which are determined by the quality of the part produced. Wendel et al. (2008) provided a summary of the comparison between various RP processes as shown in Table 2-2.

Table 2.2. Comparison between various RP methods (adapted from Wendel et al., 2008).

	Stereo lithography	Selective laser sintering	Laminated object manufacturing	Fused deposition modelling	3D Printing
Materials	Photopolymers (acrylic and epoxy resins)	Metals, sand, thermoplastics (PA12,PC,PS)	Foils (paper, polymers, metals, ceramics)	Thermoplastics (ABS, PC, ABS-PC blend, PPSU)	Thermoplastics, cement, cast-sand
Part Size(mm)	600×600×500	700×380×550	550×800×500	600×500×600	508×610×406
Accuracy	<0.05 mm	0.05-0.1mm	0.15mm	0.1mm	0.1/600×540 dpi
Curing time	No cooling off or curing time up to 30 min	Depending on geometry and bulk	Depending on geometry	No cooling off or curing time up	No cooling off or curing time up
Commercially available since	1987	1991	1990	1991	1998
Costs (T)	from 130	from 150	from 150	from 50	from 25
Relative sample costs	medium	Medium-high	low-medium	low-medium	low

2.3 FDM Part Quality

Literature on additive technologies shows that much work has been done on various RP methods such as SLS, SLA etc. but the likelihood of improvement in the Fused Deposition Modelling has not been properly addressed. In general, FDM is considered to be a slower process when compared to the other RP techniques such as SLS because of its inherent layer-by-layer method of fabrication. This layer-based fabrication produces parts with anisotropic properties and residual stresses (Ahn et al., 2002) which directly affects the mechanical strength of the parts. Another disadvantage to this layer manufacturing in FDM is the staircase effect. FDM parts are fabricated by stacking the layers upon each other to build the part geometry. This holds true for geometries such as

cubes but for a geometry with curved surfaces and inclined surfaces, the accurate dimensions cannot be achieved. The sliced information for inclined surface will experience a loss of information as the machine prints layers in a two and a half dimensional form. This loss of information results in creating a stair-like appearance on the surfaces. This effect is sometimes known as the Staircase effect. It is minimal in case of perpendicular and horizontal surfaces, but its effect is maximum in inclined or curved surfaces. Figure 2.7 shows the effect of the staircase in RP processes. Decreasing the layer thickness might seem to decrease the effect but it might lead to an increase in build time and cost. Hence an optimal value of layer thickness among the ones used for the study needs to be chosen such that it balances the build time and staircase effect.

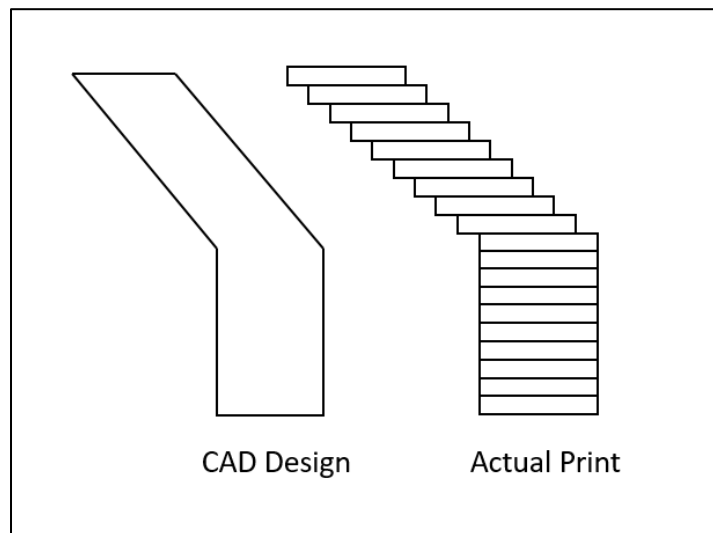


Figure 2.7. Staircase effect observed in inclined surfaces (adapted from 3Dprinterchat.com)

The loss of information due to the staircase effect is one of the reasons for dimensional inaccuracy and surface roughness in FDM parts (Chennakesava et al., 2017).

Several studies focused on improving the dimensional quality of FDM parts. Dyrbus

(2010) investigated the dimensional inaccuracy and surface roughness of parts fabricated using the FDM. The study specifically focused on the impact of parameters on the elements such as linear, angular and curved dimensions. Dao et al. (1999) in his study on shrinkage compensation in FDM parts found the shrinkage error to increase as the feature dimensions increased. From the results obtained it was concluded that FDM has a linear accuracy of about 0.1mm and angular accuracy of 0.4 degrees. Nancharaiah et al. (2010) studied the effect of process parameters such as layer thickness, road width, raster angle etc. on the dimensional accuracy and surface roughness of the FDM fabricated parts. DOE was used to set the experiments and it was found that layer thickness along with road width affected both the surface roughness and dimensional accuracy, whereas raster angle had the least effect. Chennakesava et al. (2017) found orientation to be the main parameter affecting the dimensional accuracy of the parts. It was concluded that accuracy increases with the lower value of orientations and hence parts should be fabricated at lower angles. Various studies have focused on improving the dimensional and surface roughness aspect of FDM part quality. However, the strength aspect of the FDM parts also needs to be focused in order to increase FDM applications in various fields. The process capability of any manufacturing process is determined by the ability of the process to produce parts with good mechanical performance.

The strength of FDM fabricated parts is usually less when compared to that of parts obtained from traditional manufacturing processes. Though a portion of this drawback is due to the principle involved in the manufacturing of the part in the FDM process, a major portion is due to the improper choice of the process parameters. The

print quality of an FDM prototype is greatly influenced by the choice of process parameters used in the part fabrication (Chennakesava et al., 2017). The FDM parameters set at the time of fabricating the part in FDM determine the build cost and time. Therefore, it is very crucial for designers, engineers and developers to understand the effect of process parameters to reduce build cost and increase the part quality (Katti et al., 2017). Moreover, it can be seen from the literature review in section 2.3 that the effect of parameters on the strength of the part varies from material to material. An optimal parameter for one material may not be the same for a different material. Hence, it is important to investigate the link between the properties of materials and their dependence on the process parameters. The following section talks about some of the work done so far in this direction.

2.4 Studies Done So Far

The term “rapid” in RP refers to the manufacturing build time of the parts starting from the design stage to the stage where one needs to push a button that starts the manufacturing of the part. Even though RP techniques offer a plethora of advantages such as minimal human effort and skill, etc., it has its own disadvantages in terms of build part quality. Therefore, it is suggested to understand the drawbacks involved in the individual RP processes for their recommendation in any industrial application. Kim et al. (2008) compared Rapid Prototyping techniques such as SLA, SLS, LOM, and FDM in terms of part quality such as mechanical strength, dimensional accuracy, heat resistance, build time and cost. The study presented a detailed conclusion on the advantages of each individual RP process. It was found that in terms of surface roughness, dimensional accuracy and

part hardness Stereolithography (SL) method was advantageous, whereas for less build time and cost-effective build 3D printing was suggested. Laminated Object manufacturing (LOM) was found to be advantageous in terms of heat resistance and Selective Laser Sintering (SLS) was found to be suitable to build a part with good compressive strength in less time. FDM and LOM were found to produce parts with higher impact strength but only in the build direction.

A significant amount of importance is given to the mechanical strength of the parts fabricated by the RP technologies since the mechanical properties of the fabricated parts are considered to be important indices (Deng et al., 2018) of a manufacturing process. The part quality of the FDM process mainly depends on the process parameters that were present in the machine during the part production. Improper choice of the process parameters in the FDM technique can be a crucial reason for the poor mechanical properties of the fabricated part. Literature shows that the strength of FDM parts could be improved by a proper understanding of the process conditions/parameters and controlling those. Therefore, it is very crucial to understand the influence of FDM process parameters on the part quality (Katti et al., 2017). The progress of the attempts made to improve the build quality of the FDM parts till now has been slow because of FDM's complex nature and conflicting parameters. The following sections show the previous studies done in this direction.

Said et al. (2000) investigated the impact of part orientation on the tensile strength, flexural strength and impact resistance of ABS solid models. It was found that parts printed by laying the layers along the direction of the length exhibited higher

strength over other orientations. It was reported that the anisotropic property in FDM parts is due to the weak interlayer bonding caused due to the volume shrinkage during solidification of the semi-molten filament from the nozzle in the chamber. Similarly, Górski et al. (2015) studied the effect of part orientation by performing the bending and tensile tests on the parts produced in different orientations. Results obtained showed that orientation of the part during manufacturing has a strong impact on the tensile and bending strength of the part. Changing the build orientation varied the strength index of ABS samples. The study also designated supposed ranges of critical orientations where the transition from 'yield point' to 'brittle' happens for different loads and provided a supposed range of orientation for various loads.

Bagsik et al. (2010) investigated the effect of build orientation on the ULTEM 9085 parts that were built using FDM technique. It was seen that building the part from the edge gave the part higher tensile strength when compared to the horizontal and perpendicular directions. It was also observed that the highest compressive strength was obtained while building the part in an upright direction. However, the geometry of the parts was found to be independent of the build orientation. Lee et al. (2007) studied the effect of build orientation on the compressive strength of parts produced by three different additive methods namely FDM, 3D printer and Nano-composite deposition (NCDS). Axially printed FDM parts showed higher compressive strength than the transversely printed FDM parts by almost 11.6%. Whereas, in 3D printing diagonally printed specimens were found to have a much higher compressive strength in comparison to the axially printed specimens. NCDS specimens which were printed axially had 23.6%

higher compressive strength than the transversely printed specimens. Of all the three processes NCDS was the process that was found to be most affected by the build direction. Smith et al. (2013) studied the effect of build orientation on the mechanical strength and modulus of elasticity of polycarbonate samples. It was found that repeatable measurements can be made of the ultimate tensile strength and elastic modulus in FDM printed PLA samples. Schöppner et al. (2011) studied the effect of build direction and toolpath generation on the mechanical properties of Polyetherimide (PEI) parts printed by FDM. It was reported that parts built in horizontal direction had higher yield strength and compressive modulus when compared to the parts that were built in a vertical direction.

Apart from the build orientation of the parts, some of the studies concentrated on individual parameters such as layer thickness, raster angle, raster width etc. Christiyan et al. (2016) in their study performed flexural and tensile tests on ABS + hydrous magnesium silicate composite. The samples were prepared by varying the levels of layer thickness in the FDM machine. Results obtained concluded that parts manufactured with lower layer thickness had the maximum tensile and flexural strength of the material as compared to parts manufactured with other levels of layer thickness. Another study by Ognzan et al. (2014) investigates the effect of layer thickness along with deposition angle and infill percentage on the maximum flexural force in FDM printed polylactic acid (PLA) samples. It was observed that the layer thickness had the maximum effect on the flexural strength followed by the interaction between deposition angle and infill percentage. In yet another study, Wenzheng et al. (2015) studied the effect of layer thickness

accompanied with raster angle on PEEK parts and found that both factors had a similar effect on the compressive and flexural properties. Variations in the deformation of PEEK samples was studied by varying the chamber and nozzle temperature. When compared with ABS material, results displayed that the mechanical properties of PEEK are superior to that of 3D printed ABS.

Khan et al. (2005) performed Taguchi analysis to find the optimal set of process parameters that affect the elastic performance of ABS prototypes. Process parameters such as layer thickness, air gap, etc. were varied to produce the parts and were tested using a catapult at the varied angle of displacements. Air gap was found to be the maximum contributor for lower angles of displacement whereas layer thickness was found to be the maximum contributor for higher angle of catapult displacement. In another study, Motaparti et al. (2016) investigated the effect of air gap along with build orientation and raster angle on the compressive strength of ULTEM 9085 samples. They observed that the interaction between raster angle and build direction affected the compressive strength of the ULTEM samples and air gap had the least effect. It was also found that horizontal built parts had a higher compressive strength in comparison to the vertical built for both solid and sparse specimens. Casavola et al. (2017) studied the effect of raster angle on residual stress built in the part due to rapid heating and cooling of the part. They found parts built with a raster angle of +/- 30 had the higher residual stress and the ones built with +/- 45 had the least residual stress.

While most studies concentrated on individual contribution of process parameters very few focused on the simultaneous effect of parameters. Masood et al. (2010) studied

the effect of process parameters such as air gap, raster width and raster angle on the tensile strength of polycarbonate parts made by FDM. The study also observed the comparison of tensile strength between samples produced by FDM and molded and extruded PC parts. Ahn et al. (2002) studied the influence of air gap, raster width and raster orientation on the mechanical properties of ABS samples. They observed that air gap and raster orientation have a significant effect on the mechanical properties of the part among other parameters. It was also found that built part exhibited anisotropic properties based on the build direction. Few rules for designing parts were put forward based on the experimental results.

Apart from the mechanical strength, the process parameters also have a strong impact on the build time and cost of the product. Yet, very few studies have been done in this direction. Ismail et al. (2014) found that the raster angle and orientation were important process parameters that affected the mechanical properties and production costs of ABS material. Also, samples built with zero raster angle in the horizontal direction produced parts with better mechanical properties and surface roughness with the optimum production time and cost. Rathee et al. (2017) studied the effect of spatial orientation on the build time of FDM parts. Response Surface Methodology (RSM) was used to design the experiments and investigate the effect of orientations. It was found that orientations had a major impact on build time and individual process parameter contribution varied as per the spatial orientation.

Table 2.3 gives the summary of all the literature done so far in terms of the parameters considered, the material used, output parameters and the significant parameters

obtained in the studies. An investigation of the link between the material properties and the FDM parameters would be crucial for industries and users.

Table 2.3. Summary of the literature review done so far on the effect of process parameters on strength of Fused Deposition Modelling parts

Authors	Material	Geometry or standard used for the tests	Machine used and estimated prices*	Process parameters considered	Mechanical Properties considered	Significant process parameters found	Analysis
Wenzheng et al. [2015]	PEEK	and cylinder	U-Print SE 3D printer Dog bone (\$30k)	Layer thickness, Raster angle	Compressive and flexural strength	Layer thickness and deposition orientation	Through graphs obtained from the mechanical tests
Masood et al. [2010]	PLA	ASTM D638	FDM1650 Stratasys (\$120k)	Air gap, raster angle and raster width	Tensile strength	Not applicable	Through graphs obtained from the mechanical tests
Górski et al. [2015]	ABS	Dog bone and cylinder	Dimension BST 1200 (\$60k)	Orientation	Bending and tensile strength	orientation	Through graphs obtained from the mechanical tests
Ahn et al. [2002]	ABS	ASTM D638 and ASTM D695	Stratasys FDM machine (\$60k-\$75k)	air gap, raster width and raster orientation	Tensile and Compressive strength	Raster orientation, air gap	Through graphs obtained from the mechanical tests
Ismail et al. [2014]	ABS	ASTM D638 and ASTM D790	Dimension 3D printer machine (\$70k - \$80k)	Raster angle, orientation	Tensile and flexural strength	Orientation	Through graphs obtained from the mechanical tests

Table 2.3 (continued)


Wenzheng et al. [2015]	PEEK	Dog bone and cylinder	U-Print SE 3D printer (\$30k)	Layer thickness, Raster angle	Compressive and flexural strength	Layer thickness and deposition orientation	Through graphs obtained from the mechanical tests
Masood et al. [2010]	PLA	ASTM D638	FDM1650 Stratasys (\$120k)	Air gap, raster angle and raster width	Tensile strength	Not applicable	Through graphs obtained from the mechanical tests
Gorski et al. [2015]	ABS	Dog bone and cylinder	Dimension BST 1200 (\$60k)	Orientation	Bending and tensile strength	orientation	Through graphs obtained from the mechanical tests
Ahn et al. [2002]	ABS	ASTM D638 and ASTM D695	Stratasys FDM machine (\$60k-\$75k)	air gap, raster width and raster orientation	Tensile and Compressive strength	Raster orientation, air gap	Through graphs obtained from the mechanical tests
Ismail et al. [2014]	ABS	ASTM D638 and ASTM D790	Dimension 3D printer machine (\$70k - \$80k)	Raster angle, orientation	Tensile and flexural strength	Orientation	Through graphs obtained from the mechanical tests
Khan et al., 2005	ABS	Catapult 	FDM 3000 (\$60k)	Layer thickness Air gap, raster width, raster orientation	Angle of displacement	Layer thickness and raster orientation	ANOVA and S/N ratio. P values for various angles of displacements presented

Table 2.3 (continued)

Ognzan et al. [2014]	PLA	ISO 178:2001; prismatic	Makerbot Replicator 2 (\$3k - \$20k)	Layer thickness, Deposition angle, infill density, Orientation	Flexural strength	Layer Thickness, infill density, orientation	layer thickness: $p = 0.00$ Infill angle: $p = 0.208$ Orientation: $p = 0.247$
Motaparti et al. [2016]	ULTEM 9085	ASTM D695	Fortus 400mc (\$185k)	Raster angle and air gap	Compressive strength	Air gap	Raster angle: $p < 0.0001$ Air gap: $p < 0.0816$ Build direction; $p < 0.0001$
Sandeep et al. [2017]	ABS	Cylinder	uPrint modeler (\$30k)	Spatial orientations	Build time	Slice height, air gap, raster angle and width	Response Surface Methodology

ASTM D638: Dog Bone model (tensile tests); ASTM D695: Cylinder model (compression tests).

*All the prices are a rough estimate and have been acquired from internet sources.

2.5 Research Gap, Challenges and Problems

A thorough investigation of the literature shows the following limitations:

- Most of the studies concentrated on one parameter at a time or one material property at a time. In real time fabrication of a part using FDM, several parameters come into play during production. Additionally, the parameters considered in most of the studies seem to be lacking. Hence, it is necessary to study the simultaneous effect of crucial parameters to get a better understanding of the FDM parameters.
- Some of the results obtained in the above studies seem to be inconsistent. For example, Khan et al. (2005) found that smallest layer thickness gave the best performance, while Sood et al. (2010) found that tensile strength of an FDM part first decreased and then increased as layer thickness increased. On the other hand, Ahn et al. (2002) found layer thickness to have less significance on the tensile strength. This disparity in results calls for the need for a thorough investigation of the FDM parameters.
- FDM parameters not only affect the part quality but also greatly affect the build time involved. However, studies found in the literature did not focus on the effects of process parameters on the build time.
- Most of the studies done till now focus on the materials such as ABS, PLA etc. However, from the literature, it is seen that the effect of parameter varies with the material being used. Investigating new materials would aid in overcoming the

material-limitation challenge of the FDM technique. Hence, there is a need for investigating the parameter's effect on potential materials (Mohammed, 2015).

- Not all parameters of the FDM technique have been studied. One such parameter is the printing speed that has not been investigated or used. Hence, a study on investigating the effect parameters such as printing speed on the build quality is crucial.

As discussed earlier, the quality of an FDM product mainly depends on the parameters chosen. The main concerns of any FDM user with respect to the quality are the tensile strength, compressive strength, yield strength, build time, build cost etc. Even though studies have focused on identifying the optimal parameters for improving the quality of the parts, there is still no optimal set of parameters for all types of materials and parts (Mohammed, 2015). Parts manufactured by FDM usually have lower mechanical properties than parts manufactured by traditional manufacturing processes (Mohammed, 2015) and are highly affected by various process parameters. Hence, to improve the part quality, it is very important to understand the relationship between the crucial FDM parameters and the material properties.

A review of the literature shows that the relationships between the process parameters and material properties have not been studied much, particularly for different materials processed by FDM (Mohammed, 2015). Some of the materials that can be liquified by the FDM head are ABS, PC, PLA, nylon-12, elastomer, and wax, among which ABS, PC and PPSF are widely used for FDM applications. In the direction of material properties, most of the studies concentrated on ABS parts. However, very little amount

of studies has been done in the direction of material characterization and process parameters optimization. Hence, considerable work remains to be done for process parameter optimization for other FDM processable materials.

In this study, based on the review of the literature, prominent and conflicting parameters that affect the part quality were chosen. The selected process parameters are the layer thickness, part orientation, and printing speed. This study differs from previous studies in the following ways:

- In this study, the simultaneous effect of crucial parameters such as layer thickness, orientation, and printing speed (identified from the literature) on the mechanical properties have been considered.
- This study takes into account a new FDM process parameter such as printing speed that has not been previously studied.
- Moreover, this study uses a full-factorial analysis, unlike other studies which use Design of Experiments (DOE) to reduce the number of experiments. Using full factorial analysis would minimize the loss of data from experiments.
- The simultaneous effect of FDM process parameters on the build time of the fabricated part is investigated.
- Unlike previous studies which used more typical materials in their experiments, this study uses a new material known as CFR-PEEK. This material has proved its potentiality in various fields as will be discussed in section 3.2.2.

2.6 Review

This chapter talked about the RP technologies as a whole, especially the FDM process and is divided into sections and sub-sections for simplicity and better understanding. Section 2.1 provided an overview of the RP processes, the stages involved in it and their importance. It described the CAD software and RP software that aid in analyzing the mathematical data of a designed CAD model and then transferring to the machine. It talked about the important stages involved in generating the data for the machine. Section 2.2 gives a brief summary of RP processes such as SLA, SLS, 3DP, MJM, and FDM and provided their individual advantages and disadvantages in terms of product quality. Section 2.3 talked about the problems in the FDM method and how they affect the part quality. Section 2.4 dealt with the studies done so far in the direction of investigating the effect of FDM process parameters on the mechanical strength. This section showcased the complexity of the FDM process and the necessity of understanding the process parameters' influence on the product quality. It can be stated that the progress in this particular direction has been slow due to the wide range of conflicting parameters and limitation of materials available for processing in FDM.

The availability of a large number of process parameters in FDM makes it difficult to understand the combined influence of parameters on the fabricated part quality. The wide range of conflicting parameters makes FDM a complex process. However, the build quality of an FDM part mainly depends on the process parameters. Therefore, there is a need to understand the effect of FDM parameters on the part quality. The knowledge of

parameters influences, and their optimization is very crucial to product designers, engineers, and developers for building application specific products in various industries. Though attempts have been made to understand the effect of process parameters on the part quality, the progress in this direction has not been much effective. A major portion of this slow progress is attributed to the inconsistent results obtained in different studies. A review of the literature shows that the results obtained in the studies differ greatly from one another. The parameter effects on build quality seem to be contrasting. The inconsistency in the results obtained, calls for a thorough investigation of the FDM parameters and their effect on build quality. Moreover, a review of the literature shows that further investigation is needed in choosing the right combination of parameters.

Apart from the inconsistency, studies till now have focused only on a few specific materials. Table 2-3 shows the summary of studies done in the direction of the parameter effect and the materials used in the studies. Results obtained from these studies indicate that the effect of the FDM process parameter depends on the material being used i.e. optimal parameters obtained for one material will not be optimal for another material. However, literature till now shows that studies have investigated the parameter effect only on stereotypical materials such as ABS and PLA. Therefore, there is a need to understand and investigate the effect of FDM parameters on new materials.

This study, unlike previous studies, focuses on an emerging material known as CFR-PEEK which has proven to be a potential material in various applications. It aims at investigating the effect of crucial and conflicting process parameters such as layer thickness and orientation on the build quality of the CFR-PEEK parts. Since mechanical

properties are considered to be the important indices of any manufacturing process, the part quality will be determined in terms of mechanical strength. Moreover, this study takes into account the printing speed, as a variable, that affects the part build time - which has not been studied previously. Additionally, this study also aims to establish a functional relationship between the parameters and identify the optimal (among the parameter levels used for this study) set of parameters.

CHAPTER 3

MATERIALS AND METHODS

3.1 Introduction

FDM as an RP technology has significant advantages such as ease of fabricating complex part structures layer by layer, elimination of expensive tooling and having high flexibility (Mueller et al., 2012; Bernard et al., 2002). When compared to the traditional manufacturing processes FDM has several advantages of offering parts in less time and cost (Too et al., 2002). However, the biggest challenges faced by this technology are the quality of the part fabricated and the limited availability of materials for processing, which limits its application in various fields (Kim et al., 2008). This makes it crucial to investigate the link between the material properties and the process parameters which poses a major challenge. From literature it is seen that the performance of any FDM part not only depends solely on the process parameters but also on the material being used. Unlike previous studies that have focused more on typical materials, this study uses a relatively new and a potential material known as CFR-PEEK which has not been studied yet. Exploring this new material would pave a path for CFR-PEEK into the various fields involving medical, aviation and would help industries to produce application-specific parts using FDM methodology.

To withstand the demand of raising competition, new materials have been developed over the past few years. With the increasing advancement in RP techniques

machines have now become capable of printing different materials including metals. However, the limited availability of processing materials still poses a major challenge for the FDM technique. To increase the usage of FDM parts in various fields, new materials need to be developed and examined using the FDM technique.

For a material to be used in FDM, it should have a proper range of melting and solidifying temperature, low viscosity, minimal shrinkage value since the material needs to be extruded in a semi-molten form and cool within minimal time. In the FDM process, the material is maintained at a temperature 5 degrees Celsius below the melting temperature and needs to solidify with 0.1 s after dropping on the plate (Pham et al., 2012). This property of the material helps in improving the build time. Thermoplastics such acrylonitrile butadiene styrene (ABS), polylactic acid (PLA), ABS, polycarbonate (PC) are good fits for these kinds of requirements (Hopkinson et al., 2006) and have been used by researchers for a long time.

In this study, Carbon reinforced – Polyether ether Ketone (CFR-PEEK), a thermoplastic, is being used to fabricate the specimens. This material satisfies all the necessary requirements for being used in an FDM technique and has not been sufficiently investigated. CFR-PEEK, a composite of PEEK, is a highly suitable material for medical applications, particularly in implants because of its capability to overcome the disadvantages of materials (as discussed in section 3.2.1) being currently used such as metals, ceramics, etc. in the medical field. The following sections describe the importance of implants and the suitability of CFR-PEEK as the material for implants.

3.1.1 Disadvantages of materials being used as an implant

Implants are medical devices that are manufactured to replace a missing body part, deliver medications, provide support or enhance the function of the damaged existing part. Implants can basically be used in almost every organ of the body. Some implants are intended to be in the body permanently and few can be removed once they are no longer needed. Few of the wide range applications of the implants are endoprostheses for joint replacement of worn out joints, heart valve prostheses to treat irreparable heart valve defects, stents and cochlear implants (Sternberg, 2009).

Implants remain in direct contact with the tissues of an organism and last with the organism for a longer time. Since most of the implant requirements are related to the material being used, the success of an implant depends on the type of material used for its fabrication (Tappa et al., 2018). Most commonly used orthopedic implant materials are metals, ceramics, polymers, and composites. However, these materials have some notable disadvantages which hinder them from being used as medical implants.

Metallic implants such as stainless steel, tantalum (Ta), cobalt chromium have been widely used in manufacturing medical implants. The mismatch of strength and elastic modulus of metals with bones (as they have higher strength and elastic modulus) can cause stress shielding leading to prosthetic loosening (Rui, et al., 2014). Additionally, longer in vitro presence of metals might cause allergic reactions at the implant location (Rui et al., 2014). Another disadvantage of using metals is that they are opaque to the radio waves and X-ray portion of the electromagnetic spectrum. This property affects the

ability to examine the already implanted medical implants inside the body as they would be opaque to magnetic resonance imaging (MRI).

Apart from metals, ceramics such as calcium phosphate (e.g., hydroxyapatite), glass ceramics and metallic oxides are commonly used for fabrication of implants. Despite their non-toxicity, good compatibility and bioactivity, they are undesirable for load-bearing applications because of their poor mechanical properties which include higher elastic modulus, lower ductility and fracture toughness (Kokubo et al., 2003).

Other materials being widely used in biomedical applications are Polymers (Rui et al., 2014) such as Poly-glycoside (PGA), Poly-hydroxyl-butyrates (PHB) and poly-lactic acid (PLA). However, in vitro, these polymers are too weak and flexible to fulfill the demands of orthopedic applications. The polymers also affect the sterilization process as they absorb undesirable liquids used in sterilizations process and swell (Ramakrishna et al., 2001).

Despite the ongoing development in the field of orthopedics, much attention is required to treat the traumatic injuries, joint diseases and their associated implications (Li et al., 2015). Issues such as mechanical wear, aseptic loosening, infection, instability are some of the reasons for the second replacement of implants (Li et al., 2015).

3.2 Potentiality of CFR-PEEK

PEEK, a semi-crystalline thermoplastic, developed by a group of English scientists (Eschbach, 2000) has proved to be a better substitute to the materials being currently used in orthopedic surgery, spine surgery etc. (Panayotov et al., 2016). Since its commercialization for industrial applications, PEEK has become a crucial high-performance thermoplastic substitute for metal implants in the medical field since 1998 (Skirbutis et al., 2017). Over decades, PEEK and its composites have gained wide-spread attention, because of their compatibility and bone-like properties, especially in traumatic applications, orthopedics and spinal implants (Kurtz et al., 2007).

The use of carbon fiber in the PEEK gives it more advantages. The combination of carbon and PEEK polymer stimulates bone formation and allows sufficient loads to be transmitted (Green et al., 2001). CFR-PEEK has the ability to be readily accepted by the body and to withstand prolonged fatigue strain without breaking down over time (Li et al., 2015). It can be manufactured to closely resemble the modulus of both cortical and cancellous bone densities (Li et al., 2015). Green et al. (2001) have presented a comparison of stiffness between different materials and the stiffness of human femur as shown in Figure 3-1. It can be seen that CFR-PEEK displays similar stiffness as that of a human femur with a proper selection of fiber type and concentration.

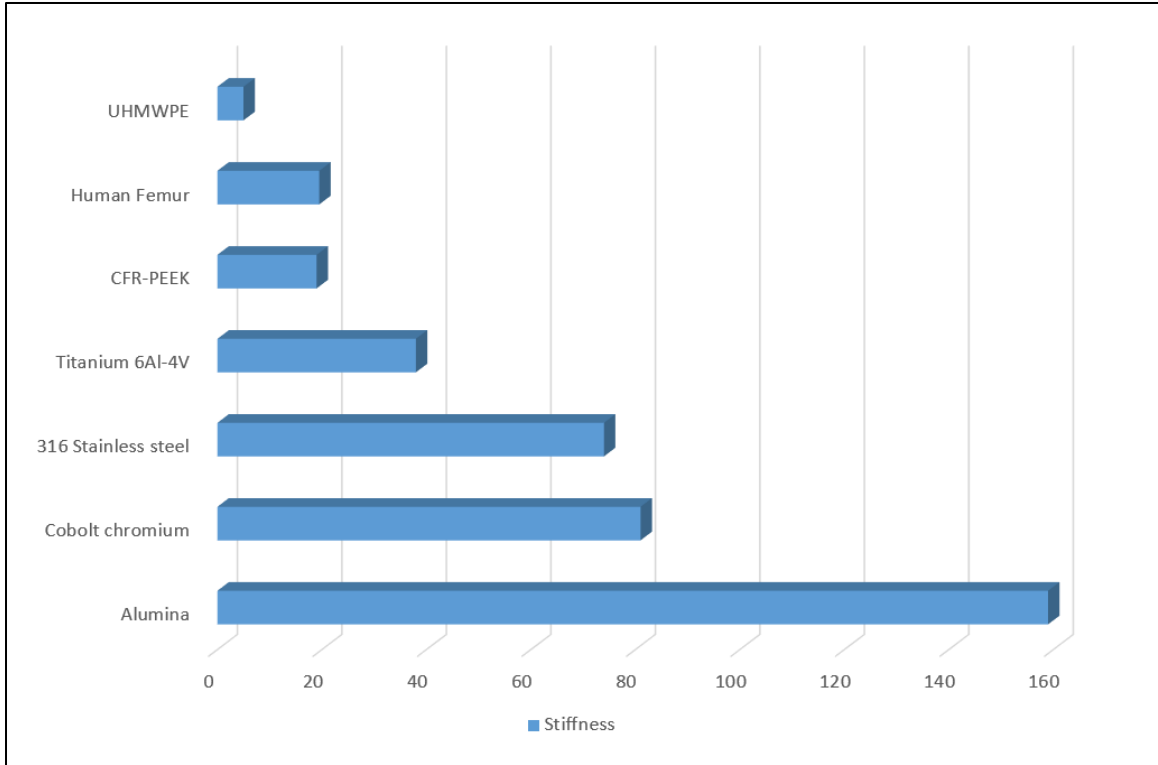


Figure 3.1. Comparison of the stiffness of different materials (adapted from Green et al., 2001)

CFR-PEEK comes in two forms, short fiber CFR-PEEK and long fiber CFR-PEEK. The 'long' fibered CFR-PEEK has fibers running along the entire length of the implant, which makes it anisotropic. This anisotropic property gives an additional advantage of tailoring the implant specific to the patients need. Additionally, the use of CFR-PEEK in implants helps in avoiding potential issues such as stress shielding, prosthetic loosening and bone resorption (the process of being reabsorbed) as commonly seen in metal implants (Li et al., 2015). The chemical structure of CFR-PEEK makes it chemically stable and resistant to high temperature (Li et al., 2015). Its stability against ionizing radiation (such as gamma radiation) makes it capable of regular sterilization cycles (Godara et al., 2007).

Furthermore, CFR-PEEK being a non-metallic material is compatible with both computed tomography and magnetic resonance imaging technologies (Li et al., 2015). Additionally, its X-ray transparency helps in visualizing the fusion. In comparison to other materials, CFR-PEEK has several advantages of compatibility, better manufacturability, reasonable cost and availability. Comparatively, PEEK and its composites seem to perform better than other alternatives in terms of implant quality (Garcia et al., 2017).

In the last two decades, research has been done to explore the suitability of CFR-PEEK in bio-medical applications. Li et al. (2015) investigated the research work done from 1950 to 2014 to assess the outcomes of CFR-PEEK in orthopedic implants. Twenty-three articles, from various regions of the world, were selected mostly concentrating on the wear and tear, mechanical strength, durability, and biocompatibility. From Li's investigation, it was concluded that CFR-PEEK performs well in comparison to other materials currently being used. In another study for analyzing the effectiveness of a CFR-PEEK used as a volar plate for distal radius fracture, none of the forty cases analyzed were found to have hardware breakage or loss of fracture reduction (<http://www.pitt.edu/~jwd30/trends.html>).

Though CFR-PEEK has been proved to be the best alternative to materials being used as an implant, very few studies have concentrated on fabricating CFR-PEEK using the Fused Deposition Modelling technique. Shen et al. (2017) developed CAD models of patient customized structures and 3D printed them with ABS using the FDM method. Computer tomography (CT) files were captured for the anatomic features of conjoined twins and were fabricated by the Fused Deposition Modelling. The five organs, of which

few are groups of the skeleton, spinal nerve and kidney, were fabricated by using the FDM technology. The printed parts closely resembled the CT files of the organs and had an overall deviation of less than 2 mm. Huang et al. (2017) did a case study on printing CFR-PEEK implants. A patient-specific fistula stent for the treatment of ECF was developed using the FDM process. These stents made of TPU (thermoplastic urethane) are implanted in a 45-year-old man who had suffered pelvic deformation and abdominal problems. The implants were reported to be highly effective in treating the fistula.

Studies done in relation to the FDM fabrication of CFR-PEEK implants show the manufacturing potential of the FDM process in medical applications. Bogdan et al. (2013) presented the FDM method as an alternative or an effective way for fabricating components of PEEK and its composites. The studies done until now have used a particular set of FDM parameters to produce the desired parts. However, the effect of the FDM process parameters on the CFR-PEEK part has not been studied. This crucial gap calls for the need to investigate the effect of FDM process parameters on product quality of CFR-PEEK material. Understanding the influence of the parameters would be crucial for fabricating and tailoring patient-specific implants in various medical applications. Not only in medical applications, the knowledge of parameter influences and the relationship between them would also be helpful for product developers and engineers in producing application specific products in various industries.

3.3 Methodology

3.3.1 Specimen Fabrication

In this study, Fused Deposition modeling (FDM) being the most popular and fastest growing three-dimensional printing method to produce large size implants (Deng, 2018) was used for the fabrication of CFR-PEEK specimens. Specimens for the experiments were fabricated using the OPTIMA FDM printer. This FDM printer was developed by APIUM Additive technologies. Figure 3-2 shows the image of the APIUM P220 series FDM printer (APIUM catalog, Accessed on 02/20/2019). The machine is capable of using a wide range of materials including high-performance polymers such as PEEK, CFR-PEEK, extreme temperature plastics such as PBI, PI, TPI, high temperature and engineering plastics among others. The Table 3-1 below gives a description of the machine's technical specifications. The CFR-PEEK material used in this study is an Apium CFR-PEEK. It was shipped from Apium in spools of 500 grams each with each thread diameter of 1.75mm. The material is a PEEK composite with 30% carbon fiber filled.

Table 3.1. Specifications of the machine (Optima PEEK printer)

Technical Specifications	
x/y Resolution	Product Resolution: 0.5 mm Machine Resolution: 0.0125 mm
z Resolution	Product: 0.1 mm, Machine: 0.05mm
Reproducibility	0.1mm
Nozzle Diameter	0.4 mm
Print Bed	Heated up to 160° C
Build Plate Size	220 x 175 mm or 155 x 155 mm
Machine Size	850 x 685 x 675 mm

**Figure 3.2. APIUM P220 Series FDM printer (Adopted from www.imakr.com)**

The 3D models for the part specimen were generated using the SolidWorks modeling software as shown in Figure 3-3a and then were converted into the STL format as shown in Figure 3-3b. The dimensions of the models conform to the ASTM standard

which will be discussed in section 3.3.2. The STL file was then transferred to the slicing software, where we get the options to set the experimental plan. At this point, the user can select the orientation, layer thickness, and printing speed as required. Once the parameters are set as required, the software then slices the model and generates the information of the required tool path. The information is then used by the printer to move the nozzle to print the part.

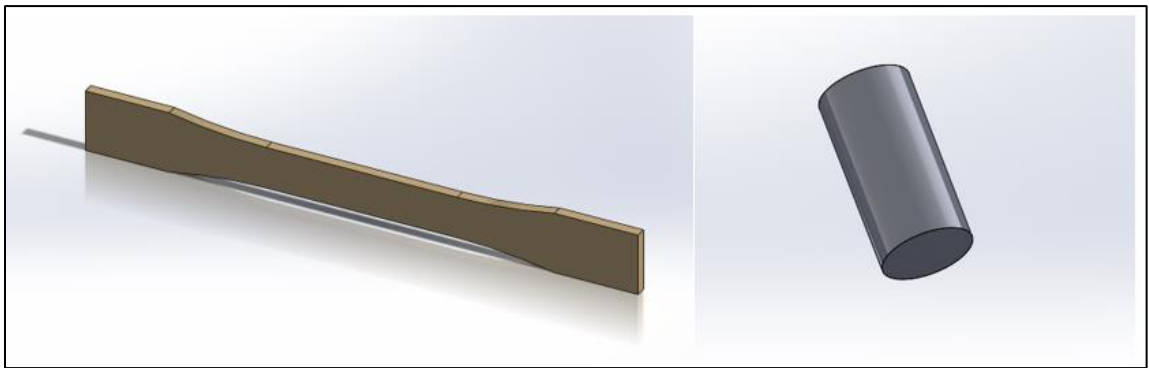


Figure 3.3 a. SolidWorks model of the parts

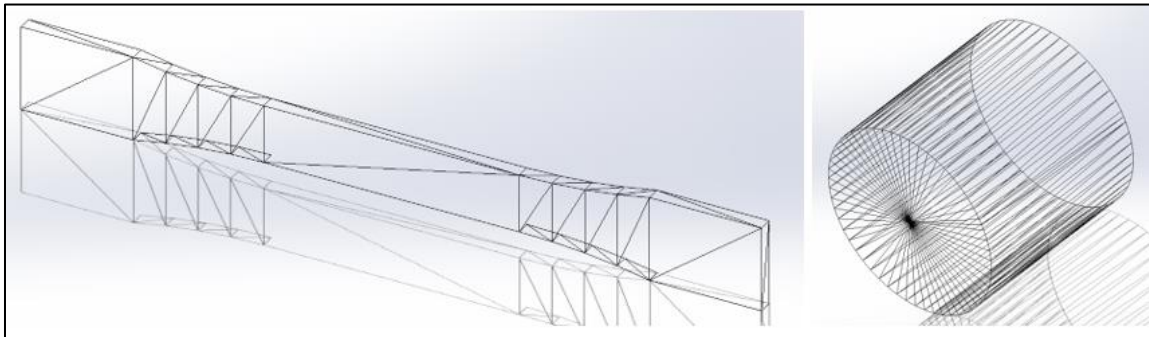


Figure 3.3 b. STL files of the SolidWorks model

The material, CFR-PEEK, was loaded onto the machine in form of a spool. Particular pair of wheels are used for holding and advancing the material from the spool to the machine. The material is heated above its solidification temperature and then extruded onto the build platform using the nozzles. The FDM machine uses two nozzles, which work

alternatively, one for depositing the build material and other for depositing the support material. For each layer, the contour is first laid to form the boundary and then the interior portion is filled as raster filling. The raster filling for each consecutive layer varies by ninety degrees to obtain adequate interlayer bonding between the layers. The extrusion head moves in X-Y direction whereas the bed moves in the Z direction. Figure 3-4 gives the schematic diagram of the working of an FDM printer (Sood, 2011).

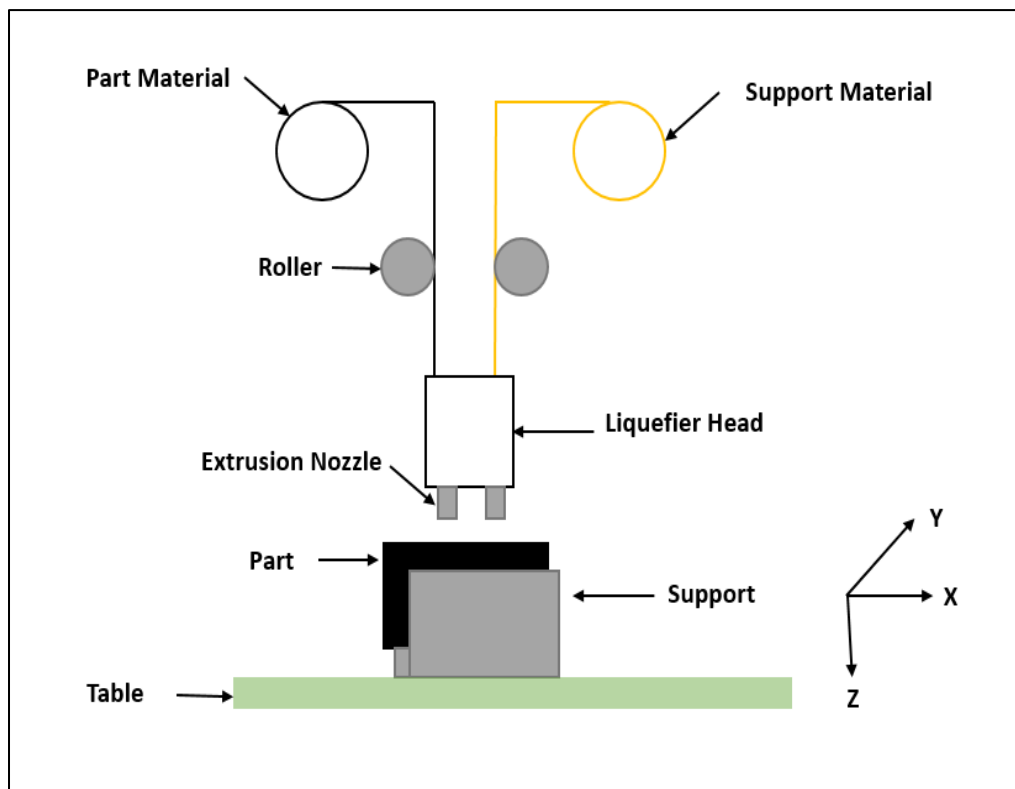


Figure 3.4. Schematic diagram showing the working of an FDM printer (adapted from Sood, 2011)

3.3.2 Test Requirements and Specifications

3.3.2.1 Tensile test

The specimens for the tensile test were designed with specifications conforming to ASTM D638-10 standard method of testing for tensile properties of plastics. ASTM D638 is the internationally accepted strength specification and is used for obtaining the tensile strength of the plastic materials (Standard Test Method for Tensile Properties of Plastics, 2018). The data from the tensile test is used for quality characterization, quality control and purposes of research and development (ASTM D638).

The measurements of the sample as per the standard are as follows. The specimen has an overall length of 63.5 mm, a depth of 3.40 mm, a narrow width of 9.53 mm, and a radius fillet of 12.7 mm (ASTM D638). Figure 3-6 shows the shape and dimensions of the test specimen for tensile tests. The tests were performed using the universal tensile material testing system with a crosshead speed of 5mm/min.

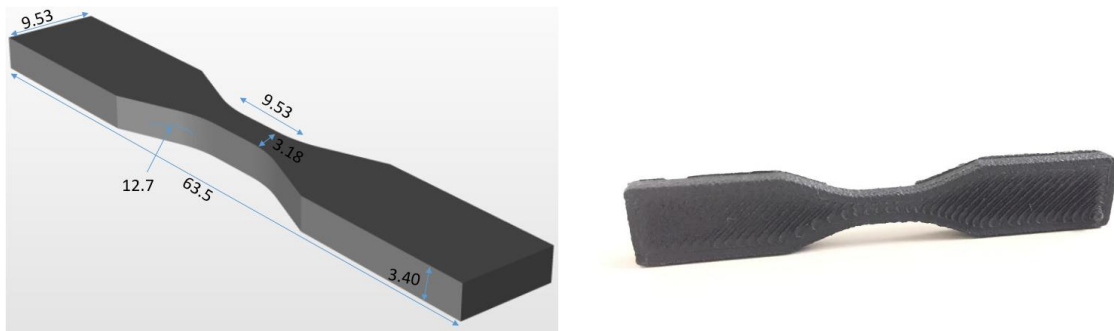


Figure 3.5. Tensile test specimen and dimensions

3.3.2.2 Compressive test

The specimens for the compressive test were designed with specifications conforming to ASTM 695 standard method of testing compressive properties of Plastics. ASTM D695 is the internationally accepted strength specification and is used for obtaining compressive strength of the plastic materials (Standard Test Method for Compressive Properties of Plastics, 2018). This test provides a standard method of acquiring data for research and development, quality control and confirmation of specifications (Standard Test Method for Compressive Properties of Plastics, 2018).

The specimen used was as per ASTM D695 which is a rectangular bar. Figure 3-6 shows the shape and dimensions of the test specimen for compressive tests. The tests were performed using the universal material testing system with crosshead speed of 1.3mm/min and load range of 50KN.



Figure 3.6 a. Compressive test specimen

Along with the compressive specimen, a fixture was designed to hold the compression specimen in place. This helps in avoiding buckling phenomenon and gives pure compression result.

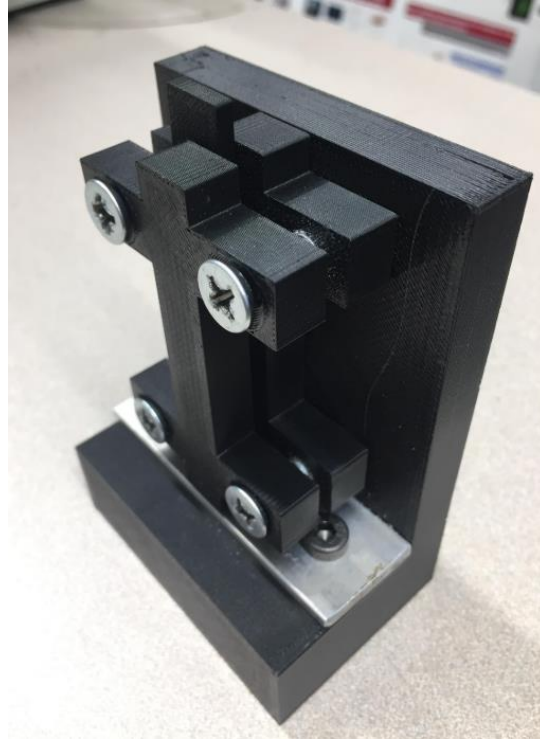


Fig 3.6 b. Fixture fabricated for performing compression test.

3.3.2.3 Number of Specimens

The number of isotropic specimens for each of the ASTM standards (i.e., ASTM D638 and D695) is five. In this study, three specimens were considered for both the standards considering the cost of CFR-PEEK and the budget of the thesis. However, literature shows investigators using three specimens instead of five specimens and obtaining a similar result. Therefore, three specimen samples are fabricated for each experiment, i.e., three specimens for the tensile testing and three specimens for the compressive testing.

3.3.2.4 Speed of testing

The speed of testing for the tension test was done at a constant speed of 5mm/min (Standard Test Method for Tensile Properties of Plastics, 2018) relative to the motion of the test fixtures. The compression tests were done at a constant speed of 1.3mm/min (Standard Test Method for Compressive Properties of Rigid Plastics, 2018) relative to the motion of the test fixtures.

3.3.2.5 Test Requirements

To understand the performance of any material, the widely accepted and common mechanical tests are the tensile and compressive tests (Swallowe, 1999). Evaluating the mechanical behavior under the tensile and compressive conditions provides the necessary material property data critical for the component design and performance assessment (Materials Evaluation and Engineering Inc., 2018). Hence in this study, the mechanical properties were evaluated using tensile and compressive tests. The machine used for the mechanical tests is called the Universal Test Machine, commonly known as UTM. The machine used in this study is the 800 series UTM machine. Figure 3-7 shows the image of the UTM.



Figure 3.7. 800 series UTM fatigue test machine (Adopted from www.testresources.net)

The tensile and compressive test machines comprise of screw driven beams, which are used to hold the parts and can be moved as per the operator's desired speed (Swallowe, 1999). Using a pair of grips, a load cell is staged on the beam. A sample is then mounted between the fixed base plate and the load cell. During the test, as the beam moves, the load cell records the force on the sample. The strain is measured using an extensometer. The next section talks about the test sample standards and the procedure of testing.

The specimens were first designed in SolidWorks as per ASTM D638 standard (for tensile test) and ASTM D695 standard (for compression test), and then transferred as an STL file to the printer. The models were then printed using the OPTIMA PEEK printer having a nozzle diameter of 0.4 mm. In the process of printing the samples, three parameters namely layer thickness, orientation and printing speed were varied at different levels. All the three process parameters were chosen based on their significance found in the literature review. The following section talks about the rationale for selecting the parameters.

3.4 Selection of Process Parameters

3.4.1 Layer thickness

Layer Thickness is defined as the measure of the layer height. It can also be stated in terms of thickness as the thickness of the deposited filament layer. Figure 3-8 shows the schematic diagram of layer thickness in an FDM environment (Zureks, 2008).

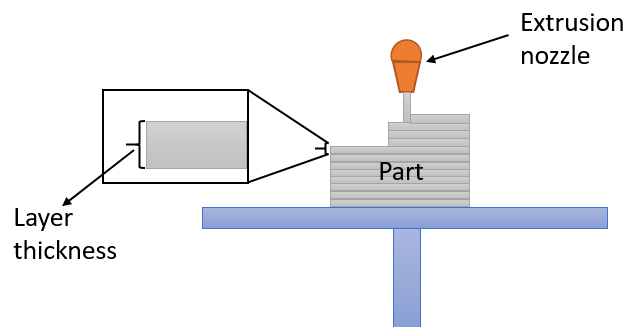


Figure 3.8. Layer Thickness

Layer height, as an FDM parameter, has been the most controversial one in terms of the results obtained in various studies. The outcome of one study in terms of layer thickness effect straightly contradicts with the outcomes of a similar study. For example, Khan et al. (2005) found that the smallest layer thickness was always included in the optimal parameter set which gave the best performance, while Sood et al. (2010) found that tensile strength of an FDM part first decreased and then increased as layer thickness increased. In yet another study, Tymrak et al. (2014) stated that the tensile strength was highest when the value of layer thickness was low. On the other hand, Ahn et al. (2002) found layer thickness to have less significance on the tensile strength. Furthermore, a peek into the literature review shows that layer thickness has a significant impact on the mechanical properties.

Given the contrasting results found in studies and its significant effect on the mechanical properties, the effect of layer thickness on material quality is still uncertain. Hence, there is a need to investigate this process parameter to understand its effect on CFR-PEEK's material properties. In this study, the levels chosen for layer thickness are 0.2mm and 0.3mm. In general, layer thickness values are fixed for a particular machine and are set based on the print resolution. Different studies used different levels of layer thickness values based on the machine. Tymrak et al. (2014) and Wu et al. (2016) used 0.3mm, and 0.4 mm of layer thickness in their study whereas Rahman et al. (2015) used 0.25 mm. Ognzan et al. (2014) used 0.2 mm and 0.3mm of layer thickness in their research, whereas Rankouhi et al. (2016) used 0.2 mm and 0.4 mm. The growing levels of layer thickness values chosen in this study would help in understanding the effect of

increasing or decreasing the thickness values on the mechanical strength of the CFR-PEEK parts.

3.4.2 Orientation

Orientation can be described as an angular difference between the planes determining the direction of manufactured object (Górski et al., 2015). Figure 3-9 shows a dog bone structure varied in different orientations along X, Y, and Z directions.

Build orientation is found to have a major impact on the mechanical properties particularly on the tensile and compressive strengths (Wenzheng et al., 2015). Smith et al. 2013, in their study found orientation to be the major contributor in effecting the tensile strength of the PLA parts. In yet another study, tensile and compressive strengths of ULTEM 9085 printed in different orientations were found to vary remarkably (Schöppner et al., 2011). Build-orientation also has a crucial impact on the part quality, geometrical accuracy, manufacturing cost and overall build time (Ullu et al., 2015). In a study by Dani et al. (2013), the orientation of FDM-manufactured rods was varied from zero to ninety degrees and its effect on the build cost was studied. It was found that variations in the orientation angle caused a significant variation in the build time, amount of build material and finally the cost involved in the fabrication. Raut et al. (2014) studied the effect of orientation on ABS materials and found that part built at zero degrees was associated with minimum cost and had good tensile

strength. In this study, orientation has been chosen as the second parameter of study because of its significant effect on part quality and build factors.

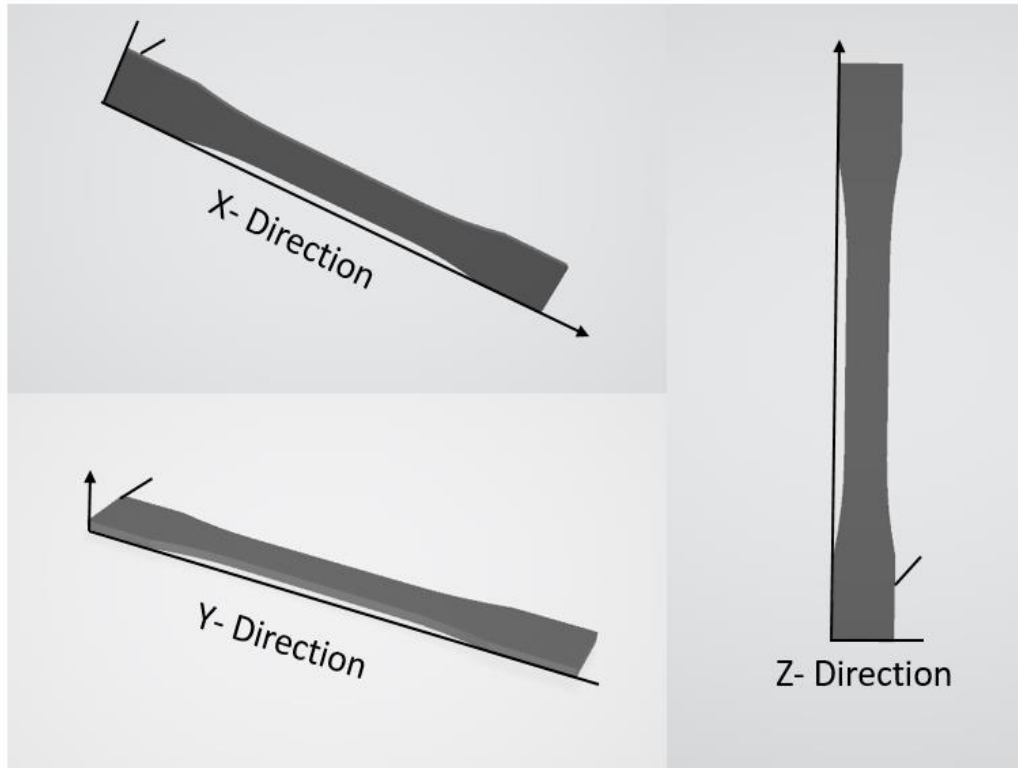


Figure 3.9. Orientation of the Dog bone structure in X, Y, and Z direction

In this study, two levels of orientations are chosen – zero degrees and ninety degrees. Based on the part geometry these are the two common orientations that would use least support material and take less time. Also, from a detailed study of the literature review, it can be deduced that maximum deviation in the mechanical properties is found at these two levels. Rahman et al. 2015 printed PEEK parts at zero and ninety-degrees orientation. It was observed that the mechanical properties of samples generated with zero orientation greatly varied with that of samples fabricated at ninety. The tensile

strength of samples generated at zero degrees was 11.6 % higher than that of the samples fabricated at ninety. Ognzan et al. (2014) studied the effect of orientation on parts built with a deposition angle of zero and sixty. It was found that mechanical properties, build time and cost varied significantly with the build orientation. Samples fabricated at zero degrees had the highest tensile strength and were associated with minimum cost. Whereas samples built at sixty degrees' orientation had the least modulus of elasticity.

3.4.3 Printing speed

Printing speed is defined as the speed at which the beads or the layer is laid from the printer's nozzle. The printing speed greatly impacts the build time of the parts (Ebubekir, 2017). It is essential for a user to understand the effect of printing speed on the build quality of the part. With the growing demand for faster production in today's world (LaSelle, 2018), it is crucial to have a knowledge of the effect of printing speed on part quality, especially the mechanical properties (3Dmatter, 2018). Attoye et al. (2018) investigated the effect of printing speed on two materials – ABS and PLA and found that printing speed had a significant effect on the part quality and build time. However, printing speed has not been studied much so far and thus has been considered as one of the parameters in this study.

Printing speeds are usually recommended based on the machine type and resolution. However, it is important to understand the effect of printing speed on the part quality since the speed of building the part directly affects the build time and part strength (Attoye et al.,2018). The APIUM printer used in this study has three printing speeds

including 1000mm/min, 1200mm/min and 1400mm/min. Table 3.2 shows the parameters and levels used for printing the samples.

The goal of the study is to identify the effect of these factors or parameters on the part strength. Research so far has focused on identifying the effect of single parameter or factors on the output responses. Studying a factor or a set of factors is a common approach usually used in engineering investigation. However, this kind of approach has several drawbacks such as conclusions are not being clear, a large number of experiments to be conducted, factor interactions that cannot be investigated etc. These challenges can be overcome by using a Design of experiments (DOE). DOE is a branch of statistics (ASQ, 2018) which helps in effectively planning, organizing and performing the experiments and improves the productivity of the experiments conducted. This method uses statistics and enables the user to understand the simultaneous effect of every single factor in experiments, which consists of a large number of input parameters or factors that control the outcomes or process (Jeff et al., 2002). One drawback of DOE is – the number of experiments increases drastically as the number of factors increase. Due to this drawback, most of the studies use Taguchi analysis to reduce the number of experiments and associated cost. However, using this analysis leads to loss of information from the eliminated set of experiments. Hence, to avoid this kind of information loss, this study uses the full factorial design of experiments. A full factorial study helps in investigating all the possible combinations without losing vital information from any combination.

Table 3.2. Values of varying process parameters

Parameter	Symbol	Unit	Level 1	Level 2	Level 3
Layer height	L	mm	0.2	0.3	-
Orientation	O	mm	0	90	-
Printing speed	P	mm/min	1000	1200	1400

Table 3-3 shows the different combinations possible with three parameters varied at different levels. Samples were printed as per the combinations mentioned in Table 3-3. Three samples are printed for every combination. For the tensile testing of the specimens, three samples are printed for each of the eighteen combinations, for a total of 54 samples. Similarly, three samples are printed for each of the eighteen combinations for the compressive test. Table 3-3 shows all the different combinations and the number of experiments.

Representations in the table:

L1: Layer thickness of 0.2mm

L2: Layer Thickness of 0.3mm

O1: Orientation of 0 degrees

O2: Orientation of 90 degrees

P1: Printing speed of 1000mm/min

P2: Printing speed of 1200 mm/min

P3: Printing speed of 1400 mm/min

Table 3.3. Possible combinations using all the three parameters

Experiment Number	Factors		
	Layer Thickness	Orientation	Printing Speed
1	L1	O1	P1
2	L1	O1	P2
3	L1	O1	P3
4	L2	O1	P1
5	L2	O1	P2
6	L2	O1	P3
7	L1	O2	P1
8	L1	O2	P2
9	L1	O2	P3
10	L2	O2	P1
11	L2	O2	P2
12	L2	O2	P3

To avoid the noise factor, the order in which the experiments are being conducted was randomized. Randomization is a technique which is used for balancing the effect of uncontrollable conditions or parameters that can impact the results of an experiment. Randomizing the experiments reduces the chance of results getting biased by experimental conditions and materials. It also helps in estimating the inherent variations in the materials and conditions and helps in making valid inferences based on the experimental data (Minitab 18, 2/19/2019).

Table 3.4 a. The order in which the experiments were conducted for tensile test

Tensile Test (Dog Bone Structure)					
Standard Order	Run Order	Layer Thickness	Orientation	Printing Speed	Combination
21	1	0.3	0	1400	L2O1P3
20	2	0.3	0	1200	L2O1P2
35	3	0.3	90	1200	L2O2P2
15	4	0.2	0	1400	L1O1P3
3	5	0.2	0	1400	L1O1P3
24	6	0.3	90	1400	L2O2P3
4	7	0.2	90	1000	L1O2P1
16	8	0.2	90	1000	L1O2P1
28	9	0.2	90	1000	L1O2P1
17	10	0.2	90	1200	L1O2P2
10	11	0.3	90	1000	L2O2P1
23	12	0.3	90	1200	L2O2P2
25	13	0.2	0	1000	L1O1P1
31	14	0.3	0	1000	L2O1P1
33	15	0.3	0	1400	L2O1P3
7	16	0.3	0	1000	L2O1P1
19	17	0.3	0	1000	L2O1P1
8	18	0.3	0	1200	L2O1P2
14	19	0.2	0	1200	L1O1P2
27	20	0.2	0	1400	L1O1P3
32	21	0.3	0	1200	L2O1P2
5	22	0.2	90	1200	L1O2P2
18	23	0.2	90	1400	L1O2P3
11	24	0.3	90	1200	L2O2P2
22	25	0.3	90	1000	L2O2P1
2	26	0.2	0	1200	L1O1P2
34	27	0.3	90	1000	L2O2P1
9	28	0.3	0	1400	L2O1P3
12	29	0.3	90	1400	L2O2P3
1	30	0.2	0	1000	L1O1P1
13	31	0.2	0	1000	L1O1P1
36	32	0.3	90	1400	L2O2P3
6	33	0.2	90	1400	L1O2P3
30	34	0.2	90	1400	L1O2P3
29	35	0.2	90	1200	L1O2P2
26	36	0.2	0	1200	L1O1P2

The Table 3-4 a show the order in which the experiments were conducted for the tensile test with respect to the parameter levels and their representation.

Table 3.4b. The order in which the compressive tests are being performed.

Compression Test (Cylinder Structure)					
Standard Order	Run Order	Layer Thickness	Orientation	Printing Speed	Combination
14	1	0.2	0	1200	L1O1P2
24	2	0.3	90	1400	L2O2P3
22	3	0.3	90	1000	L2O2P1
21	4	0.3	0	1400	L2O1P3
19	5	0.3	0	1000	L2O1P1
13	6	0.2	0	1000	L1O1P1
17	7	0.2	90	1200	L1O2P2
20	8	0.3	0	1200	L2O1P2
23	9	0.3	90	1200	L2O2P2
16	10	0.2	90	1000	L1O2P1
15	11	0.2	0	1400	L1O1P3
18	12	0.2	90	1400	L1O2P3
10	13	0.3	90	1000	L2O2P1
1	14	0.2	0	1000	L1O1P1
3	15	0.2	0	1400	L1O1P3
9	16	0.3	0	1400	L2O1P3
4	17	0.2	90	1000	L1O2P1
12	18	0.3	90	1400	L2O2P3
7	19	0.3	0	1000	L2O1P1
6	20	0.2	90	1400	L1O2P3
8	21	0.3	0	1200	L2O1P2
11	22	0.3	90	1200	L2O2P2
2	23	0.2	0	1200	L1O1P2
5	24	0.2	90	1200	L1O2P2
29	25	0.2	90	1200	L1O2P2
36	26	0.3	90	1400	L2O2P3
27	27	0.2	0	1400	L1O1P3
26	28	0.2	0	1200	L1O1P2
32	29	0.3	0	1200	L2O1P2
28	30	0.2	90	1000	L1O2P1
35	31	0.3	90	1200	L2O2P2
31	32	0.3	0	1000	L2O1P1
33	33	0.3	0	1400	L2O1P3
30	34	0.2	90	1400	L1O2P3
25	35	0.2	0	1000	L1O1P1
34	36	0.3	90	1000	L2O2P1

Table 3.4b shows the order in which the experiments were conducted for the compressive test. All the experiments were conducted as per the run order mentioned in Tables 3.4a and 3.4b to avoid any noise in the experiments.

CHAPTER 4

RESULTS AND DISCUSSION

In this study, a full factorial analysis is done. This analysis helps in preventing the loss of some critical information that may occur in other designs such as Taguchi designs.

4.1 Tensile Specimen

Tensile strength of the material was determined by experimenting with samples made from a nozzle diameter of 0.2 mm. All the values obtained were in the 95% confidence interval. The results obtained for all the 12 combinations are as shown in table 4.1.

It was also found that the data obtained was 89.42% accurate. This indicates that the tensile strength for CFR-PEEK can be defined by or varied by these three parameters with a probability of 89.42%. This result strengthens the statement provided earlier which points to the use of layer thickness, orientation and printing speed as the three important parameters.

Table 4.1. Combinations and the obtained tensile strengths in Mpa

Combinations	L	O	P	Tensile strength (Mpa)
L1O1P1	0.2	0	1000	118.3130474
L1O1P1	0.2	0	1000	124.2934933
L1O1P1	0.2	0	1000	132.1743418
L1O1P2	0.2	0	1200	116.4885455
L1O1P2	0.2	0	1200	105.0313954
L1O1P2	0.2	0	1200	114.3066402
L1O1P3	0.2	0	1400	115.1562892
L1O1P3	0.2	0	1400	113.3334884
L1O1P3	0.2	0	1400	116.97909
L1O2P1	0.2	90	1000	94.65581975
L1O2P1	0.2	90	1000	99.61700367
L1O2P1	0.2	90	1000	95.99622611
L1O2P2	0.2	90	1200	99.52509473
L1O2P2	0.2	90	1200	92.33174522
L1O2P2	0.2	90	1200	91.44651188
L1O2P3	0.2	90	1400	91.09525261
L1O2P3	0.2	90	1400	89.34843642
L1O2P3	0.2	90	1400	96.45362449
L2O1P1	0.3	0	1000	90.19289718
L2O1P1	0.3	0	1000	89.74420274
L2O1P1	0.3	0	1000	90.74697098
L2O1P2	0.3	0	1200	81.84883166
L2O1P2	0.3	0	1200	88.35211691
L2O1P2	0.3	0	1200	71.65862342
L2O1P3	0.3	0	1400	78.70230645
L2O1P3	0.3	0	1400	83.56194014
L2O1P3	0.3	0	1400	81.83687119
L2O2P1	0.3	90	1000	63.59329411
L2O2P1	0.3	90	1000	70.65750048
L2O2P1	0.3	90	1000	61.37944258
L2O2P2	0.3	90	1200	66.9523254
L2O2P2	0.3	90	1200	66.64966771
L2O2P2	0.3	90	1200	79.53205441
L2O2P3	0.3	90	1400	70.22772741
L2O2P3	0.3	90	1400	69.73546423
L2O2P3	0.3	90	1400	73.34611214

Figure 4.1 shows the variation of the tensile strength using the stress-strain graphs obtained for combination in MPA values along with the parameter values.

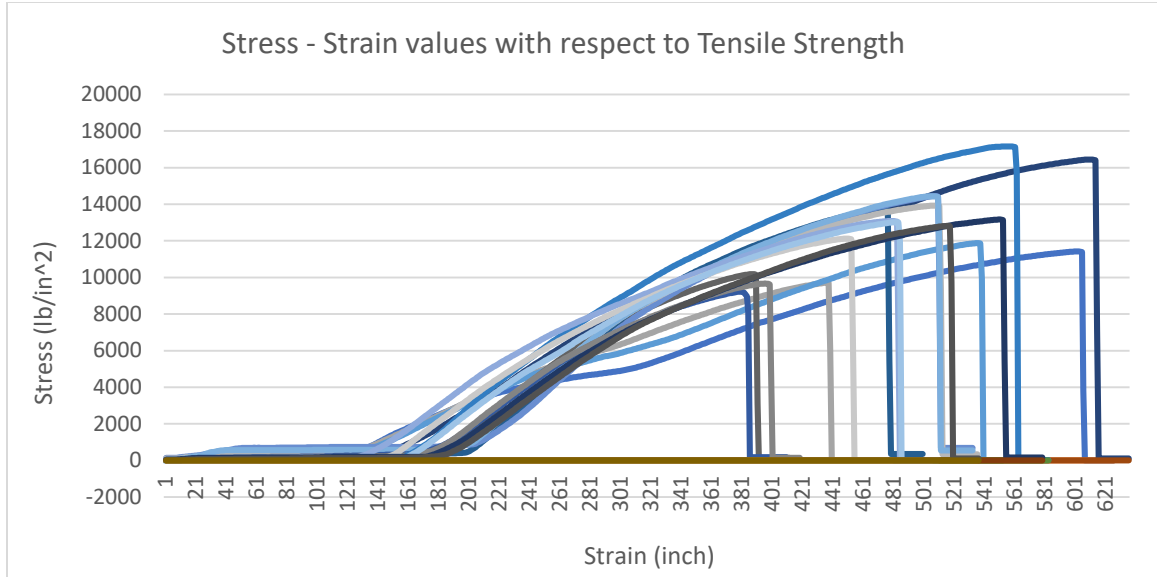


Figure: 4.1 Stress-strain graphs obtained for various combinations of tensile strength

4.1.1 ANOVA Analysis

The ANOVA analysis was performed on the using MINITAB 18 software to identify the effect of individual factors on the tensile strength. Interactions among the parameters was only taken into consideration for the analysis. The results obtained are as shown in table 4.1.1.

Table 4.1.1 is a snip from MINITAB results section. In the source column L stands for layer thickness, O for Orientation and P for printing speed. L*O is for interaction between layer thickness and orientation, L*P is interaction between layer thickness and printing speed, and O*P is for interaction between orientation and printing speed. L*O*P is the interaction between all the three parameters.

Table 4.1.1 Analysis of variance table for tensile test results

Analysis of Variance					
Source	DF	Adj SS	Adj MS	F-Value	P-Value
L	1	7738.9	7738.95	323.49	0
O	1	3214.5	3214.47	134.37	0
P	2	165.8	82.91	3.47	0.048
L*O	1	140.2	140.71	5.86	0.023
L*P	2	65	32.48	1.36	0.276
O*P	2	280.2	140.08	5.86	0.008
L*O*P	2	33.4	16.71	0.7	0.507
Error	24	574.2	23.92		
Total	35	12212.1			

In the figure, the p-value (probability value) shows the significance of the effect of parameters on the output which is tensile strength in this case. Any p-value less than 0.05 is considered to be significant. From the p-value column in table 4.1.1 it is seen that all parameters and interactions except for L*P and L*O*P have p-values less than 0.05. This shows that all the three parameters (layer thickness, orientation and printing speed) have significant effects on tensile strength of CFR-PEEK. The main effects plot was found based on the 'Larger is better' property in MINITAB. This particular option is chosen with an interest to look at the effect of parameters levels to obtain the highest tensile strength. The Figure 4.1.2 shows the main effect plot for all the individual parameters.

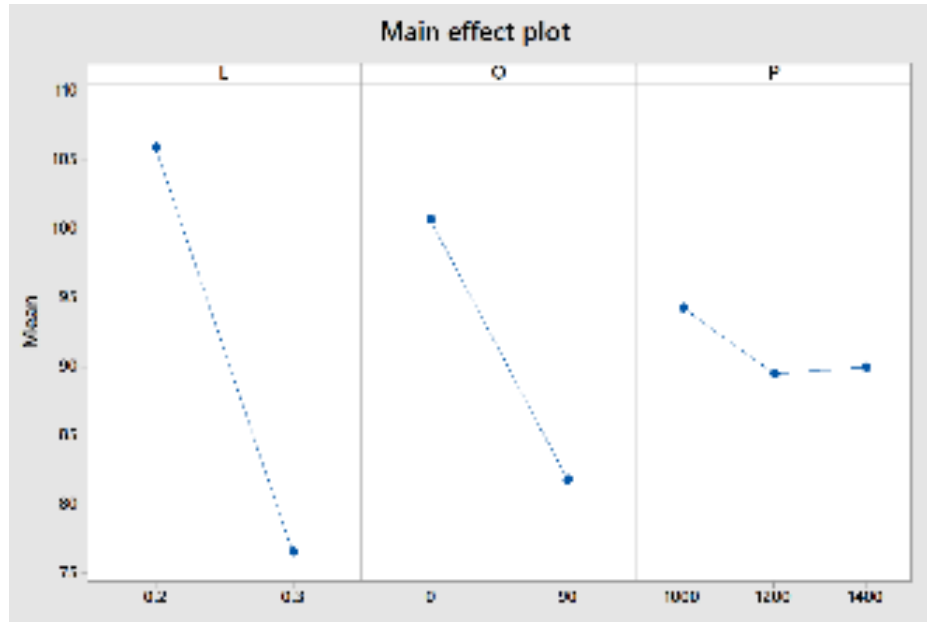


Figure 4.1.2. Tensile: Main effects plot

The p-values also suggest that there are interactions between layer thickness and orientation and between orientation and printing speed. These interactions seem to have significant effects (based on p-values) on the tensile strength of CFR-PEEK material. An interaction occurs when effect of one parameter depends on the effect of the other parameter and it means that parameters are not independent. Interactions mean that the results from the main effects cannot be relied upon completely. However, to understand interactions is to look at a special graph known as the interactions plot shown in Figure 4.1.3. For example, without looking at the interactions plot we cannot determine from main effects plot that 0-degree orientation has the highest tensile strength.

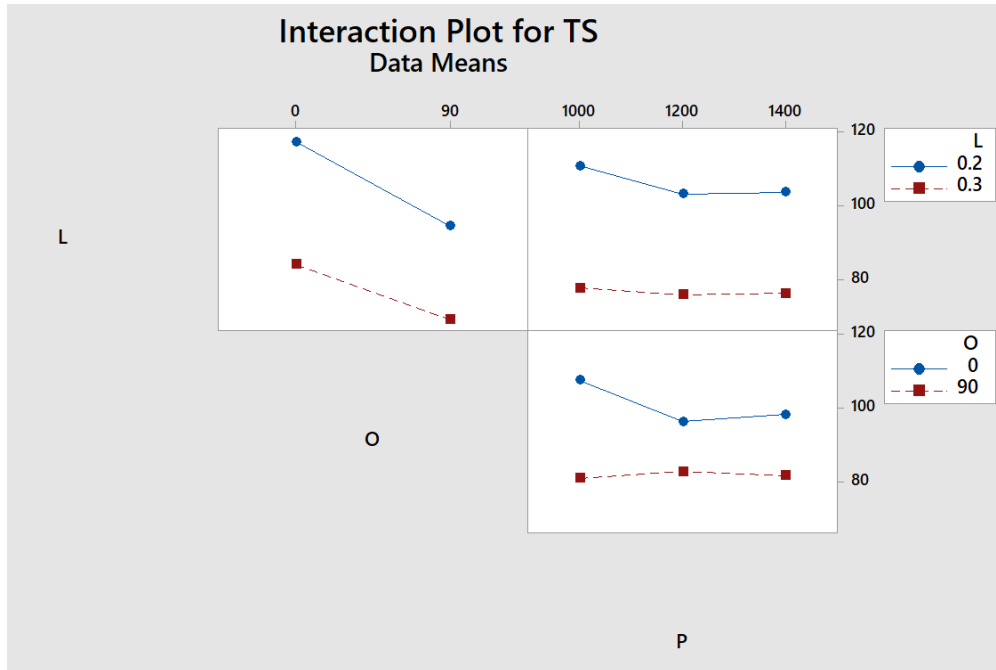


Figure 4.1.3. Interactions plot for tensile strength

The Interactions plot graph shows the values of independent variables on X -axis and dependent variables on Y - axis. Parallel lines in the interaction plot indicate that there is no interaction between the parameters whereas lines with different slopes indicate that an interaction might be present. Lines in the L-O graph have converging slopes which will cross each other at some point towards the right. The crossing of lines in L-O graph states that there is a significant interaction between layer thickness and orientation as indicated by the p-value. To understand the importance of interactions plot we will consider the effect of orientation on the tensile strength. From the main effects plot we can see that 0 degrees orientation leads to higher tensile strength whereas 90 degrees orientation leads to lower tensile strength. However, we cannot conclude the statement without considering the interactions plot since there is a significant interaction between both the parameters. From the first graph in Figure 4.1.3, it can be seen that the

point (0.2,0 degrees) is at higher tensile strength than the point (0.2,90 degrees) which in turn is at higher tensile strength than the point (0.3,0 degrees) which is again higher than (0.3,90 degrees).

The result obtained from main effects plot is in fact true given the levels of parameters chosen in the study. However, if we extend the lines in the L-O graph along the path, at some given levels of orientation (X, Y) with associated tensile strength of A, B, C on the y axis, the graph would look like this. Now, the result from main effects plot would not hold true. In this case, the effect of orientation cannot be based completely on the main effect plot results as orientation depends on the layer thickness chosen. A (0.3, X) and a (0.2, Y) would give a higher tensile strength than a (0.2, X) and (0.3, Y). Therefore, both orientation of X and orientation of Y give higher tensile strength. Graph in Figure 4.1.4 was created to explain the importance of interaction plots.

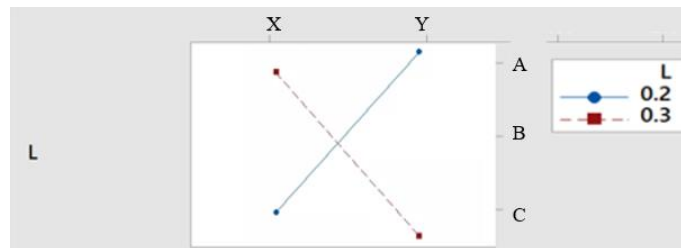


Figure 4.1.4. Interaction plot figure created to understand the interactions

However, from the results obtained in this study, the main effect plots for layer thickness, orientation and printing speed display the same result as the interactions plot.

As can be deduced from Figures 4.1.2 and 4.1.3, layer thickness of 0.2 mm has a better tensile strength than 0.3 mm of layer thickness. Hence, it can be said that a lower layer thickness produces CFR-PEEK parts of higher strength. The decrease in tensile

strength with increasing layer thickness can be attributed to the fact that for a sample with lower layer thickness, layers are closely stacked upon each other creating a higher inter-layer bonding among them when compared to parts with higher layer thickness. One other reason for this result can be due to the presence of micro voids between layers in layer by layer method techniques which act as stress risers (Shubham et al., 2016). Smaller layer thickness has smaller voids whereas higher layer thickness has larger micro voids leading to lesser bonding which ultimately leads to lower tensile strength.

Similarly, Orientation of 0 degrees produces higher tensile strength than an orientation of 90 degrees as shown in Figures 4.1.2 and 4.1.3. Hence, fabricating parts with a 90 degree orientation will lead to weaker tensile strength than parts fabricated horizontally. The reason for this result is from the fact that at 90 degrees the stacked layers in the part are perpendicular to the force applied and thus can be easily pulled apart. Whereas when printed at zero degree angle the layers stacked in the part are parallel to the tensile force and hence have higher strength (Figure 4.1.5).

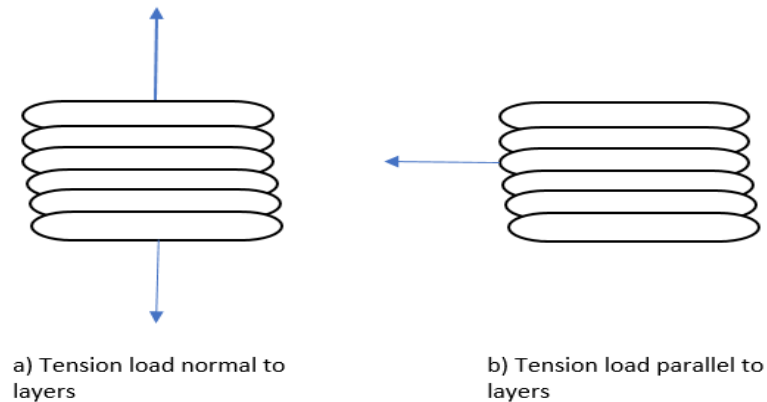


Figure 4.1.5. Effect of tension load (tensile strength) on the layers of the part stacked (adapted from 3D hubs).

Printing speed, however, seems to have a different type of effect on tensile strength. As seen from Figures 4.1.2 and 4.1.3, 1000mm/min speed seems to produce CFR-PEEK parts with higher tensile strength than the other speeds. However, in the figure, 1200mm/min speed seems to produce a slightly lower tensile strength than 1400 mm/min to speed. This result can be linked to the fact that at higher speeds there is minimal time for a section of layer to bond with the adjacent section which results in micro-voids and hence lower strength.

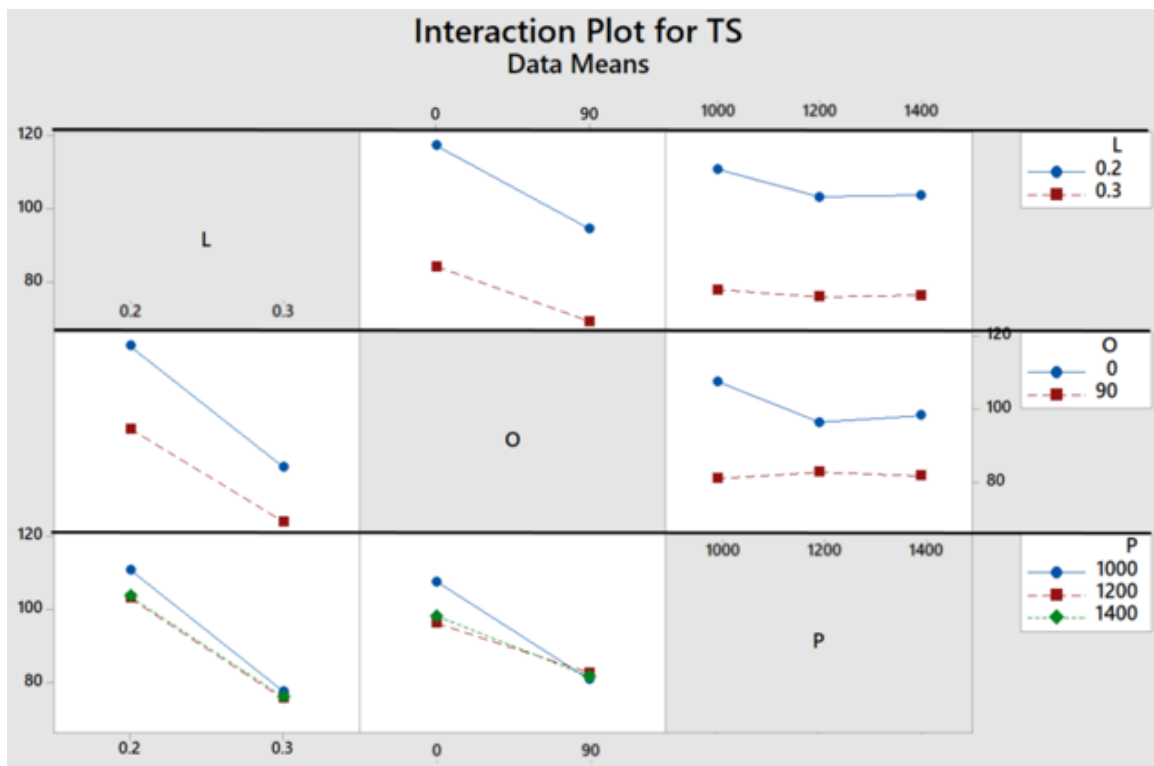


Figure 4.1.6. Full set of interaction plots for tensile strength

The full set of interaction plots helps in comparing the effect of any two-parameter combination on the tensile strength of CFR-PEEK conveniently when compared to the

interaction plot in Figure 4.1.3. For example, the top-right graph in Figure 4.1.6 shows the effect of layer thickness and printing speed on the tensile strength. Using this graph, we can see that a layer thickness of 0.2mm and a printing speed of 1000 mm/min (0.2, 1000) is essential for a higher tensile strength. Similarly, using the bottom-left graph, we can conclude that a layer thickness of 0.2mm and printing speed of 1000 mm/min (0.2,1000) is better than layer thickness of 0.2mm and 1200 mm/min (0.2,1200). Plotting the points (mm, mm/min) in the bottom-left graph in mathematical equation in terms of tensile strength we can say that:

$$(0.2,1000) > (0.2,1200) = (0.2,1400) > (0.3,1000) > (0.3,1200) = (0.3,1400)$$

The full plot matrix gives an overall picture of the effect of two individual parameters on the tensile strength.

The process parameters of FDM seem to highly affect the tensile strength of CFR-PEEK. The combination L1O1P1 seems to be the combination with the highest tensile strength and the combination L2O2P3 seems to have the least tensile strength. The whiskers box plot below in Figure 4.1.7 shows the variation of tensile strength between all the combinations.

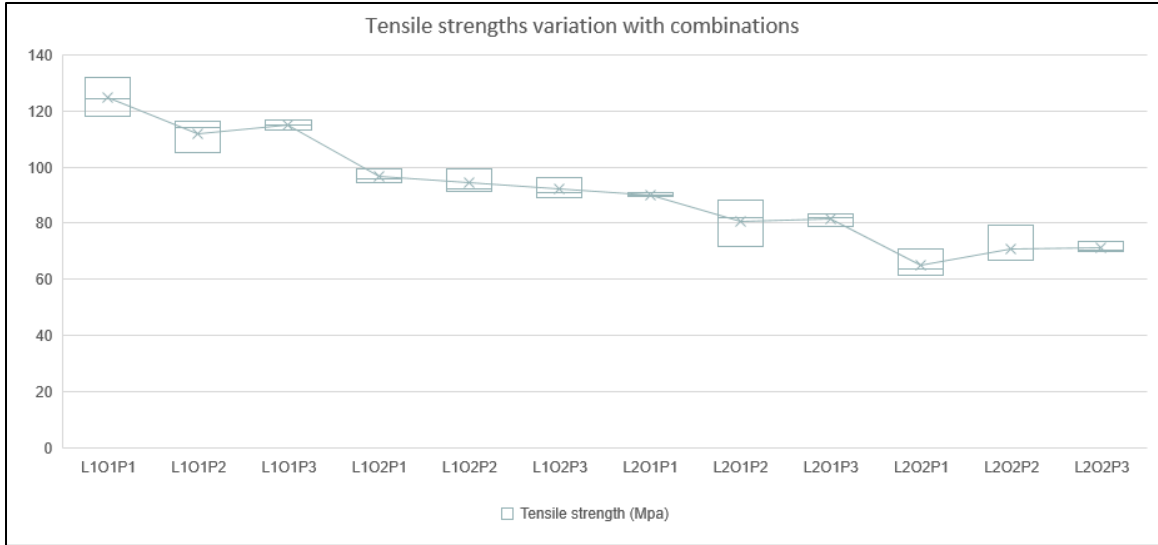


Figure 4.1.7. Variations in tensile strengths of parts printed with various combinations of process parameters

Regression equation obtained for tensile strength is

Tensile strength = 209.1 -40.8(O) -13.9(P) -46.8(L) + 7.9(L*O) + 5 (O*P) with an R square value of 93.37%.

4.1.2 Contour plots for tensile strength

Contour plots also known as level plots are used to view three-dimensional plots on a two-dimensional surface (statisticshowto.com). Using the MINITAB software contour plots for tensile strength with respect to layer thickness, printing speed and orientation are reviewed. The following figures show the contour plots obtained.

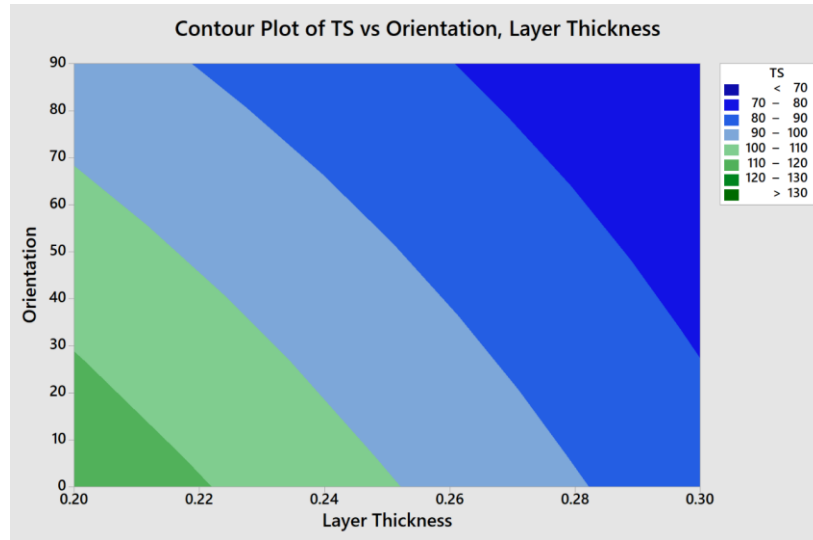


Figure 4.1.8. Contour Plot: Tensile strength vs Orientation, Layer thickness

Using the contour plots, it is easy to understand the tensile strength that could be obtained with under specific parameters or any parameters between those. For example, in this given study we have two levels: 0.2mm and 0.3mm. However, using the below contour plots one can look at other levels of layer thickness such as 0.22 or 0.28, and correspondingly, printing speed such as 1100 or 1300 mm/min.

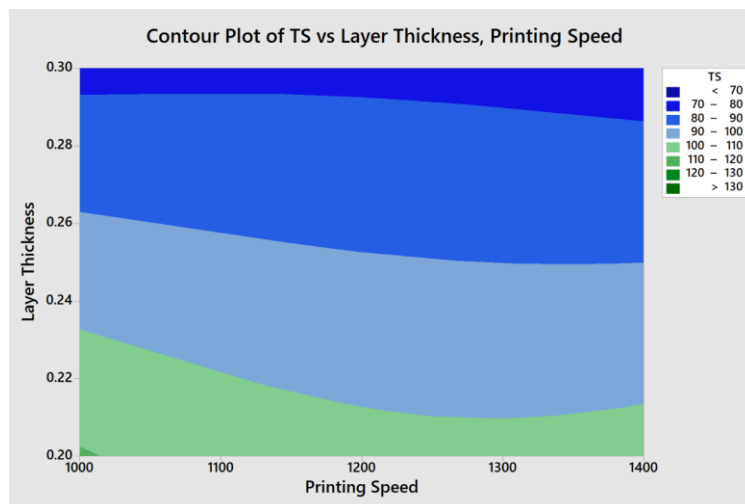


Figure 4.1.9. Tensile strength vs Layer thickness, Printing speed

From the below figure, a printing speed of 1000 mm/min and an orientation of 20 degrees has a tensile strength range of 110 – 120 MPa. The same printing speed of 1000 mm/min and an orientation of 50 degrees has a tensile strength range of 90 – 100 MPa whereas an orientation of 80 degrees has a tensile strength range of 80 MPa and below. Another fact that can be deduced from the below figure is that with a printing speed of 110 mm/min and above, it is not possible to obtain a tensile strength of more than 100 MPa.

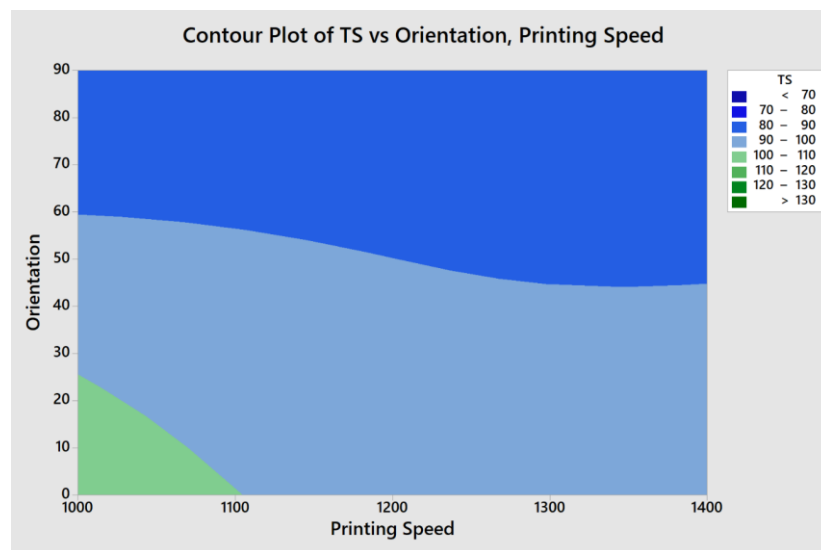


Figure 4.1.10. Tensile strength vs Orientation, Printing speed

4.1.3 Surface Plots

Surface plots are three-dimensional graphs that are used to depict the relationship among a fixed variable which is dependent and two more independent variables (netdna-ssl.com). Surface plots are created for tensile strengths with respect to Printing speed, Orientation and Layer thickness. The following figures show the surface plots:

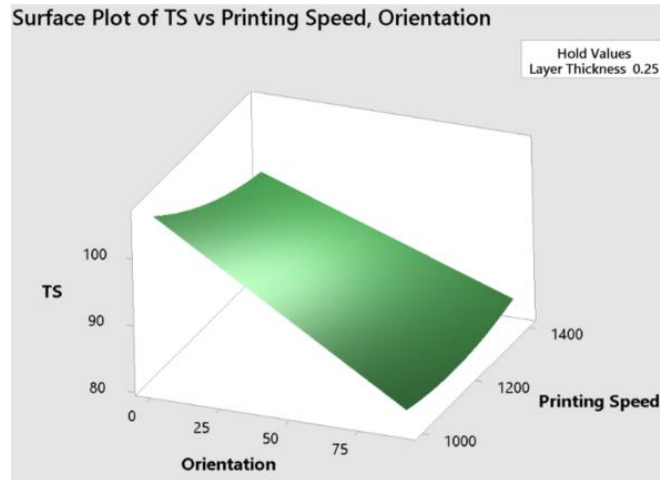


Figure 4.1.11. Surface Plot: Tensile strength vs Orientation, Printing speed

Figures 4.1.11 to 4.1.13 give a similar idea of results obtained from ANOVA analysis in a 3D plane. The planes show the effect of two parameters on tensile strength while keeping an average value of the third parameter.

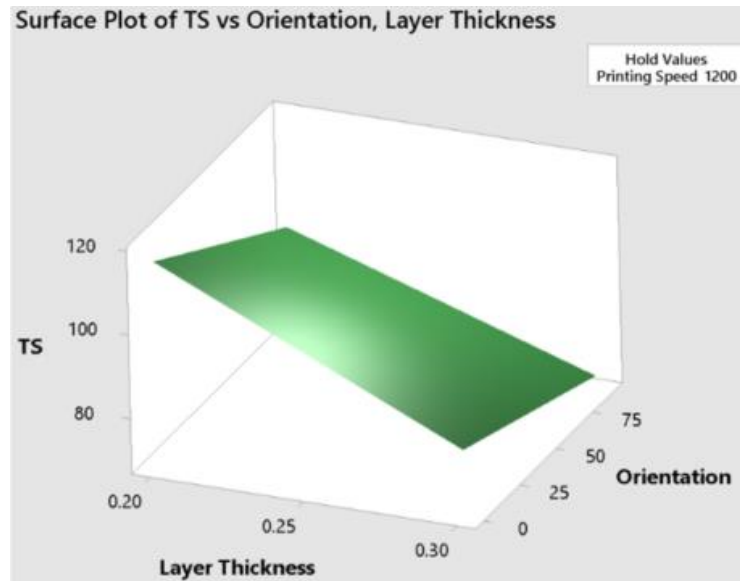


Figure 4.1.12. Surface plot: Tensile strength vs Orientation, Layer thickness

Figure 4.1.19 shows the variation in tensile strength with respect to orientation and layer thickness. These 3D planes help in selecting the parameters for any particular value of the tensile strength. For example, to understand the parameters required for a tensile strength of 98 MPa, one draws a line from the z-axis (tensile strength axis) towards the 3D plane. From the point on the 3D plane, a line then follows through the layer thickness (L) and orientation (O) plane. From the point on the L-O plane, one then should draw lines towards L axis and O axis. Those points on the L and O axis would be the desired levels. Similarly, desired levels for L, O and P can be obtained for tensile strengths.

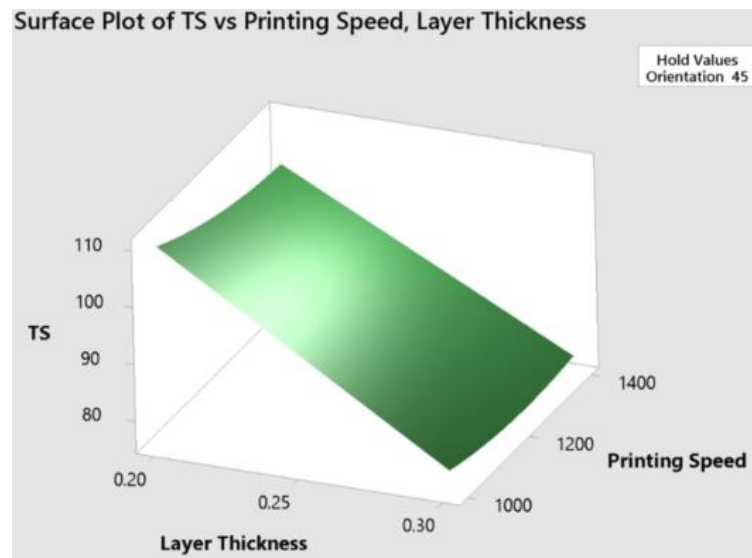


Figure 4.1.13. Surface Plot: Tensile strength vs Layer thickness, Printing speed

4.1.4 Optimal factors for tensile strength

Using the MINITAB software, the optimal (among the parameter levels used for this study) levels for each parameter have been identified for tensile strength. The levels shown in

red (in Figure 4.1.18) are the ones that are optimal (among the parameter levels used for this study). The following snip shows the optimal (among the parameter levels used for this study) factors obtained:

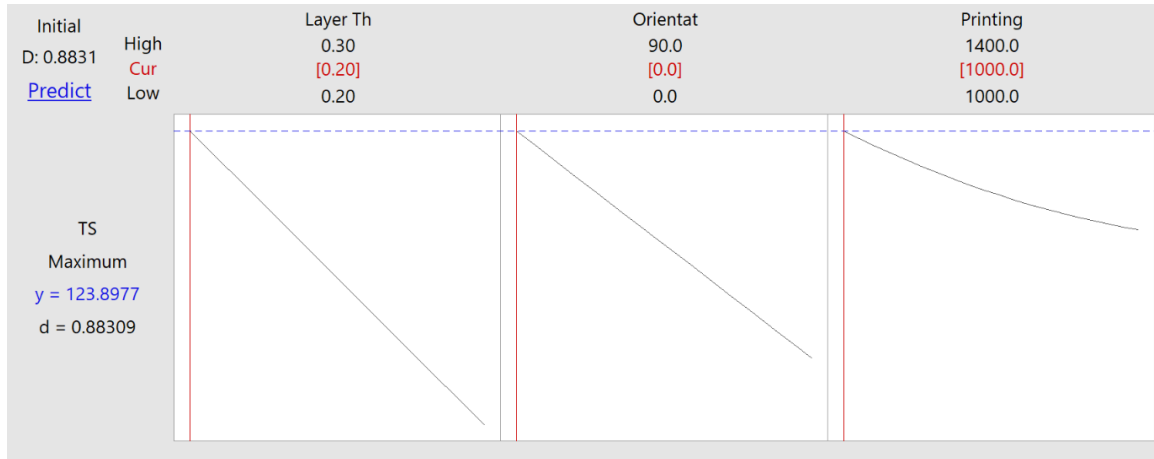


Figure 4.1.14. Tensile: Optimal (among the parameter levels used for this study) factors obtained using MINITAB software

Lower layer thickness means lesser gaps between the layers and therefore higher bonding between them. Also, a part build with lower layer thickness has a greater number of bonding layers in it than a part build with higher layer thickness and less bonding layers. Therefore, a lower layer thickness is better for higher tensile strength.

An orientation of 0 degrees resulted into a higher tensile strength since the dog bone structure at zero degrees has a longer raster filling inside than the structure built at ninety degrees. Longer bonding areas mean higher bonding and higher strength.

At lower printing speed, the material coming out of the nozzle in the form of a layer has more time to cool and bond with the previous layer and hence there is better bonding between the layers and higher strength in the part.

4.2 Compression Specimen

Compression strength of CFR-PEEK was determined by experimenting with samples made from a nozzle diameter of 0.2 mm. All the values obtained were in the 95% confidence interval. The results obtained for each combination of compression strength are as shown in table 4.2.

Table 4.2. Combinations and their compression values obtained

Combinations	L	O	P	Compressive Strength (Mpa)
L1O1P1	0.2	0	1000	76.99676346
L1O1P1	0.2	0	1000	64.09461286
L1O1P1	0.2	0	1000	82.6722472
L1O1P2	0.2	0	1200	82.89400337
L1O1P2	0.2	0	1200	71.35992484
L1O1P2	0.2	0	1200	76.27707462
L1O1P3	0.2	0	1400	73.78449477
L1O1P3	0.2	0	1400	67.17442631
L1O1P3	0.2	0	1400	61.97731204
L1O2P1	0.2	90	1000	91.98850897
L1O2P1	0.2	90	1000	92.453464
L1O2P1	0.2	90	1000	88.19812845
L1O2P2	0.2	90	1200	88.33596159
L1O2P2	0.2	90	1200	85.4431823
L1O2P2	0.2	90	1200	91.76755949
L1O2P3	0.2	90	1400	92.36368044
L1O2P3	0.2	90	1400	89.72404226
L1O2P3	0.2	90	1400	88.09018408
L2O1P1	0.3	0	1000	60.73311399
L2O1P1	0.3	0	1000	51.35126168
L2O1P1	0.3	0	1000	67.82434362
L2O1P2	0.3	0	1200	66.62810621
L2O1P2	0.3	0	1200	62.7607319
L2O1P2	0.3	0	1200	69.06463166
L2O1P3	0.3	0	1400	55.03258847
L2O1P3	0.3	0	1400	68.11585063
L2O1P3	0.3	0	1400	64.30608135
L2O2P1	0.3	90	1000	83.34326593
L2O2P1	0.3	90	1000	76.7849909
L2O2P1	0.3	90	1000	75.65263689
L2O2P2	0.3	90	1200	72.67834085
L2O2P2	0.3	90	1200	82.8862054
L2O2P2	0.3	90	1200	78.35490018
L2O2P3	0.3	90	1400	75.47277328
L2O2P3	0.3	90	1400	87.46026502
L2O2P3	0.3	90	1400	81.30284445

4.2.1 ANOVA Analysis

The ANOVA analysis was performed using MINITAB 18 software to identify the effect of individual factors on the compression strength. Interactions among the

parameters were also taken into consideration during the analysis. The results obtained are shown below.

Analysis of Variance					
Source	DF	Adj SS	Adj MS	F-Value	P-Value
L	1	959.37	959.37	30.12	0
O	1	2487.57	2487.57	78.09	0
P	2	24.44	12.22	0.38	0.686
L*O	1	0.25	0.25	0.01	0.93
L*P	2	64.71	32.35	1.02	0.377
O*P	2	122.57	61.28	1.92	0.168
L*O*P	2	12.96	6.48	0.2	0.817
Error	24	764.54	31.86		
Total	35	4436.42			

Table 4.2.2 Analysis of variance table for compression test results.

Table 4.2.2 is a snip from MINITAB results section. In the source column, as mentioned in section 4.1.1, L stands for layer thickness, O for Orientation and P for printing speed. L*O is for interaction between layer thickness and orientation, L*P is interaction between layer thickness and printing speed, and O*P is for interaction between orientation and printing speed. L*O*P is the interaction between all the three parameters. From the p-value column in table 4.2.2, it is seen that the parameters - layer thickness and orientation

have p-values less than 0.05. Since the associated p-values are less than 0.05, layer thickness and orientation have significant effects on the compression strength of CFR-PEEK. The Figure 4.2.3. shows the main effect plot for all the individual parameters.

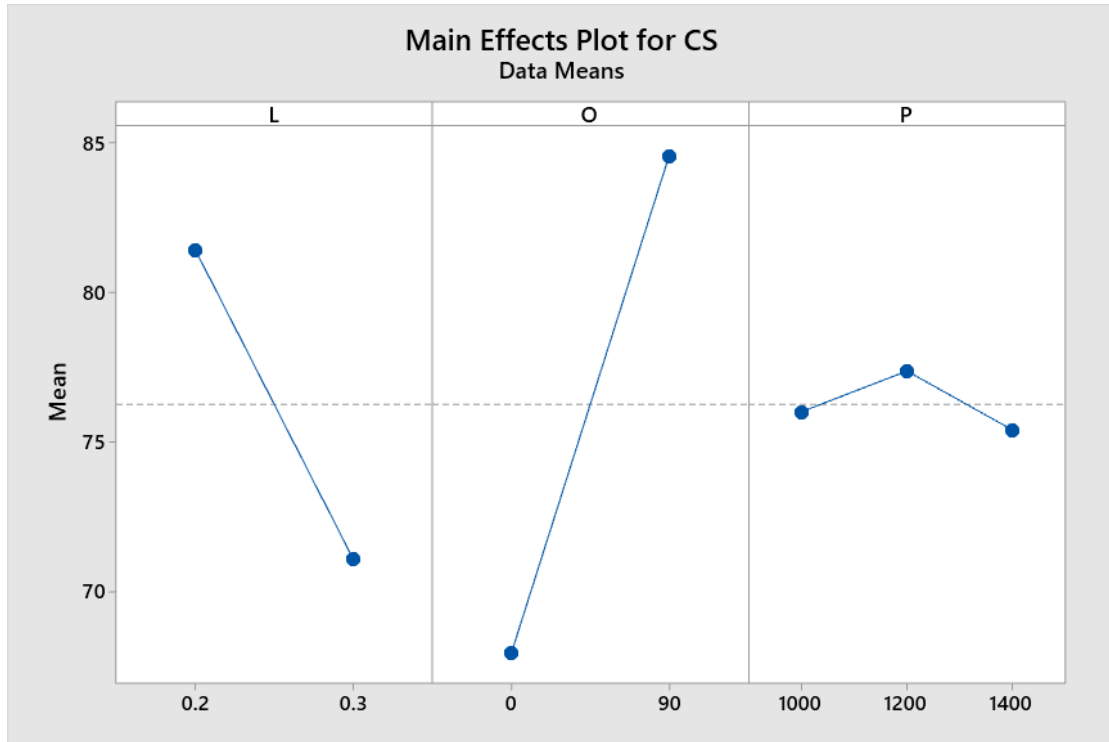


Figure 4.2.3. Compression: Main effects plot

The main effects plot was generated based on the 'Larger is better' property in MINITAB. This particular option is chosen with an interest to obtain the parameter levels which result in a higher compressive strength. From the ANOVA analysis, it is found that unlike tensile strength, compressive strength is not affected by printing speed but only by the parameters - orientation and layer thickness. One other interesting result obtained from ANOVA analysis of compressive strength is that there are no interactions between the parameters. This shows that the effect of both layer thickness and orientation on the tensile strength are independent. As discussed in section 4.2.1, an interaction occurs

when effect of one parameter depends on the effect of another parameter. Interactions mean that the results from the main effects cannot be relied upon completely. However, in this case, since there are no interactions, results from the main effects plot are to be considered solely. To understand interactions, we need to look at a special graph known as interactions plot. Figure 4.2.4 shows the interaction plot of compression strength.

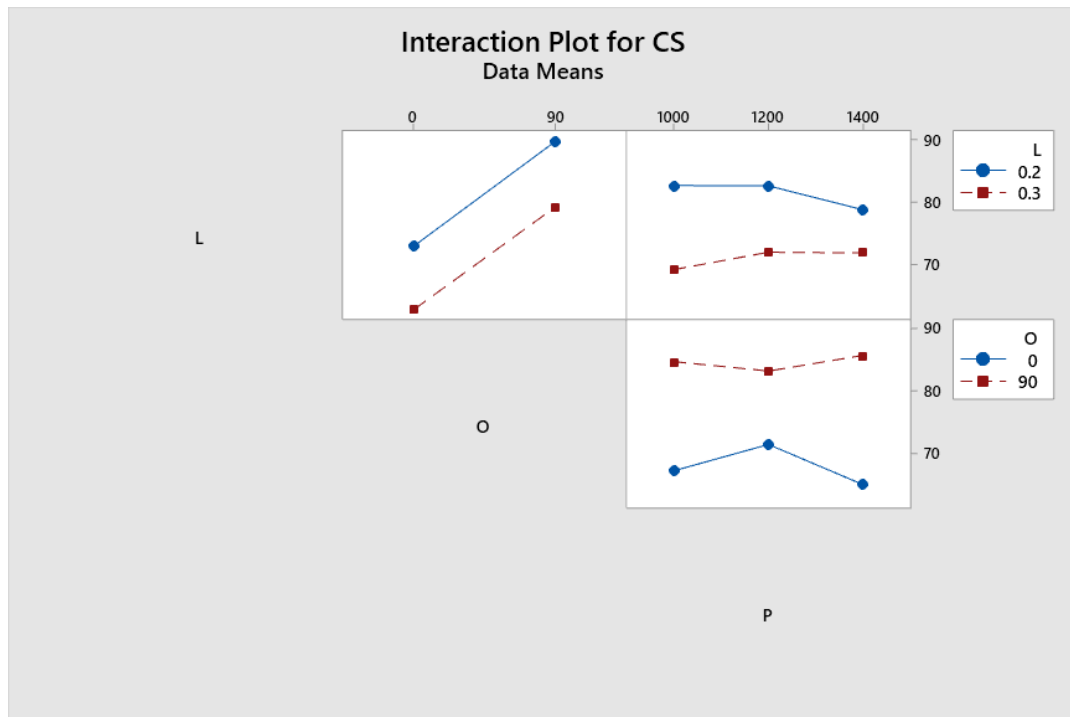


Figure 4.2.4. Interactions plot for compression strength

The parallel lines in the interaction plots state that there are no interactions between the parameters as indicated by the p-values.

As can be deduced from Figure 4.2.3, layer thickness of 0.2 mm layer thickness produces a better compression strength than 0.3 mm of layer thickness. For fabricating parts with higher compression strength, lower layer thickness should be used. The increase in compressive strength with decreasing layer thickness can be attributed to the

fact that the layers are closely stacked upon each other creating a higher inter-layer bonding among them when compared to parts with higher layer thickness. One other reason for low compressive strength in higher layer thickness values can be due to the presence of micro voids between layers which act as stress risers (Shubham et al., 2016). Smaller layer thickness has smaller voids whereas higher layer thickness has larger micro voids leading to lesser bonding which ultimately leads to lower compressive strength.

Similarly, Orientation of 90 degrees produces higher compression strength than an orientation of 0 degrees as shown in Figure 4.2.3. Hence, fabricating parts with a 0-degree orientation will lead to weaker compression strength than parts fabricated vertically. The reason for this can be due to the fact that at 90 degrees the stacked layers in the part are perpendicular to the force applied and thus resist the compressive force. Whereas when printed at zero-degree angle, the layers stacked in the part are parallel to the compressive force and can create a gap between layers decreasing the strength.

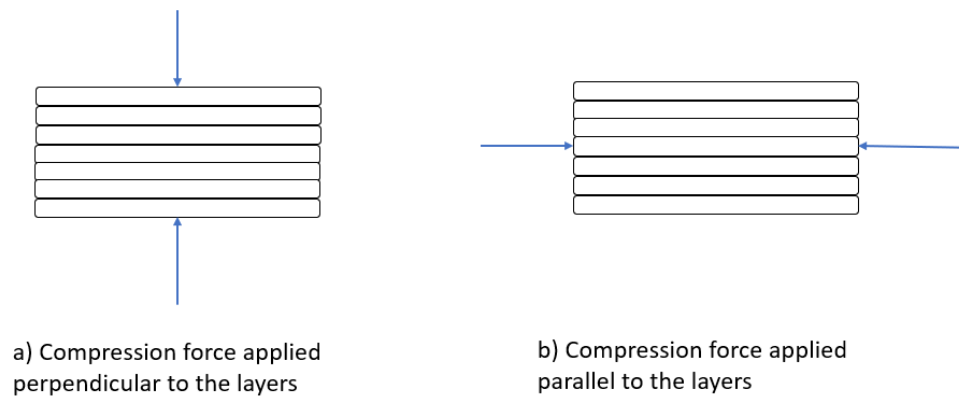


Figure 4.2.5. Effect of compression load (compressive strength) on the layers of the part stacked (adapted from 3D hubs).

Printing speed, however, seems to have a different type of effect on compression strength. As shown, 1200mm/min speed seems to produce CFR-PEEK parts with a higher compression strength than the other speeds. However, in the figure, 1400mm/min speed seems to have a slightly lower compression strength than that of 1000 mm/min speed. Lower speeds seem to give better bonding time with the previous layer due to which it exhibits a stronger bond.

Figure 4.2.6. shows the set of interaction plots for compression strength.

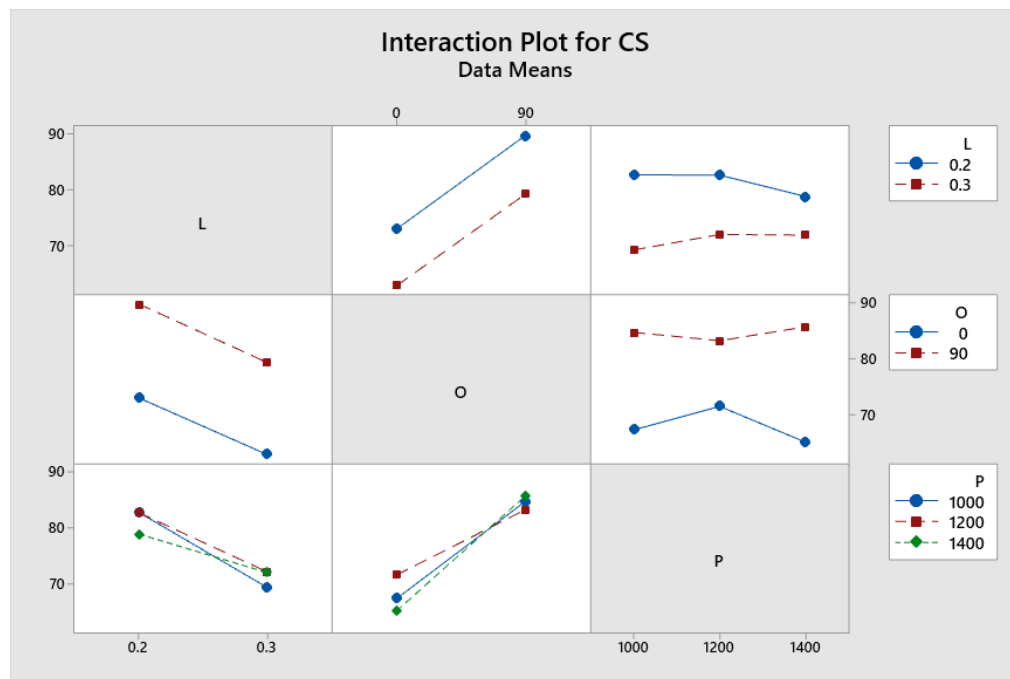


Figure 4.2.6. Full interaction plots for compression strength

The full set of interaction plots helps in identifying and comparing the effect of any two parameters on the compression strength of CFR-PEEK. For example, the top-right graph in Figure 4.2.5 shows the effect of layer thickness and printing speed on the compression strength. Using this graph, we can see that a layer thickness of 0.2mm and a printing

speed of 1000 mm/min is essential for a higher compression strength. The combination of (0.2mm, 1200mm/min) produces a higher compression strength than the combination (0.3mm, 1400 mm/min). Similarly, using the bottom-left graph, we can conclude that a layer thickness of 0.2mm and printing speed of 1200 mm/min (0.2mm, 1200 mm/min) produces parts with higher compression strength than a combination of similar layer thickness but 1400 mm/min (0.2mm, 1400 mm/min). The full plot matrix gives an overall picture of the effect of two individual parameters on the compression strength.

The process parameters of FDM seem to highly affect the tensile strength of CFR-PEEK. The combination L1O2P1 seems to be the combination with highest compression strength, and the combination L2O1P1 seems to have the least compression strength. The whiskers box plot below in Figure 4.2.7 shows the variation of compression strength between all the combinations. One interesting thing to note in this graph is all the three combinations L1O2P2, L1O2P1, and L1O2P3 seem to have the same and highest compression strength. In all three combinations, the similar parameters are seen to be the layer thickness of 0.2mm and Orientation of 90 degrees. But the printing speed is different in all the combinations. This underlines the result from ANOVA analysis that neither printing speed nor any interactions has any effect on the compression strength and only layer thickness and orientation affect the compression strength of CFR- PEEK the most.

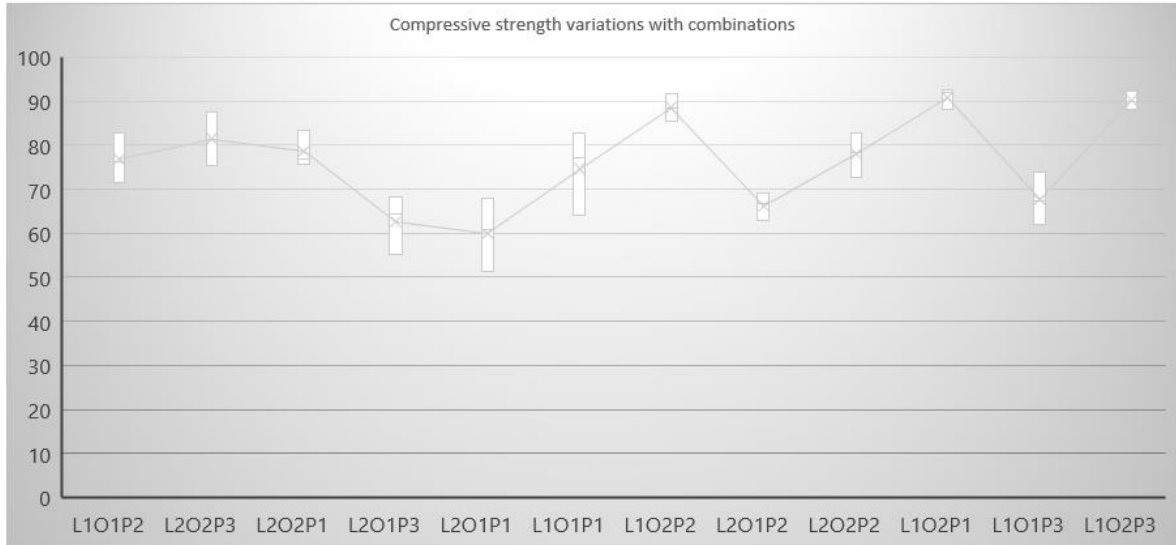


Figure 4.2.7. Variations in compression strengths of parts printed with various combinations of process parameters

Regression equation obtained for compression strength is

$CS=66.81+16.6O-10.3L$ with an R square value of 77.70%.

4.2.2. Contour Plots

Contour plots are used to view the three-dimensional plot on a two-dimensional surface (statisticshowto.com). Using the MINITAB software, contour plots for compression strength with respect to layer thickness, printing speed and orientation are generated.

The following figures show the contour plots obtained.

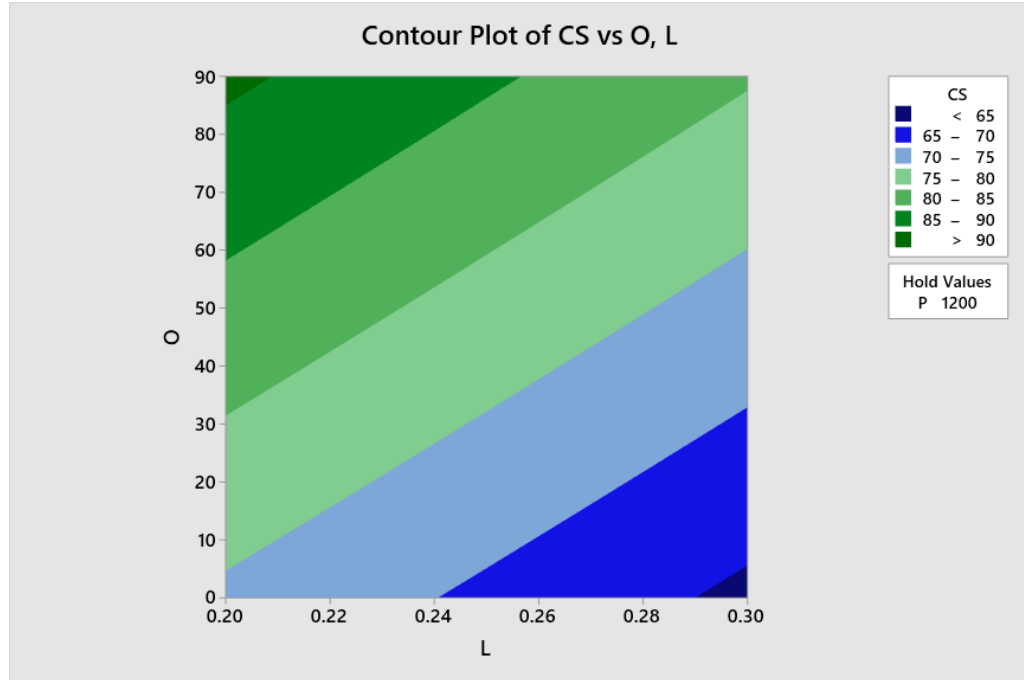


Figure 4.2.8. Contour Plot: Compression strength with respect to Layer Thickness and Orientation

From the above figure, it can be deduced that lower layer thickness and higher orientation will lead to a higher compression strength. This contour plot was generated by averaging the printing speed value to 1200 mm/min. From Figure 4.2.8, layer thickness of 0.20 mm and 70 degrees will lead to a compression strength range of 85-90 MPa. While maintaining the same layer thickness of 0.20 mm, if the orientation is reduced by half, compression strength is reduced by 5-10 MPa. However, it is advisable to choose a proper orientation than layer thickness to reduce the amount of time and cost for building support structures. In the FDM technology, orientation affects the build time and cost whereas the layer thickness affects the build time. Higher the layer thickness, lower the build time.

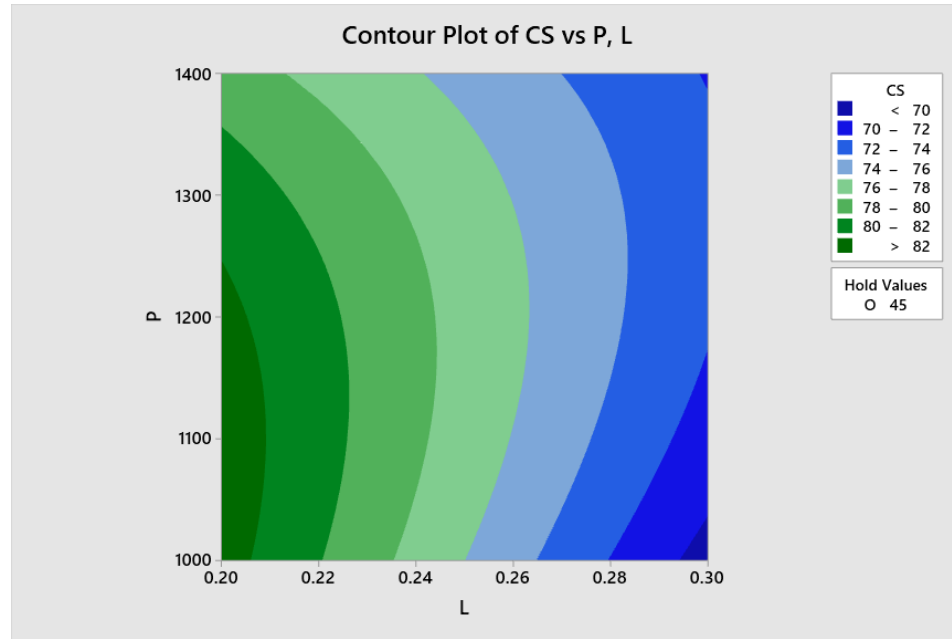


Figure 4.2.9. Contour Plot: Compression strength with respect to Layer thickness and Printing speed

From Figure 4.2.9, it can be seen that a lower layer thickness and lower printing speeds can lead to higher compression strength of CFR-PEEK material. This graph is plotted by averaging the orientation value to 45 degrees. One interesting thing to note is – while maintaining the same layer thickness of 0.20 mm if we increase the printing speed to 1200+20 mm/min, the compression strength obtained remains the same. Also, looking at the graph closely, it is clear that the layer thickness has a greater effect on the compressive strength of CFR-PEEK. For every 0.02 mm change in layer thickness, the compressive strength changes by 2 MPa. The strength values remain almost the same horizontally in the graph for various range of printing speed. This statement supports the higher p-value obtained from ANOVA analysis stating minimal or no effect of printing speed on compressive strength. This graph in relative terms is more dispersed than the other contour plots for O-P (Figure 4.2.8) and O-L (Figure 4.2.10).

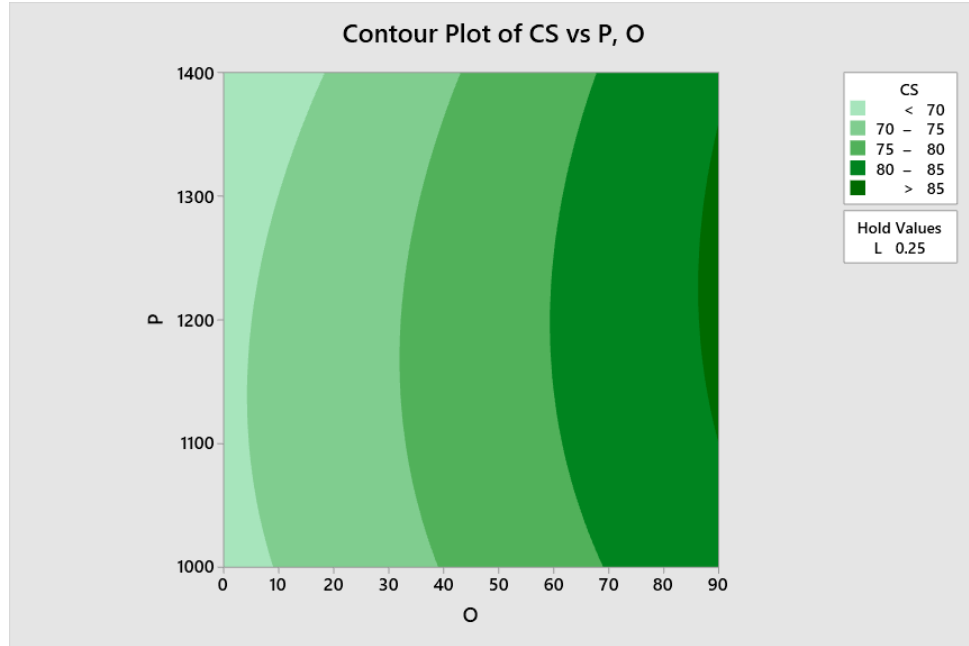


Figure 4.2.10. Contour Plot: Compression strength with respect to Printing speed and Orientation

Figure 4.2.10 looks more relaxed when compared to the contour plots in Figure 4.2.8 and Figure 4.2.9. This contour plot was generated by averaging the layer thickness to a value of 0.25 mm. Given the levels of parameters, an orientation of 90 degrees and a printing speed of 1150 mm/min to 1250 mm/min gives a higher compressive strength. An interesting thing to note here is that the compressive strength seems to be more affected by the orientation than by the printing speed. This statement supports the higher p-value for printing speed obtained from ANOVA analysis stating minimal or no effect of printing speed on compressive strength. For every change of 20-30 degrees, the compressive strength values change by 5 MPa.

4.2.3 Surface Plots

As mentioned in section 4.1.3, Surface plots are three-dimensional graphs that are used to depict the relationship among a fixed variable which is dependent and two more independent variables (netdna-ssl.com). Surface plots are created for compression strengths with respect to Printing speed, Orientation and Layer thickness. The following figures show the surface plots generated in MINITAB.

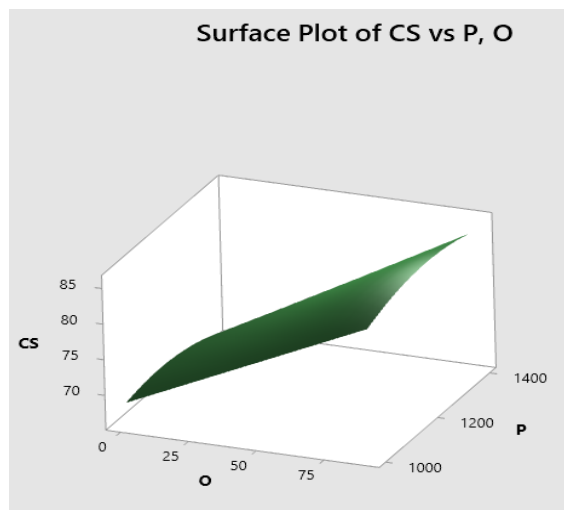


Figure 4.2.11. Surface Plot: Compression strength with respect to Orientation and printing speed

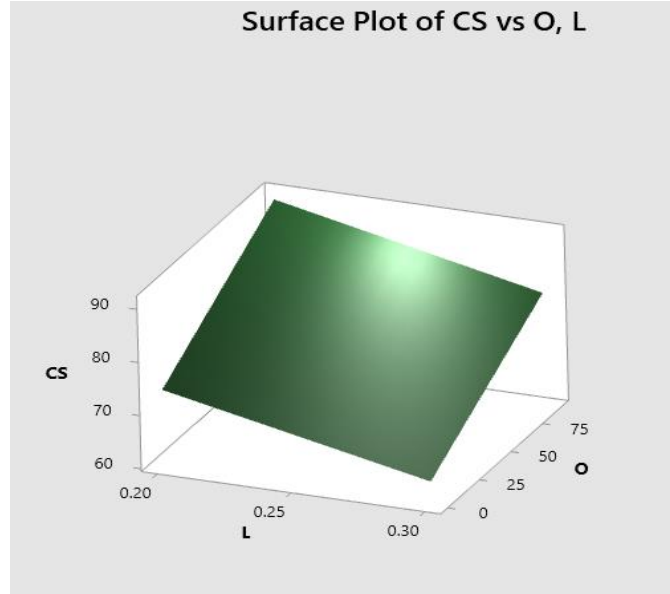


Figure 4.2.12. Surface Plot: Compression strength with respect to Layer Thickness and Orientation

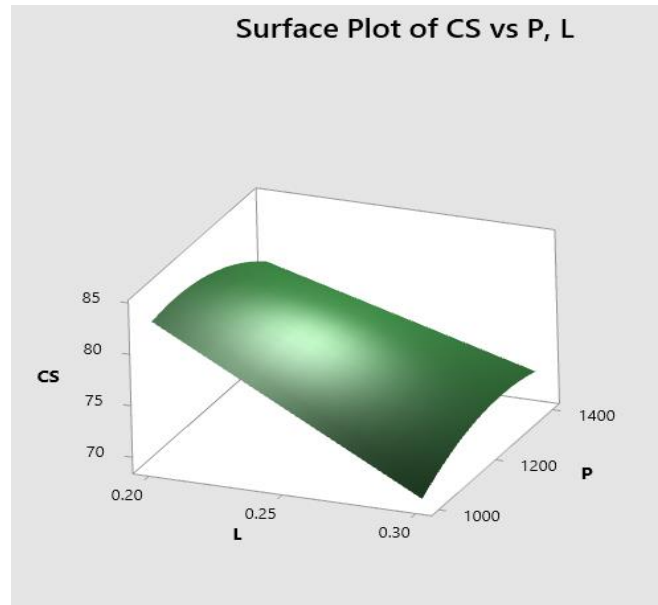


Figure 4.2.13. Surface Plot: Compression strength with respect to Layer Thickness and Printing speed

4.2.4 Optimal Factors for Compression Strength

Using the MINITAB software, the optimal (among the parameter levels used for this study) levels for each parameter have been identified for compression strength. The levels shown in red and stated as Cur (in Figure 4.2.14) are the ones that are optimal (among the parameter levels used for this study). The optimal (among the parameter levels used for this study) printing speed in this case is defined as 1133.33 mm/min as per MINITAB, since the graph coincides at that particular point. Theoretically, it would be correct but in general, FDM printers would not have such decimal values of printing speed. In this case, the speed available on the machine and is closest to the obtained value in MINITAB is 1200 mm/min. The following snip shows the optimal (among the parameter levels used for this study) factors obtained.

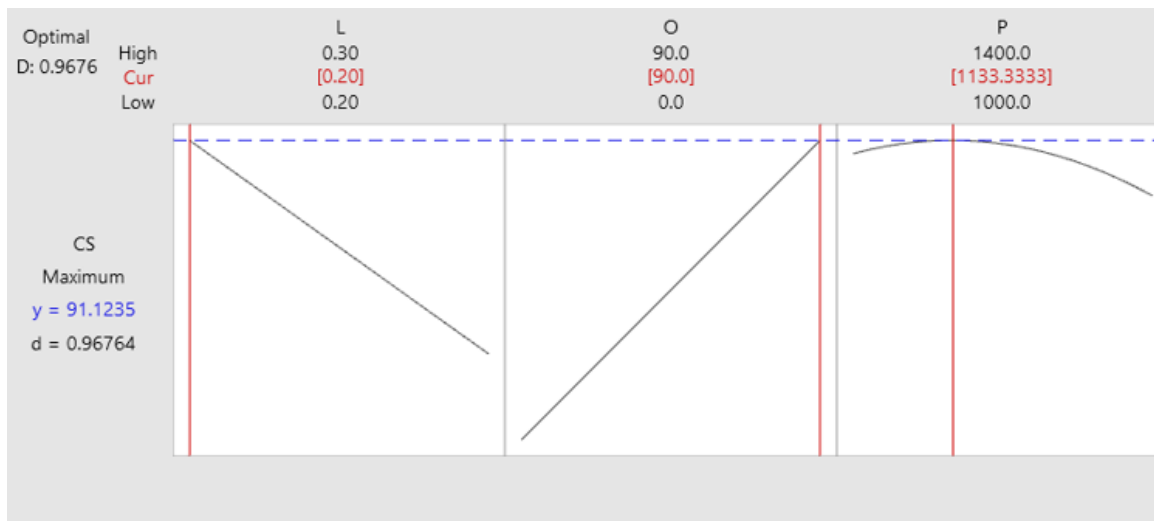


Figure 4.2.14. Compressive: Optimal (among the parameter levels used for this study) factors obtained using MINITAB software

Lower layer thickness means lesser gaps between the layers and therefore higher bonding between them. Also, a part build with lower layer thickness has a greater number of bonding layers in it than a part build with higher layer thickness and less bonding layers. Therefore, a lower layer thickness is better for higher tensile strength. Printing speed seemed to have no effect on the compression strength.

4.3 Comparison with Other Studies

Velineni et al. (2018) has conducted a similar study to learn about the effect of process parameters on the dimensional accuracy of 3D printed parts. In comparison to this study, Velineni et al.'s study used ABS material and studied the geometric variability in parts for different process parameters. Her study did not focus on the mechanical properties of the parts. In contrast, the present study focuses on the mechanical properties of CFR-PEEK for different combinations of process parameters. The parameters used in both the studies are layer thickness, printing speed and orientation. Both the studies have used a full factorial analysis.

CHAPTER 5

CONCLUSION

Fused Deposition Modelling is a non-traditional technique of fabricating any geometry in a temperature-controlled environment by extruding layers in a sequential manner. The layer-by-layer method gives an advantage of minimal tooling and manual support which aids in building complex parts. FDM has a proven track of being comfortable to use with minimal cost when compared to the conventional methods (Liu et al., 2005). However, one major drawback of this technology is the dependency of part quality on the parameters of FDM. Parts fabricated through FDM largely depend on the processing parameters used to obtain the part. The principle involved in FDM for fabricating parts is a major reason for the limited usage of FDM technology (Onuh et al., 1999; Kai et al., 1997). Other major reason is due to the minimum amount of materials available for processing in FDM. There is a need to investigate more materials for its processability using FDM. The present work lays stress on both the limitations of improving part quality by understanding the effect of process parameters and investigating new materials. Han et al. (2019) studied the mechanical properties of CFR-PEEK samples printed with a unique set of parameters and levels. A layer thickness of 0.2mm, Printing speed of 40mm/s along with other parameter levels were used to print the samples. The tensile strength was obtained to be 101.41Mpa whereas the compression strength obtained was 137.11Mpa.

Findings

In this study, a new material known as CFR-PEEK is used to understand the effect of process parameters on the mechanical properties of parts built using FDM. Two major mechanical properties considered in this study are the tensile and compressive strength of CFR-PEEK. Based on the literature review and studies done so far, three major parameters are taken into consideration – layer thickness and orientation. Along with these a new parameter – printing speed is considered. The effect of these parameters on the mechanical properties are as follows:

- All three parameters layer thickness (L), orientation (O) and printing speed (P) have significant effects on the tensile strength of the CFR-PEEK.
- The interaction between layer thickness and orientation; orientation and printing speed and between all three L, O and P have significant effects on the tensile strength.
- For tensile strength – 0.2mm, 0 degrees and a printing speed of 1000 mm/min produce CFR- PEEK of highest tensile strength.
- Parameter levels – 0.3 mm, 90 degrees and 1200 m/min produce CFR- PEEK with lowest tensile strength among the given level of parameters.
- The optimal parameters need to be chosen based on the tensile strength required.

There is a drastic variation in tensile strength with respect to the 12 parameter combinations as shown in Figure 4.1.14. The combination L1O1P1 (layer thickness of 0.2 mm, build orientation of 0 degrees, and Printing speed of 1000 mm/min) gives the highest

tensile strength whereas the combination of L2O2P3 (Layer thickness of 0.3 mm, build orientation of 90 degrees and printing speed of 1400 mm/min) produces least tensile strength. For the compression test of CFR-PEEK the results look at lot different as follows:

- Two of the three parameters – Layer thickness and Orientation were found to have significant effects on the compressive strength of CFR-PEEK.
- Printing speed was found to have no or minimal effect on the compressive strength of CFR-PEEK.
- No interactions are found between the parameters which means that the effect of layer thickness and orientation is independent.
- For compressive strength – layer thickness of 0.2mm, build orientation of 90 degrees and printing speed of 1200 mm/min are found to give the maximum compressive strength.
- Parameter levels – 0.3 mm, 0 degrees of build orientation and printing speed of 1400 mm/min produce the least compressive strength in CFR-PEEK parts.
- The optimal parameters need to be chosen based on the compressive strength required.

Similar to the tensile strength, there is a drastic variation in compressive strength too, with respect to the 12 parameter combinations as shown in Figure 4.2.13. The combination L1O2P2 (layer thickness of 0.2 mm, build orientation of 90 degrees, and Printing speed of 1200 mm/min) and L1O2P1 (layer thickness of 0.2 mm, orientation of 90 degrees and printing speed of 1000 mm/min) produce the highest compressive

strength in CFR-PEEK material, whereas the combination of L2O1P1 (Layer thickness of 0.3 mm, build orientation of 0 degrees and printing speed of 1000 mm/min) produce least compressive strength in CFR-PEEK material.

A part with good tensile and compressive strength can be obtained if the following levels are used. A lower layer thickness, and lower printing speed. In this study, a layer thickness of 0.2mm and printing speed of 1000 mm/min. Orientation angle can be chosen based on the shape of the part which gives least support material and less time.

5.1 Uniqueness of This Study

- In this study, the effects of crucial parameters (identified from the literature study done) such as layer thickness and orientation on the major mechanical properties of CFR-PEEK have been considered.
- This study considers an FDM process parameter (printing speed) that has not been much studied previously.
- This study uses a full-factorial analysis that minimizes loss of data from experiments.
- Unlike previous studies which used cliché materials in their experiments, this study uses a new and very potential material known as CFR-PEEK. This material has proved its potentiality in various fields as was discussed in section 3.2.2.

5.2 Scope of Future Work

The present study leaves a scope for investigators to extend the present study to include other aspects of FDM technology. Some suggestions for future work are:

- Investigate the effect of additional parameters such as raster width, air gap, temperature, raster orientation and angle, etc. on the mechanical properties of CFR-PEEK.
- Investigate the effect of process parameters on additional mechanical properties like impact strength, surface roughness, flexural strength, etc.
- Investigate the effect of process parameters with additional levels to understand the interaction effects between the parameters. For example, in this study only two levels were considered for every parameter due to cost constraints. In future studies, investigators can use a larger range with more factor levels.
- Comparative evaluation of mechanical properties of CFR-PEEK parts produced using various RP methods.

REFERENCES

ASTM D638-14. (2014). "Standard test method for tensile properties of plastics". West Conshohocken, PA, United States: ASTM International. (Accessed on 15th October 2018). <http://www.dept.aoe.vt.edu/~aborgolt/aoe3054/manual/expt5/D638.38935.pdf>

ASTM D695-15. (2015). "Standard test method for compressive properties of rigid plastics". West Conshohocken, PA, United States: ASTM International. (Accessed on 15th October 2018).

<http://www.dept.aoe.vt.edu/~aborgolt/aoe3054/manual/expt5/D695.6642.pdf>

ASQ. <https://asq.org/quality-resources/design-of-experiments>. (Accessed on August 2nd, 2018).

APIUM P220 Series FDM printer. (Accessed on March 2nd, 2019). <https://www.imakr.com/apium-3d-printers/1961-apium-p200.html>

Ahn S.H., Montero M., Odell D., Roundy S. and Wright P.K. (2002). "Anisotropic material properties of Fused Deposition Modelling ABS". Rapid prototyping journal, vol. 8(4), 248-257.

Bak D. (2003). "Rapid prototyping or rapid production? 3D printing processes move industry towards the latter". Assembly automation, 23(4), 340-345.

Bellini A. (2002). "Fused deposition of ceramics: a comprehensive experimental, analytical and computational study of material behavior, fabrication process and equipment design."

Bernard A. and Fischer A. (2002). "New trends in rapid product development". CIRP Annals Manufacturing Technology, Volume 51, Issue 2, pp. 635-652.

Bagsik A., Schöppner V. and Klemp E. (2010). "FDM part quality manufactured with ULTEM 9085". Proceedings of the 14th international scientific conference on polymeric materials, Halle (Saale), Germany. 15–17 September 2010; pp. 307–315.

Blockland forums. "Crysis 2 Tessellation". (Accessed August 23rd, 2018). <https://forum.blockland.us/index.php?topic=302085.0>.

Barequet G. and Kaplan Y. (1998). "A data front-end for layered manufacturing". Computer Aided Design, Vol. 30, Pp. 231-243.

Bogdan V., Ziga K., Tomaz B., Andrew A. and Drstvensek I. (2013). "Processing poly (ether etherketone) on a 3d printer for thermoplastic modelling". Material in Tehnologies. 47. 715-721.

CAD design of Staircase effect. (Accessed on Feb 24th, 2019). <https://3dprinterchat.com/design-guidelines-for-3d-printing/staircase-effect/>.

Casavola C., Cazzato A., Moramarco V. and Pappalettere C. (2016). "Orthotropic mechanical properties of Fused Deposition Modelling parts described by classical laminate theory". Mater. Des. 90 (2016), pp. 453-458.

Chacón J. M., Caminero M.A., García-Plaza E. and Núñez P.J. (2017). "Additive manufacturing of PL structures using Fused Deposition Modelling: Effect of process parameters on mechanical properties and their optimal selection". Mater. Des. 2017, 124, 143–157.

Chennakesava P. and Shivraj Narayan Y. (2017). "Fused Deposition Modeling – Insights". International conference on advances in design and manufacturing (ICAD&M'14).

Chowdary B. V. (2007). "Back-propagation artificial neural network approach for machining center selection". Journal of Manufacturing Technology Management, vol. 18(3), pp. 315-332.

Christiyan K. J, Chandrasekhar U. and K. Venkateswarlu. (2016). "A study on the influence of process parameters on the mechanical properties of 3D printed ABS composite". In IOP

Conference Series: Materials Science and Engineering (Vol. 114, No. 1, p. 012109). IOP Publishing.

Cotteleer M. and Joyce J. (2014). "3D opportunity additive manufacturing paths to performance, innovation, and growth". Deloitte Review, no. 14, 5-19.

Chua C.K., Leong K.F. and Lim C.S. (2010). "Rapid prototyping: principles and applications". (with companion CD-ROM). World Scientific Publishing Company.

Contour plots. (Accessed on 3rd August 2019). <https://www.statisticshowto.datasciencecentral.com/contour-plots/>

Cooper K.G. (2001). "Rapid Prototyping Technology": selection and application. CRC press.

Dani T., Kamdi P., Nalamwar G., Borse V. (2013). "Multi objective optimization of built orientation for rapid prototyping of connecting rod". International journal of scientific research and management 1(1), 13-18

Dao Q., Frimodig J.C., Le H.N., Li X., Putnam S.B., Golda K., Foyos J., Noorani R. and Fritz B. (1999). "Calculation of shrinkage compensation factors for rapid prototyping (FDM 1650)." Computer Applications in engineering education, 7(3), 186-195.

Deger K. O., & Deger A. H. (2012). "An application of mathematical tessellation method in interior designing". Procedia-Social and Behavioral Sciences, 51, 249-256.

Deng, X., Zeng, Z., Peng, B., Yan, S., & Ke, W. (2018). "Mechanical Properties Optimization of Poly-Ether-Ether-Ketone via Fused Deposition Modeling". Materials (Basel, Switzerland), 11(2), 216

Dyrbuš, G. (2010). "Investigation on quality of rapid prototyping FDM method".

Ebubekir C., Mustafa A., Ferhat Y., Meltem G., Bünyamin K. (2017). "Investigation of the FDM process performance at different printing parameters".

Eschbach L. (2000). "Nonresorbable polymers in bone surgery". Injury, 31, D22-D27.

Formlabs. (Accessed on 24th October 2018). <https://formlabs.com/blog/what-is-selective-laser-sintering/>.

Palermo E. Fused Deposition Modelling: Most Common 3D Printing Method. September 19th, 2013. (Accessed on 23rd October 2018). <https://www.livescience.com/39810-fused-deposition-modeling.html>

Garcia-Gonzalez D., Jayamohan J., Sotiropoulos S.N, Yoon S.H, Cook J., Siviour C.R, Arias A. and Jérusalem A. (2017). "On the mechanical behaviour of PEEK and HA cranial implants under impact loading". Journal of the mechanical behavior of biomedical materials, 69, 342-354.

Gebisa, A. W., & Lemu, H. G. (2018). "Investigating Effects of Fused-Deposition Modeling (FDM) Processing Parameters on Flexural Properties of ULTEM 9085 using Designed Experiment". Materials, 11(4), 500.

Gebhardt, A. (2003). "Rapid prototyping".

Godara A., Raabe D. and Green S. (2007). "The influence of sterilization processes on the micromechanical properties of carbon fiber-reinforced PEEK composites for bone implant applications". Acta Biomater. 3, 209–220.

Górski F., Wichniarek R., Kuczko W., Zawadzki P. and Buń P. (2015). "Strength of ABS parts produced by Fused Deposition Modelling technology – a critical orientation problem." Advances in Science and Technology Research Journal, 9(26), 12-19.

Green S. & Schlegel, J. (2001). "A polyaryletherketone biomaterial for use in medical implant applications". Polym for the Med Ind Proc, Brussels, 14-15.

Green, S. (2007). "CFR PEEK composite for surgical applications". Medical Device Link, MDDI.

Hopkinson N., Hagur R.J.M., and Dickens P.H. (2006). "Rapid manufacturing: An industrial revolution for the digital age".

Hon K. K. B. (2007). "Digital additive manufacturing: from rapid prototyping to rapid manufacturing". In Proceedings of the 35th International MATADOR Conference (pp. 337-340). Springer, London.

Huang J.J., Ren J.A., Wang G.F. (2017). "3D-printed fistula stent designed for management of entero-cutaneous fistula: an advanced strategy". World journal of gastroenterology, 23(41), 7489.

Inzana J. A., Olvera D., Fuller S. M., Kelly J. P., Graeve O. A, Schwarz E.M., Kates S.L. and Awad H. L. (2014). "3D printing of composite calcium phosphate and collagen scaffolds for bone regeneration". Biomaterials, 35(13), 4026-4034.

Ismail D. and Ertan R. (2014). "Experimental investigation of FDM process for improvement of mechanical properties and production cost". Rapid Prototyping Journal, 20(3), 228-235.

Jamshidi P., Haddad M. and Mansour S. (2005). "A new database approach to improve STL files correction algorithms". 18th International Conference on Production Research. Jeff Wu C. F. and Michael Hamada. (2002). "Experiments: planning, analysis, and parameter design optimization." (Vol. 552). John Wiley & Sons.

Kai C.C. and Fai L.K. (1997). "Rapid prototyping principles and applications in manufacturing". World Scientific Publishing Co., Inc.

Katti D.R., Sharma A., Katti K.S. (2017). "Materials and devices for bone disorders, predictive methodologies for design of bone tissue engineering scaffolds". In Materials for bone disorders (pp. 453-492). Academic Press.

Khan Adil. (2016). "Design and characterizing of an innovative acoustic resonator".

Khan Z.A, Lee B.H. and Abdullah J. (2005). "Optimization of rapid prototyping parameters for production of flexible ABS object". Journal of materials processing technology, 169(1), 54-61.

Kim G.D. and Oh Y.T. (2008). "A benchmark study on rapid prototyping processes and machines: Quantitative comparisons of mechanical properties, accuracy, roughness, speed, and material cost". Proceedings of the Institution of Mechanical Engineers, Part B: Journal of Engineering Manufacture, 222(2), 201-215.

Kitsakis K. & Moza Z. & Iakovakis V. & Mastorakis N, Kechagias J. (2015). "An investigation of dimensional accuracy of Multi-Jet Modeling parts". In Proceedings of the International Conference in Applied Mathematics, Computational Science and Engineering, Crete, Greece.

Kokubo T., Hyun-Min K. and Masakazu K. (2003). "Novel bioactive materials with different mechanical properties". Biomaterials, 24(13), 2161-2175.

Kruth J. P., Levy G., Schindel R., Craeghs T., and Yasa E. (2008). "Consolidation of polymer powders by selective laser sintering." In Proceedings of the 3rd International Conference on Polymers and Molds Innovations (pp. 15-30)

Kulkarni P., Marsan A. and Dutta D. (2000). "A review of process planning techniques in layered manufacturing". Rapid prototyping journal, 6(1), 18-35.

Kurtz S.M. and Devine J.N. (2007). "PEEK biomaterials in trauma, orthopedic and spinal implants". Biomaterials, 28(32), 4845-4869.

LaSelle R. (2018). The future looks bright for additive manufacturing. (Accessed on December 9th, 2018). <https://www.jabil.com/insights/blog-main/future-of-3d-printing-additive-manufacturing-looks-bright.html>

Lee C., Kim S., Kim H. and Ahn S. (2007). "Measurement of anisotropic compressive strength of rapid prototyping parts". Journal of materials processing technology, 187, 627-630.

Levy G. N., Schindel R. and Kruth J. P. (2003). "Rapid manufacturing and rapid tooling with layer manufacturing (LM) technologies, state of the art and future perspectives". CIRP annals, 52(2), 589-609.

Li C. S., Vannabouathong C., Sprague S. and Bhandari M. (2015). "The use of carbon-fiber-reinforced (CFR) PEEK material in orthopedic implants: A systematic review". Clinical medicine insights: Arthritis and musculoskeletal disorders, 8, CMAMD-S20354.

Liu and Chen-Yu. (2013). "A comparative study of rapid prototyping systems" (Doctoral dissertation, University of Missouri--Columbia).

Liu Q., Leu M.C., and Schmitt S.M., "Rapid Prototyping in Dentistry: Technology and Application". The international journal of advanced manufacturing technology, 29(3-4), 317-335.

Ma D., Lin F., and Chua C.K. (2001). "Rapid prototyping applications in medicine. Part 2: STL file generation and case studies". The International Journal of Advanced Manufacturing Technology, 18(2), 118-127.

Mahesh M., Fuh J.Y.H., Wong Y.S., and Loh H.T. (2005). "Benchmarking for decision making in rapid prototyping systems". In IEEE International Conference on Automation Science and Engineering, 2005. (pp. 19-24). IEEE.

Masood S.H., Mau K. and Song W.Q. (2010), "Tensile properties of processed FDM polycarbonate material". In Materials Science Forum (Vol. 654, pp. 2556-2559). Trans Tech Publications.

Masood S. and Soo A. (2002). "A rule based expert system for rapid prototyping system selection". Robotics and Computer-Integrated Manufacturing, 18(3-4), 267-274.

Materials Evaluation and Engineering Inc. (Accessed on 6th December 2018). <https://www.mee-inc.com/laboratory-expertise/tension-compression-testing/>

Mohammed S.H., Espalin D., Ramos J., Perez M., & Wicker R. (2014). "Improved mechanical properties of fused deposition modeling-manufactured parts through build parameter modifications". *Journal of Manufacturing Science and Engineering*, 136(6).

Motaparti K.P., Taylor G., Leu M.C., Chandrashekhara K., Castle J. and Matlack M. (2016). "Effects of build parameters on compression properties for ULTEM 9085 parts by Fused Deposition Modeling". In *Proceedings of the 27th Annual International Solid Freeform Fabrication Symposium*, Austin, TX, USA (pp. 8-10).

Mueller B. (2012). "Additive manufacturing technologies: rapid prototyping to direct digital manufacturing". *Assembly Automation*, 32(2).

Muthu S., Senthilkannan S. and Mahesh M. (2016). "Handbook of sustainability in additive manufacturing". (Vol. 1, pp. 31-42). Hong Kong: Springer.

Nancharaiah T., Raju D.R. and Raju V.R. (2010). "An experimental investigation on surface quality and dimensional accuracy of FDM components". *International Journal on Emerging Technologies*, 1(2), 106-111.

Ognzan L., Dejan M. and Miroslav P. (2014). "Effect of layer thickness, deposition angle and infill on maximum flexural force in FDM built specimens". *Journal for Technology of Plasticity*, 39(1), 49-58.

Onuh S. O. and Yusuf Y. Y., "Rapid Prototyping Technology: Applications and Benefits for Rapid Product Development," *Journal of intelligent manufacturing*, 10(3-4), 301-311.

Panayotov I.V., Orti V., Cuisinier F., and Yachouh J. (2016). "Poly-ether-ether-ketone (PEEK) for medical applications". *Journal of Materials Science: Materials in Medicine*, 27(7), 118.

Pham, D. T., & Gault, R. S. (1998). "A comparison of rapid prototyping technologies. *International Journal of machine tools and manufacture*". 38(10-11), 1257-1287.

Pham, D., & Dimov, S. S. (2012). "Rapid manufacturing: the technologies and applications of rapid prototyping and rapid tooling." Springer Science & Business Media.

P-value. <https://en.wikipedia.org/wiki/P-value> . (Accessed on 18th August 2019).

Rajpurohit, S. R., & Dave, H. K. (2018). "Effect of process parameters on tensile strength of FDM printed PLA part". Rapid Prototyping Journal, 24(8), 1317-1324.

Rankouhi, B., Javadpour, S., Delfanian, F., & Letcher, T. (2016). "Failure analysis and mechanical characterization of 3D printed ABS with respect to layer thickness and orientation." Journal of Failure Analysis and Prevention, 16(3), 467-481.

Ramakrishna S., Mayer J., Wintermantel, E., & Leong, K. W. (2001). "Biomedical applications of polymer-composite materials: a review." Composites science and technology, 61(9), 1189-1224.

Rahman K.M., Letcher T. and Reese R. (2015). "Mechanical properties of additively manufactured peek components using fused deposition filament fabrication". In ASME 2015 International Mechanical Engineering Congress and Exposition (pp. V02AT02A009-V02AT02A009). American Society of Mechanical Engineers.

Rathee S., Srivastava M., Maheshwari S. and Siddiquee A.N. (2017). "Effect of varying spatial orientations on build time requirements for FDM process: A case study". Defence technology, 13(2), 92-100.

Raut S., Jatti V.S., Khedkar N.K. and Singh T.P. (2014). "Investigation of the effect of built orientation on mechanical properties and total cost of FDM parts". Procedia materials science, 6, 1625-1630.

Rodrigo M., Volpato N., Stolfi J., Gregori R. M., and DaSilva M. V. (2017). "An optimal algorithm for 3D triangle mesh slicing". Computer-Aided Design, 92, 1-10.

Rui M. and Tang T. (2014). "Current strategies to improve the bioactivity of PEEK". International journal of molecular sciences, 15(4), 5426-5445.

Russel G.A, Wu B.M., Borland S.W., Cima L.G., Sachs E. M. and Cima M.J. (1997). "Mechanical properties of dense polyaltic acid structures fabricated by three-dimensional printing". *Journal of Biomaterials Science, Polymer Edition*, 8(1), 63-75.

Said E. O. S, Foyos J., Noorani R., Mandelson M., Marloth R. and Pregger B.A. (2000). "Effect of layer orientation on mechanical properties of rapid prototyped samples". *Materials and Manufacturing Processes*, 15(1), 107-122.

Saffarzadeh M., Gillispie G., and Brown P. (2016). "Selective laser Sintering (SLS) Rapid Prototyping technology: A review of medical applications"

Attoye S. O. (2018). "A Study of Fused Deposition Modeling (FDM) 3-D Printing Using Mechanical Testing and Thermography". (Doctoral dissertation).

Shen S., Wang H., Xue Y., Yuan L., Zhou X., Zhao Z., Dong E., Liu B., Liu W., Cromeens B. (2017). "Freeform fabrication of tissue-simulating phantom for potential use of surgical planning in conjoined twin's separation surgery". *Scientific reports*, 7(1), 11048.

Schöppner V. and KTP. K. P. (2011). "Mechanical properties of fused deposition modeling parts manufactured with Ultem* 9085". In *Proceedings of 69th Annual Technical Conference of the Society of Plastics Engineers (ANTEC'11)* (Vol. 2, pp. 1294-1298).

Shofner M. L., Lozano K., Rodriguez-Macias F.J. and Barrera E.V. (2003). "Nanofiber-reinforced polymers prepared by fused deposition modeling". *Journal of applied polymer science*, 89(11), 3081-3090.

Shubham P., Sikidar A. and Chand T. (2016). "The Influence of Layer Thickness on Mechanical Properties of the 3D Printed ABS Polymer by Fused Deposition Modeling". In *Key Engineering Materials* (Vol. 706, pp. 63-67). Trans Tech Publications.

Skirbutis G., Dzingutė A., Masiliūnaitė V., Šulcaitė G., Žilinskas J. (2017). "A review of PEEK polymer's properties and its use in prosthodontics". *Stomatologija*, 19(1), 19-23.

Smith W.C and Dean R.W. (2013). "Structural characteristics of Fused Deposition Modeling polycarbonate material". *Polymer testing*, 32(8), 1306-1312.

Sood A.K., Ohdar R.K. and Mahapatra. S.S., (2010). "Parametric appraisal of mechanical property of Fused Deposition Modelling processed parts". *Materials & Design*, 31(1), 287-295.

Sood A.K., (2011). "Study on parametric optimization of used deposition modelling (FDM) process". (Doctoral dissertation).

Sood A. K., Ohdar, R. K., and Mahapatra, S. S. (2012). "Experimental investigation and empirical modelling of FDM process for compressive strength improvement". *Journal of Advanced Research*, 3(1), 81-90.

Staircase effect image. (Accessed on 13th November 2018). Printerchat.com <https://3dprinterchat.com/2016/06/design-guidelines-for-3d-printing/staircase-effect/>.

Sternberg K. (2009). "Current requirements for polymeric biomaterials in otolaryngology". *GMS current topics in otorhinolaryngology, head and neck surgery*, 8.

Steve U., & Fletcher R., (2003). "The rapid prototyping technologies". *Assembly Automation*, 23(4), 318-330.

Subburaj K. and Ravi B. (2008). "Computer aided rapid tooling process selection and manufacturability evaluation for injection mold development". *Computers in Industry*, 59(2-3), 262-276.

Surface plots. (Accessed on 3rd August 2019). https://ncss-wpengine.netdna-ssl.com/wp-content/themes/ncss/pdf/Procedures/NCSS/3D_Surface_Plots.pdf

Swallowe G.M. (1999). "Mechanical properties and testing of polymers". an A-Z reference (Vol. 3). Springer Science & Business Media.

Tak A., Ingavale P., Khopatkar C., Bhure S., Barve V. and Rajurkar A. (2015). "Effect of 3D printing parameters on dimensional accuracy and shrinkage on printed parts".

Tappa K., Jammalamadaka U. (2018). "Novel biomaterials used in medical 3D printing techniques". *Journal of functional biomaterials*, 9(1), 17.

"The use of carbon-fiber reinforced polyetheretherketone in orthopedic surgery". (<http://www.pitt.edu/~jwd30/trends.html>). (Accessed on 23rd October 2018). Interesting Engineering Event.

Too M.H., Leong K.F., Chua C.K., Du Z.H., Yang S.F., Cheah C. M., and Ho S. L. (2002). "Investigation of 3D non-random porous structures by Fused Deposition Modeling". *The International Journal of Advanced Manufacturing Technology*, 19(3), 217-223.

Tymrak, B. M., Kreiger, M., & Pearce, J. M. (2014). "Mechanical properties of components fabricated with open-source 3-D printers under realistic environmental conditions". *Materials and Design*, 58, 242–246.

Vaezi S. (2011). "Mechanical properties of Fused Deposition Modeling parts manufactured with ULTEM 9085". In *Proceedings of 69th Annual Technical Conference of the Society of Plastics Engineers (ANTEC'11)* (Vol. 2, pp. 1294-1298).

Velineni A., Günay E. E., Park K., Okudan Kremer G. E., Schnieders T. M., and Stone R. T. (2018). "An Investigation on Selected Factors that Cause Variability in Additive Manufacturing".

Wiedemann B. and Jantzen H.A. (1999). "Strategies and applications for rapid product and process development in Daimler-Benz AG". *Computers in Industry*, 39(1), 11-25.

Wendel B., Rietzel D., Kühnlein F., Feulner R., Hülner G., and Schmachtenberg E. (2008). "Additive processing of polymers". *Macromolecular materials and engineering*, 293(10), 799-809.

Wenzheng W., Geng P., Li G., Zhao D., Zhang H. and Zhao J. (2015). "Influence of layer thickness and raster angle on the mechanical properties of 3D-printed PEEK and a comparative mechanical study between PEEK and ABS". *Materials*, 8(9), 5834-5846.

Wohler, T. (1992). "CAD meets rapid prototyping". Computer-Aided Engineering, Vol. 11, No. 4

Xingting Han, Dong Y., Chuncheng Y., Sebastian S., Lutz S., Ping Li, Dichen Li, Jürgen G. and Frank R. (2019). "Carbon Fiber Reinforced PEEK Composites Based on 3D-Printing Technology for Orthopedic and Dental Applications". Journal of clinical medicine, 8(2), 240.

Zureks. (2008). (Accessed on 23rd October 2018). Image of the FDM Process. Retrieved from https://upload.wikimedia.org/wikipedia/commons/4/42/FDM_by_Zureks.png.

3Dmatter Unlocking material properties. (2018). <http://my3dmatter.com/what-is-the-influence-of-color-printing-speed-extrusion-temperature-and-ageing-on-my-3d-prints>. Accessed on 9th December 2018.

800 series UTM fatigue test machine. Accessed on March 2nd, 2019. <https://www.testresources.net/test-machines/dynamic-fatigue-test-machines/800-series-fatigue-test-machines/>

APPENDIX

Today, quite a large number of RP processes are available and many of these processes have similarities since they appeared simultaneously (Kulkarni et al., 2000). Though there are various ways of categorizing the RP processes, one of the best ways to do that is to categorize them by the form of the material used (Bellini, 2002). In this manner all the RP methods can be grouped into:

1. Liquid-form based,
2. Solid-form based, and
3. Powder-form based (Kai et al., 1997).

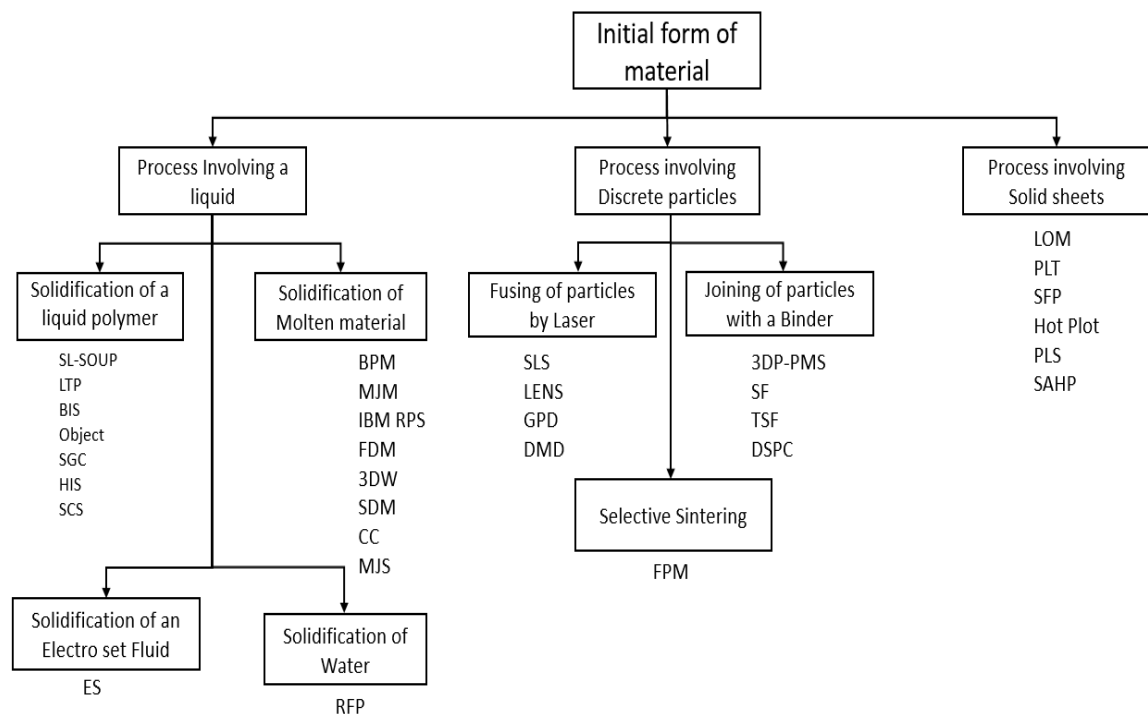


Figure 2.6. Categorization of RP processes based on the initial material form (adapted Bellini, 2002).

Figure 2-6 shows the categorization of the LM processes and also the processes that fall into the category. Some of the known RP technologies are Selective Laser Sintering (SLS), 3D Printing (3DP), Laminated Object Printing (LOM), MultiJet Printing (MJM) and Fused Deposition Modeling (FDM). Given the number of RP processes available, selecting the appropriate RP process for a particular job depends on several decision criteria such as cost, build time, geometry of the desired part, product quality, etc. Many studies are done relevant to the development of support systems to help RP users in identifying the appropriate RP process. Mahesh et al. (2005) developed a database of features of all the RP processes that help in finding the particular RP process based on the RP user queries. Masood et al. (2002) suggested the development of an RP selector, that used the machine cost, build time, accuracy and surface finish as the criteria, to select an RP process. Each individual RP process, in turn, consists of different types of machines based on the user's need. Chowdary (2007) developed a model which helps in selecting the suitable SLA machine based on part weight, beam diameter, operating system, and build envelope among others. Subburaj et al. (2008) provided a similar selection platform for the Rapid Tooling (RT) process.

The following sections give a brief idea on some of the most commonly used RP methods.

SELECTIVE LASER SINTERING

Selective laser sintering commonly known as SLS was developed at the University of Texas by Carl Deckard and Joseph Beaman. This RP technique uses a CO₂ laser beam

to fabricate parts. It starts with a 2D slice data being fed into the machine that controls that exposure path of the CO₂ laser beam (Saffarzadeh et al., 2016). With the information received from the slicing software, the laser traces the contour to sinter the powder surface. Sintering, here, means the laser heats up the powder to the melting temperature where the powder particles fuse together along the scanned path and also to the previous layer (Chua, 2010). Once that layer is formed the platform lowers by a layer thickness and the same procedure gets repeated until the part is completely built as shown in Figure 7.1. Once the part is built, the un-sintered powder can be brushed off.

The advantage of this technique is that SLS can have a passive support structure. In other words, the unfused powder in each layer acts as a support structure for the model. Additionally, the parts built by this technique can be reused by converting them to powder (Kruth et al., 2008).

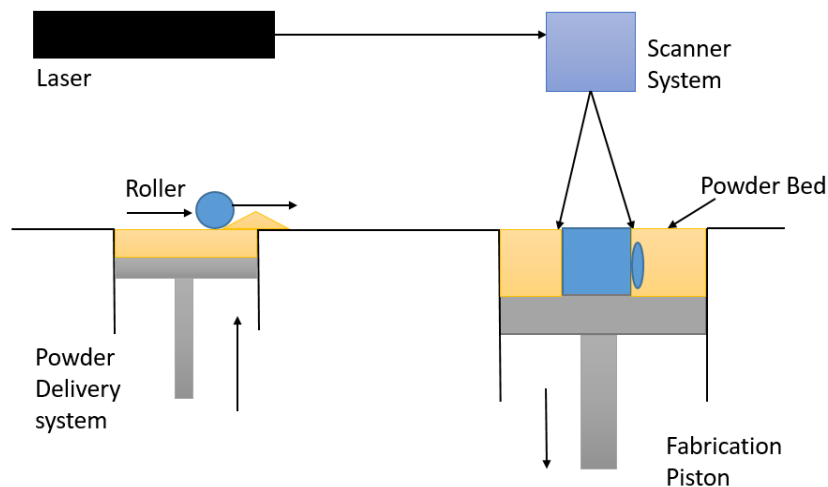


Figure 7.1. Schematic diagram of selective laser sintering

Most commonly used materials in SLS are nylon, metals, sand, ceramics etc. (Pham et al., 1998). Some challenges in this technique are warping and shrinkage that might be caused due to the extensive heating and cooling of the powder (Saffarzadeh et al., 2016). Additionally, because of the large size of the powders used, parts fabricated by this technique tend to have a poorer surface finish (Liu et al., 2013).

3D PRINTING

3D Printing also known as 3DP was invented by Massachusetts Institute of Technology (MIT) (Sood, 2011) and was commercialized by Z Corporation in 1997 (Chua et al., 2010). This technology uses the binding agents to join the powdered materials through jet deposition. The process starts with a roller leveling and distributing the powder on the top of a build chamber. The ink-jet printing head jets the binding solution selectively onto the powder material along the contour of the 2D surface. The powder particles, along with the path in which the nozzle sprayed the binder solution, stick together to form a layer (Chua et al., 2010). The remaining unprocessed powder material provides passive support to the part. Once a layer is formed the bed moves down by a slice thickness and the procedure gets repeated until the part is formed. The completed part surrounded by the unprocessed powder is then obtained by brushing off the loose powder. Figure 7.2 gives a schematic diagram of 3D printing.

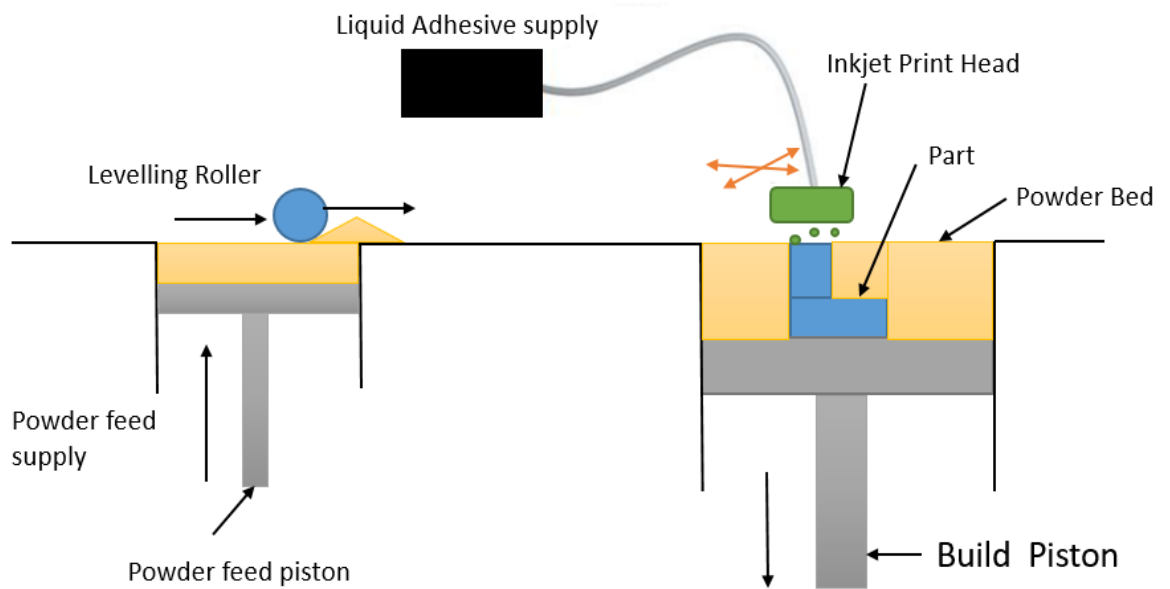


Figure 7.2. Schematic diagram of 3D printing

Some of the materials (powder) used are metals, polymers, and ceramics. The major disadvantage of this technique is the fragile nature and poor strength of the parts produced, poor surface finish and the need for post-processing (Steve et al., 2003).

LAMINATED OBJECT MANUFACTURING (LOM)

Laminated Object Printing, introduced by Helisys, California (Sood, 2011), has a very unique way of manufacturing products. LOM can be considered as both subtractive and additive process. In this technique, sheets of paper or such kind of material with adhesive on the bottom side are used as the layers for the part. A heated roller passes

over the material making it to stick to the platform. A laser beam then traces the contour of the slice as per information received from the slicing software, cutting through the sheet in the shape of the cross section (Cooper, 2001). The laser then crosshatches all of the material outside which helps in removal of the unwanted material but remains in its place while fabricating to act as passive supports (Pham et al., 2012). After this stage, a new sheet of material is rolled over and gets stuck to the earlier sheet and the same procedure is repeated thus forming the second layer. Figure 7.3 shows a schematic diagram of the working of the laminated object printing method.

Once the part is obtained, the supports are removed by hand. The disadvantage of this technique is the difficulty involved in removing the support material which might cause undercuts and geometrical inaccuracies. The other disadvantage is the necessity of an inert gas chamber to avoid any fire hazards.

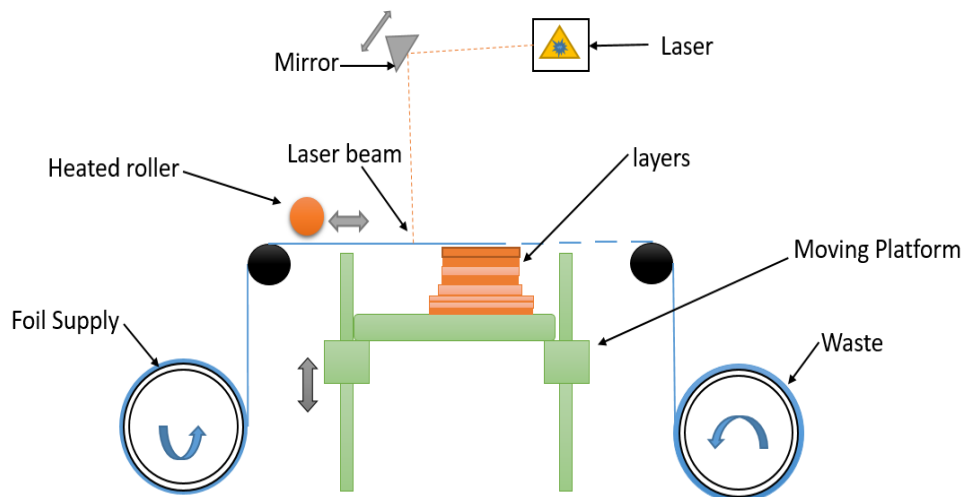


Figure 7.3. LOM mechanism (adapted from Wikipedia on 12th November 2018)

MULTI JET MODELLING

This technique uses materials such as photopolymers to build the part and wax for supporting the build structures. The printer head selectively drops the fusing material which mostly comprises of the photopolymers along the contour of the 2D surface as per information received from the slicing software. Ultraviolet light is then used to solidify the photopolymers to obtain the shape (Kitsakis et al., 2015). Once the material gets solidified a planerizer is used to fatten the layers to the specified layer thickness. This procedure is repeated until the part is completely built and later the part is obtained by removing the support material. The disadvantage of using this method is the limited number of materials available for processing and relatively slower build process (Cotteleer et al., 2014). Figure 7.4 gives a schematic diagram of the MJM process.

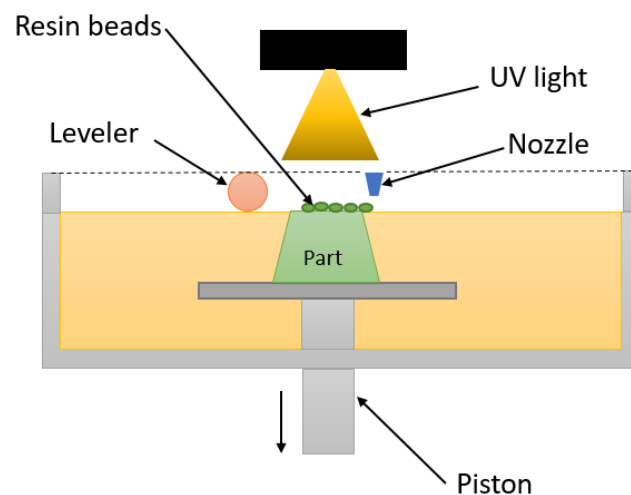


Figure 7.4. Multi Jet Modelling (adapted from Wikipedia on 12th November 2018)